

**PREPARATION OF METAL OXIDE NANOPARTICLE-MODIFIED
CARBON ELECTRODES FOR OXYGEN EVOLUTION REACTION**

BY

MOHAMMED AMEEN AHMED QASEM

A Thesis Presented to the
DEANSHIP OF GRADUATE STUDIES

KING FAHD UNIVERSITY OF PETROLEUM & MINERALS

DHAHRAN, SAUDI ARABIA

In Partial Fulfillment of the
Requirements for the Degree of

MASTER OF SCIENCE

In

CHEMICAL ENGINEERING

DECEMBER, 2017

KING FAHD UNIVERSITY OF PETROLEUM & MINERALS
DHAHRAN- 31261, SAUDI ARABIA
DEANSHIP OF GRADUATE STUDIES

This thesis, written by **MOHAMMED AMEEN AHMED QASEM** under the direction his thesis advisor and approved by his thesis committee, has been presented and accepted by the Dean of Graduate Studies, in partial fulfillment of the requirements for the degree of **MASTER OF SCIENCE IN CHEMICAL ENGINEERING**.



Dr. Sagheer A. Onaizi
(Advisor)



Dr. Mohammed Ba-Shammakh
Department Chairman


MD. ABDUL AZIZ

Dr. Md. Abdul Aziz
(Member)

28/12/2017



Dr. Mohammed Ba-Shammakh
(Member)



Dr. Salam A. Zummo
Dean of Graduate Studies



3/1/18
Date

© Mohammed Ameen Ahmed Qasem

2017

This work is dedicated to all who helped me to be patient during my life including my
parents, brothers, sisters, wife and two kids (Alshima and Alqasem)

ACKNOWLEDGMENTS

I am so thankful to Allah for making everything easy, so helping me to finish this work.

I would like to thank my thesis advisor, Dr. Sagheer Onaizi for his guidance, support, and help in this work. Also, I would like to thank the member of my thesis committee, Dr. Md. Abdul Aziz since he significantly helped me in this thesis. Where he introduced me to all the staff in the CENT at RI at KFUPM Moreover, I would like to thank the chairman of the Chemical Engineering department, Dr. Mohammed Ba-Shammakh, who was one of the committee members, for his advice. Also, I thank the Chemical Engineering master program coordinator, Dr. Mamdouh Al-Harhi for his cooperation.

All my thanks and acknowledgment to the King Fahd University of Petroleum and Minerals (KFUPM) for its financial support during my undergraduate and graduate study.

Moreover, I would like to thank the CENT at IR/KFUPM, which is its rector, Zain Yamani, for funding support and for allowing me to use their facilities. Besides, my deepest thanks go to all doctors in the chemical engineering department at KFUPM.

I will not forget my family including my parents, wife and all my village residents in Yemen for their love and support.

I would like to thank my friends including Saddam AL-Hammadi, Mohammed Al-ezzi and Galal Atef, Galal Aqial Madyan, Talal, Zaid, Ammar, Mazen, Hasan, Ibrahim and Qais.

TABLE OF CONTENTS

ACKNOWLEDGMENTS	VI
TABLE OF CONTENTS	VII
LIST OF FIGURES	X
LIST OF ABBREVIATIONS	XII
ABSTRACT	XIII
ملخص الرسالة	XV
CHAPTER 1 INTRODUCTION	1
1.1 Nickel Oxide Nanoparticles (NiO NPs)	3
1.2 Tricobalt Tetraoxide Nanoparticles (Co ₃ O ₄ NPs)	4
1.3 Objectives	5
1.4 Methodology	5
CHAPTER 2 LITERATURE REVIEW	7
2.1 NiO Nanoparticle	10
2.2 Nano-Co ₃ O ₄	14

CHAPTER 3 INFLUENCE OF PAMOIC ACID AS A COMPLEXING AGENT IN THE THERMAL PREPARATION OF NIO NANOPARTICLES: APPLICATION TO ELECTROCHEMICAL WATER OXIDATION	17
3.1 Introduction	18
3.2 Experimental	22
3.2.1 Materials	22
3.2.2 Preparation of the FPCE.....	22
3.2.3 Preparation of NiO NPs and the NiO NPs-Modified FPCE	23
3.3 Instrumentation	24
3.4 Results and discussion.....	25
3.4.1 Interaction between the Na₂PA and Ni(NO₃)₂·6H₂O	25
3.4.2 TGA Analysis of the Ni-PA Complex.	28
3.4.3 Effect of the Extent of Heat Treatment on the Crystallinity of the NiONPs	30
3.4.4 Morphological Characterization of the NiONPs Prepared at 520°C	32
3.4.5 Morphological Characterization of the NiONPs-Modified FPCE	36
3.4.6 Electrocatalytic Activities of NIO NPs Toward Water Oxidation in an Alkaline Medium	38
3.5 Conclusions	40
CHAPTER 4 PREPARATION OF NANO-CO₃O₄ BY DIRECT THERMAL DECOMPOSITION OF CO(NO₃)₂·6H₂O FOR ELECTROCHEMICAL WATER OXIDATION	41
4.1 Introduction	42

4.2 Experimental	44
4.3 Results and discussion	45
4.4 Conclusion	52
CHAPTER 5 EFFECTS OF CALCINATION TEMPERATURE ON THE OXYGEN EVOLUTION REACTION PERFORMANCE OF CO₃O₄NP/FPCE CATALYSTS	54
5.1 Introduction.	55
5.2 Experimental.	58
5.2.1 Materials and Instruments.	58
5.2.2 Preparation of Filter Paper Derived Carbon Electrode(FPCE)	58
5.2.3 Preparation of Co ₃ O ₄ NPs and Co ₃ O ₄ NPs-Modified FPCE Catalyst	59
5.3 Electrochemical Measurements	60
5.4 Results and Discussions	60
5.4.1 Characterizations of Co ₃ O ₄ NPs Formed at Different Calcinations Temperatures.....	61
5.4.2 Electrochemical measurements.....	67
5.4.3 Calculation of Electrochemically Active Surface Area(ECSA)	71
5.5 Conclusion.....	75
CHAPTER 6 CONCLUSIONS AND RECOMMENDATIONS.....	76
REFERENCES.....	78
VITAE	90

LIST OF FIGURES

Figure 1: Structure-1 shows pamoic acid (Na ₂ PA)	12
Figure 2: Photograph of the used FPCE.	23
Figure 3: Structure-2 Plausible structure of the complex formed in the interaction with Ni(NO ₃) ₂ and Na ₂ PA.	26
Figure 4: (A) FT-IR spectrum, and (B) XPS spectrum of the resultant dried reaction mass obtained after mixing Na ₂ PA and Ni(NO ₃) ₂ ·6H ₂ O in ethanol, followed by evaporation of the ethanol with heating.	27
Figure 5: TGA curves of the resultant Ni-PA complex	29
Figure 6: XRD patterns of NiO prepared by thermal decomposition of the Ni-PA complex at different temperatures: (a) 420°C, (b) 520°C, and (c) 620°C.....	31
Figure 7: SEM images of NiO prepared by the thermal decomposition of a Ni-PA complex formed in the presence (a, b) or absence (c, d) of Na ₂ PA at 520°C..	33
Figure 8: TEM image (a), HRTEM (b), and SAED (c) data collected from NiONPs prepared by thermal decomposition of a Ni-PA complex at 520°C.....	35
Figure 9: FESEM images of a FPCE modified with NiONPs prepared (a) with Na ₂ PA and (c) without Na ₂ PA. (b) and (d) show magnified views of (a) and (c), respectively.....	37
Figure 10: Linear sweep voltammogram of (a) the FPCE, and an FPCE modified with NiONPs prepared (b) with and (c) without Na ₂ PA, in 0.1 NaOH (aq). Scan rate: 100 mVs ⁻¹	39
Figure 11: (a) TGA curve of Co(NO ₃) ₂ ·6H ₂ O at the selected temperature zone. (b) XRD pattern of the product of subjecting Co(NO ₃) ₂ ·6H ₂ O to a temperature of 520 °C for three hours.	47
Figure 12: (a, b) FESEM images, (c, d) TEM images, (e) HRTEM image, and (f) SAED pattern of the nano-Co ₃ O ₄ prepared by heating Co(NO ₃) ₂ ·6H ₂ O at 520 °C for three hours in an aerial atmosphere.	49
Figure 13: (a) FESEM image of a nano-Co ₃ O ₄ /FPCE. (b) Corresponding EDS spectrum of red boxed area of (a).....	51
Figure 14: Linear sweep voltammograms of FPCE (a) and nano-Co ₃ O ₄ /FPCE (b) in 0.1 M NaOH (aq.).....	52
Figure 15: XRD patterns for CO ₃ O ₄ NPs at different temperatures (320,420,520, and 620°C)	64
Figure 16: FTIR spectra of prepared CO ₃ O ₄ NPs sintered at 320-620°C.....	65
Figure 17: SEM images of CO ₃ O ₄ NPs on ITO substrate at magnification of 400KX for various calcination temperature of (a)320, (b)420, (c)520, and (d) 620°C.	66
Figure 18: TEM images of as-prepared CO ₃ O ₄ NPs at different calcination temperatures of (a)320, (b)420, (c)520 and (d)620 °C and the insets show XRD diffraction for every temperature.	67

Figure 19: (a) Cycles of Linear sweep voltammograms of prepared Co_3O_4 NPs on FCE at (a) 420 °C, (b)520 °C,(c) 320 °C and (d)620°C in 0.1 M NaOH (aq.), the inset in the same part(a) shows the redox reactions at the four different temperatures and (b) scan rates versus current density using Co_3O_4 NPs/ FCE prepared at different tmperatures :320,420,520 and 620°C in 0.1 M NaOH (aq.),too.	70
Figure 20: Cyclic voltammograms of Co_3O_4 NPs- modified FPCE at sintered temperatures of (a)320, (b)420, (c)520, and (d) 620°C with different scan rates started from 10 to 60mvs ⁻¹ in 0.1 M NaOH (aq.) .insets in plots are the relative anodic peaks current densities vs. the square roots of scan rates. 71	71
Figure 21: Chronoamperometry curves of Co_3O_4 NPs /FPCE CVs in 0.1M NaOH at various sintering temperatures: 320,420,520 and 620 °C.....	74
Figure 22: The schematic diagram of electrochemical cell setup for oxygen evolution reaction(OER).....	75

LIST OF ABBREVIATIONS

OER	Oxygen Evolution Reaction
NPs	Nanoparticles
NiO NPs	Nikel Oxide Nanoparticles
Co₃O₄ NPs	Tricobalt Tetraoxide Nanoparticles
FPCE	Filter paper derived carbon electrode
Na₂PA	disodium salt of Pamoic Acid
TEM	Transition Electron Microscopy
SEM	Scanning Electron Microscopy
FTIR	Fourier Transform Infrared Spectroscopy
BET	Brunauer–Emmett–Teller
TGA	Thermogravimetric Analysis
XRD	X-Ray Diffraction
XPS	X-ray photoelectron spectroscopy

ABSTRACT

Full Name : [Mohammed Ameen Ahmed Qasem]
Thesis Title : [Preparation of metal oxide Nanoparticle-modified carbon electrodes for oxygen evolution reaction]
Major Field : [chemical engineering]
Date of Degree : [December,2017]

Electrochemical / photoelectrochemical water oxidation (i.e. oxygen evolution) reaction (OER) is one of the most important approaches to convert renewable energy like the solar energy to usable fuels. Generally, the oxygen evolution reaction is kinetically slow (i.e. it needs high overpotential) at commonly employed electrode in both electrochemical or photoelectrochemical OER. As a result, the modification of the electrode with a suitable catalyst is needed to reduce the required energy and increase the rate of reaction. Thus, catalyst plays an important role in this process, resulting in minimizing the process cost. Therefore, several studies have been conducted with the objective of catalyst preparation and characterization. Most researchers have used high cost materials as substrate electrodes such as gold and platinum. In this work, we used low cost substrate electrode, porous carbon electrode (PCE). We prepared the FPCE by simply heating the normal filter papers in nitrogen atmosphere in tubular furnace. Then, the metal oxides nanoparticles are deposited on the prepared PCE. We deposited the pre-synthesized NiO and Co₃O₄ NPs using drop-drying method. Here, we optimized the deposition parameters such as the applied current and time in order to get the highest possible efficiency in OER. For the case of NiOx NPs, we developed a novel method to prepare NiOx NPs. Initially, we mixed carboxylic acid functionalized organic molecules and nickel precursor

in organic solvent, and then the solution was heated to remove the solvent. Finally, the raw catalyst was flame-treated in ambient atmosphere to obtain the monodisperse spherical NiO_x NPs. Next, the NiO_x NPs were drop-casted on the FPCE to check its efficiency in electrochemical water oxidation. Similarly, Co₃O₄ NPs were prepared from only cobalt precursor by thermal decomposition and deposited on FPCE by drop-casting method. The NiO_x and Co₃O₄ NPs -modified electrode showed significantly high electrocatalytic properties in OER. The used NPs (both NiO_x and Co₃O₄) and NPs-modified PCE were characterized in detail by various modern techniques such as scanning electron microscopy (SEM), transmission electron microscopy (TEM), X-ray photoelectron spectroscopy (XPS), X-ray diffraction (XRD), Fourier transform infrared spectroscopy (FT-IR) and thermogravimetric analysis (TGA). In conclusion, the prepared catalysts are cheap and have high efficiency, which make them attractive for water oxidation (i.e., sustainable and clean energy production).

ملخص الرسالة

الاسم الكامل: محمد أمين أحمد قاسم

عنوان الرسالة: تحضير أقطاب إلكتروكيميائية من الكربون معدلة بإضافة أكاسيد المعادن ذات الأحجام النانوية ومن ثم استخدامها في تفاعل توليد الأكسجين

التخصص: هندسة كيميائية

تاريخ الدرجة العلمية: ديسمبر لعام سبعة عشر وألفين

من إحدى مصادر الطاقة المتجددة عملية أكسدة الماء. حيث يمكن أن تستخدم المواد الناتجة (بروتونات والإلكترونات) من هذه العملية في تحويل ثاني أكسيد الكربون إلى حمض الفورميك الذي يمكن أن يستخدم كوقود. وهناك طرق عديدة لأكسدة المياه : واحدة من هذه الطرق تتم باستخدام قطب كهربائي (باستخدام كهرباء) أو ضوئي (باستخدام ضوء الشمس) وينتج عن ذلك أكسجين وإلكترونات (e^-) وبروتونات (H^+). وهذا العملية تسمى تفاعل نشوء أو توليد الأكسجين . ولكن من المعوقات التي تواجه هذه الطريقة هي أن معدل التفاعل بطيء ، ويحتاج إلى جهد كهربائي عالي لتوليد الأكسجين بالإضافة إلى قلة نشاط الحوافز مع الركائز اتجاه هذه العملية . لذلك نحن حضرنا حوافز مع ركائز بطريقة معينة ؛ لمواجهة هذه التحديات وتقليلها . وفي هذه الرسالة استخدمنا الإلكترود الكهربائي فقط لذلك الغرض؛ لسهولة إعداده وتحضيره. وحيث أن الحوافز لها دور كبير في تحفيز هذا الإلكترود فإن الجزء الأكبر في هذه الرسالة هو تحضير حوافز نانوية من أكاسيد المعادن مع أقطاب من مادة الكربون . وقد تم تحضير أكسيدين (أكسيد النيكل (NiO)) وأكسيد الكوبلت (Co_3O_4)) ذاتا الأحجام النانوية على النحو الآتي: بالنسبة لأكسيد النيكل فلقد تم خلط كمية معينة من حمض البومك (Na_2PA) المحتوي على ثنائي ملح الصوديوم مع كمية معينة من نيتريد النيكل المشبع بالماء ($Ni(NO_3)_2 \cdot 6.H_2O$) في محلول الإيثانول. ومن ثم خلط الناتج من ذلك خلطا جيدا حتى يصير المحلول بما فيه متجانسا بشكل جيدا. ومن ثم يتم تبخير الإيثانول برفع درجة الحرارة إلى حوالي 65 درجة مئوية . وبعد ذلك يأخذ المركب الناتج من ذلك لتجفيفه بالفرن طيلة الليل عند درجة حرارة 40 درجة مئوية ، ومن ثم يوضع المنتج الصلب في قارب صغير مصنوع من الألومنيوم الذي بدوره يوضع في أنبوب زجاج الموجود في داخل الفرن ؛ للحصول على مادة ذات حجم نانوي، علما بأن درجة الحرارة ترتفع فيه (الفرن) كل دقيقة عشرة درجات حرارية مئوية حتى تصل إلى الخمسمائة وعشرين درجة مئوية. وبعد ذلك تستمر درجة الحرارة ثابتة لمدة ثلاث ساعات عند الخمسمائة وعشرين . ومن ثم يتم خفض درجة الحرارة خمس درجات كل دقيقة . ومن ثم يتم أخذ المادة الناتجة (أكسيد النيكل) ذات الأحجام النانو مترية (عشر أس سالب تسعة متر) ووضعها على الداعم (القطب) الذي يتم صنعه من مادة أوراق الترشيح تحت درجة حرارة تصل إلى 850

درجة مئوية لمدة خمس ساعات بحيث يتم استخلاص الكربون ذات الغشاء النافذ. بعد ذلك يتم دمج تلك المواد النانوية بالقطب الكربوني المستخلص بترسيب أكسيد النيكل على الكترود (قطب) الكربون ذات الغشاء النافذ بتقطير (قطرة بقطرة) محلول أكسيد النيكل (مللي جرام من المادة مع ملليمتر من الماء) ذات الأحجام النانوية على قطب الكربون الذي بدوره يعمل كركيزة أو داعم للمادة الحافزة (أكسيد النيكل). ومن ثم يتم تجفيف ذلك على مدى ليلة كاملة. وبعد ذلك يتم استخدام قطب الكربون المعدل بذرات أكسيد النيكل في عملية التحليل الكهربائي في محلول هيدروكسيد الصوديوم باستخدام الآلة (CHI (760E)). بالنسبة لتحضير أكسيد الكوبلت ذات الأحجام النانوية على قطب الكربون واستخدامه في عملية التحليل الكهربائي تمت بنفس طريقة أكسيد النيكل ماعدا أن أكسيد الكوبلت تم إعداده بتسخين أو حرق نتريد الكوبلت المشبع بالماء ($\text{Co}(\text{NO}_3)_2 \cdot 6\text{H}_2\text{O}$) فقط بدون إضافة أي مادة أو محلول في الفرن. لقد كانت النتيجة كالآتي: أن التيار الناتج من العملية باستخدام قطب الكربون المعدل مع أكسيد المعدن أعلى بكثير من استخدام قطب الكربون بدون أي إضافة. بالإضافة إلى أن أكسدة الماء حدثت عند جهد كهربائي أقل بالنسبة للأقطاب المعدلة بذرات أكسيدات المعدنين (النيكل والكوبلت) مقارنة بأقطاب الكربون بدون إضافة. أما بالنسبة لحافز أكسيد النيكل مع حمض بوميك فإن نشاطه على قطب الكربون اتجاه أكسدة الماء (تفاعل نشوء أو توليد الأكسجين) أكبر من نشاطه بدون الحمض المذكور سابقا. بالإضافة إلى أن كثافة التيار الناتج من التحليل الكهربائي مع قطب الكربون المعدل بأكسيد النيكل المعد مع حمض البومك أكبر من ذلك القطب المعد بدون الحمض. وهذا يؤكد أهمية الحمض المذكور سابقا في تحضير ذرات أكسيد النيكل. بالإضافة إلى ما سبق فقد تم دراسة تأثير اختلاف درجة الحرارة على أكسيد الكوبلت (Co_3O_4). وكذلك تم تعيين خصائص القطبين المعدلين بأكسيدات النيكل والكوبلت، بالإضافة إلى تعيين خصائص كل من أكسيدات النيكل والكوبلت النانوية باستخدام عدة أجهزة: جهاز الأشعة لتعيين المركبات الكيميائية (XRD) X-Ray (Diffraction)، وجهاز التحليل الحراري (TGA) Thermogravimetric Analysis، وأجهزة تعيين الشكل الخارجي للبلورة المتكونة وشكل السطح الخارجي (SEM) Scanning Electron Microscopy و (TEM) Transition Electron Microscopy وجهاز تعيين الروابط الكيميائية بين المجموعات الوظيفية وبين العناصر والذرات (FT-IR) Fourier Transform Infrared Spectroscopy وجهاز تعيين نشاط العناصر (XPS) X-ray photoelectron spectroscopy

CHAPTER 1

INTRODUCTION

Nowadays, the progress towards a comprehensive and sustainable development needs a huge amount of fossil fuels such as natural gas, oil and coal. However, these resources are not renewable since they need millions of years to be naturally generated. Such reality has forced many companies and countries to search for alternative renewable energy sources to meet their energy consumption[1].

One of these alternative sources for renewable energy is water oxidation, the so-called oxygen evolution reaction which is part of water splitting process[2]. This process oxidizes water to molecular oxygen, four electrons in addition to four protons as shown in the following equation:



This means that the electrons, protons and molecular oxygen are the products. Thus, the two products including the electrons and protons are the two alternative sources for renewable energy. However, to successfully achieve water oxidation or convert water to desirable products (current and protons), energy will be needed for initiating the reaction[2]. Additionally, to reduce the activation energy and speed up the reaction, high-performing catalysts should be utilized[2].

Thus, appropriate selection of catalyst is a key factor in the process of water oxidation since catalyst can significantly enhance the products formation and thus considerably reduce the cost. There are three common classes of catalysts used in water oxidation process. Their classifications depend on how they are synthesized and used. The three types are electro catalysts [3-15], photo catalysts [16-18] and other chemical catalysts. Therefore, many researchers [19-23] have tried to synthesis very efficient and cheap catalysts and many of them have claimed that they have fabricated catalysts with very high activity [24-27]

In details, the electro catalysts are the catalysts which help a reaction in taking place between the reactants and electrodes and /or assist an overall half-reaction (assisting the chemical transformation of an intermediate) to occur. Therefore, electrons are transferred between the reactants and electrodes leading to increasing the rate of the reaction without consuming the electro catalysts. These catalysts are deposited on the surfaces of electrodes (Note: some electrodes have electro-chemically active surfaces).

Unlike electro-electro-catalysts, photocatalysts accelerate chemical reaction rate, energy in the form of electromagnetic waves must be used to activate them and/or substrates instead of continuous current used for activating electrocatalysis [3, 28, 29]. The third type is chemical catalysts which are only different in how they are prepared and used compared to the previous ones. However, herein we are interested in only electrocatalysts for water oxidation since they can be synthesized and prepared in similar ways compared to photocatalysis and chemical catalysts.

Although the electro catalysts technique was discovered in the beginning of the last century, it was gained momentum only after 1960, which is evident from the number of publications. Despite the significant number of publications ,water oxidation is still not feasible for energy production [2] since most of the developed electro catalysts are expensive [30],have low catalytic activity [31],require high over-potential [2],have low current efficiency ,have low stability[31] or not easily prepared [5, 6].

In this work, we will use cheap materials to prepare nanoparticles -modified electrodes as electro-catalysts. Then, we will use the prepared electro-catalyst for oxygen evolution reaction process. Two NPs, NiO and Co_3O_4 will be prepared and used for OER.

1.1 Nickel Oxide Nanoparticles (NiO NPs)

We developed a thermal decomposition method for preparing NiO nanoparticles (NiO NPs) using disodium salt of pamoic acid (Na_2PA) as a complexing agent and Ni (NO_3)₂·6.H₂O as a nickel precursor. Prior to thermal decomposition, a nickel precursor, Ni (NO_3)₂·6.H₂O, was mixed with Na_2PA in ethanol, and the ethanol was evaporated to obtain the dried reaction mass. The dried reaction mass was characterized using Fourier transform infrared spectroscopy, X-ray photoelectron spectroscopy, and thermal gravimetric analysis. Thermal decomposition was then performed in air to obtain the NiONPs. The role of Na_2PA in the synthesis of NiONPs was evaluated by preparing the NiONPs according to the protocol described above without the addition of Na_2PA . The X-ray diffraction data indicated that crystalline NiO (bunsenite, cubic crystal system) formed with or without Na_2PA ; however, field emission scanning electron microscopy images showed that smaller monodisperse NiONPs formed only with the addition of

Na₂PA. Without Na₂PA, the obtained NPs were quite large and polydispersed. The sizes of the NiONPs prepared in the presence of Na₂PA were determined using TEM imaging to be 19.1 ± 3.2 nm. The crystallinity of the NiONPs prepared with Na₂PA was further confirmed using high-resolution transmission electron microscopy and the corresponding selected area diffraction patterns. The electrocatalytic activity of the NiONPs toward water oxidation under alkaline conditions was evaluated by immobilizing the NPs onto an in-house prepared filter paper derived carbon electrode, and compared with NPs prepared without Na₂PA.

1.2 Tricobalt Tetraoxide Nanoparticles (Co₃O₄ NPs)

Co₃O₄ NPs were prepared using a simple, straightforward method that involved thermal decomposition of Co(NO₃)₂·6H₂O without any pretreatment with an organic or inorganic component. The prepared Co₃O₄ NPs were characterized using X-ray diffraction, field emission scanning electron microscopy, and transmission electron microscopy. These analyses confirmed the formation of short nanorods of single Co₃O₄ phase. The electrocatalytic properties of the Co₃O₄ NPs were evaluated after immobilizing them on a carbon electrode derived from normal filter paper. The modified electrode showed good electrocatalytic properties toward water oxidation in an alkaline solution.

1.3 Objectives

- (1) Develop carbon electrode (PCE) as novel substrate material
- (2) Prepare metal oxide (MO_x NPs)
- (3) Incorporate metal oxide MO_x NPs into PCE using a proper method
- (4) Characterize the MO_x NPs-modified -PCE in order to get insight into their crystallinity and morphology
- (5) Apply the resultant MO_x NPs -modified PCE (as a catalyst) for oxygen evolution reaction (OER)

1.4 Methodology

To prepare the porous carbon electrodes, filter papers (FP) will be modified as follows: firstly, filter papers will be cut to approximately 2 cm² in area. Secondly, they will be burned on oven with under nitrogen gas for around nine hours at 850°C. Finally, the copper tape, scissor, paper puncher and strong adhesive tape will be used to make only 0.2 cm² of porous carbon subjected to the reaction with nanoparticles (NPs) catalysts. After preparing FPCE, NiO_x NPs will be fabricated as follows: a certain amount of mixture of an organic solvent and a nickel precursor will be sonicated for 10 minutes. Then, a small amount of carboxylic acid will be added, and the mixture will be sonicated for 30 minutes. Next, the solution will be stirred at certain rpm and temperature until the ethanol evaporates. After that, the product will be dried overnight in the oven at 40°C. Then, the produced catalyst will be crushed, and the obtained powder will be calcinated

in a tubular furnace for few hours at constant temperature. Then, the powder will be cooled at room temperature. This treatment will lead to the formation of the prepared NiOx NPS, which will be deposited on FPCE and left overnight. Afterwards, NiOx NPs modified- porous carbon electrode will be ready for electrochemical measurement for water oxidation using CHE instrument model 760e. On the other hand, the pre-synthesized Co₃O₄ NPs will be deposited on FPCE by method of galvanic static deposition manipulating the current and time for optimizing and getting efficient monodispersed NPs catalysts. Thus, Co₃O₄ NPs modified-FPCE will be electrochemically measured using CHE instrument model 760e. Transmission electron microscopy (TEM), scanning electron microscopy (SEM), X-ray photoelectron spectroscopy (XPS), X-ray diffraction (XRD), Brunauer–Emmett–Teller (BET), thermogravimetric analysis (TGA) and Fourier transform infrared spectroscopy (FTIR) will be used to characterize the FPCE, relevant metal precursors, Co₃O₄ NPs and NiO NPs and (Co₃O₄ and NiO) NPs modified –PCE in details.

CHAPTER 2

LITERATURE REVIEW

The advantages of technology in the renewable energy field attracts the research and industrial community to devote a tremendous effort to make a breakthrough in this area. Currently, most available energy sources are not sustainable, and they are considered as a source of pollution. As a result, development a new generation of energy sources that are environmentally friendly, clean and sustainable are urgent. As an example of a cheap renewable energy sources is water oxidation (oxygen evolution reaction (OER)).

For achieving a high-water oxidation (WO) activity, active catalysts should be utilized. Different catalysts (chemical ,electrochemical [3-15] and phot-electrochemical [16-18]) have been synthesized by several researchers and used for OER. However, in this study we will focus on the electrochemical catalysts owing to simpler preparation compared to other catalysts.

Class of these catalysts is transitional metals oxide where many of them, such as IrO_2 , Rh_2O_3 , CoO_4 , Mn_2O_3 and RuO_2 [19-23], could be used in many application like water oxidation[16-18]. However, most of the previous catalysts are rarely available, so they are expensive and some of them have low activity. Furthermore, their preparations are a little bit complex. In addition, expensive substrate electrodes like ITO[5, 6] have been used in these catalysts (transitional metal oxides). Therefore, an alternative inexpensive

metal oxide with simple preparation, cheap substrate electrode and high catalytic activity is needed.

Therefore, extensive effort has been devoted to obtain electro catalysts with these following features: well efficient, lower cost, higher stability[2].Most of these properties can be achieved by using some of transitional metals including (Co, Ni and son on) [2].However, only the nickel and cobalt based compounds like Nickel and cobalt oxides, Co_3O_4 and NiO_x ,will be particularly investigated here in this work because of their positives ,which will be mentioned below.

Regarding to Nickel oxide nanoparticles (NiO_x NPs), they have been suggested as a suggestion for this purpose (making NPs- modified electrode and using them in OER) because they have the good features mentioned above. Moreover, NiO_x NPs could be synthesized and used in many industrial applications such as supercapacitors[32] catalysts[33, 34] , electrochemical films[35, 36], gases sensors [37],batteries[38-40], magnetic substances[41, 42] and dye photocathodes[43]. In addition, the nickel oxide catalyst has been considerably studied for oxygen evolution reaction since this catalyst has high activity and low cost [44-48] .

Another suggestion, one of these compounds used for water oxidation(WO) is cobalt - based spinel oxide, which has been extensively studied ,where it has considered in alkaline solution as a higher efficient and stable catalyst[24-27].Therefore, high effort has been devoted to fabricate nanomaterial of spinel oxides like cobalt based spinel oxides with smaller sizes and bigger surface area for enhancing electro catalytic features of these

oxides[25, 49-54].Specifically, Co_3O_4 , is one of spinel oxides, which has been significantly and recently investigated because of many reasons: its own unique physical and chemical proprieties ,applications in interconversion between chemical and electrical energies as well as storage[55-58].In regarding to its applications, it can be used in many applications such as supercapacitors, water splitting and batteries of lithium-ion [55-58].

However, drawbacks could be appeared such as non-homogenous, non-spherical and big particles because of different methods used for preparation of NiO_x and Co_xO_y NPs. Thus, the activity of the catalyst will be considerably decreased. Therefore, the method of preparations of NPs significantly effects on the catalyst activity and consequently its application. However most of these ways, such as self-assembly[59], Ni-based molecular complexes(electrodeposition)[47], and solvothermal[48] are not simple.

As it is known, the fabricated conditions for preparation of NPs plays a significant role in determining the basic characteristics of synthesized nanoparticle including shape, size, size of distribution, crystals and mutual alignment. Thus, using various conditions in fabrication of nanoparticles results in different findings. Therefore, the preparation method of NPs will be considered.

In this work, we will prepare nickel and cobalt oxide nanoparticles via a novel method. With respect to nickel oxide NPs, thermal treatment method with very important change (using carboxylic acid), will be investigated where nickel nitrates($\text{Ni}(\text{NO}_3)_2 \cdot 6\text{H}_2\text{O}$) precursor with carboxylic acid(PA-Na_2) will be used for preparation of NiO_x NPs and applied for oxygen evolution reaction. On the other hand ,the same method without any

changes will be investigated with preparation of cobalt oxide NPs, too. Also, porous carbon electrodes will be used as substrates to electrochemically enhance the catalytic activity instead of carbon nanotubes and graphene, which have been investigated recently[59-63].

Our expectation was that the carboxylic acid will control most of key features, mentioned above, of NiOx NPs and increase the activity of oxygen evolution reaction. In regarding to CoxOy, we expected that Co₃O₄ NPs formed will have small sizes and will be monodispersed. For knowing that, many techniques were used in characterization of the both NPs, NiOx and Co₃O₄, such as scanning electron microscopy (SEM), transmission electron microscopy (TEM), X-ray photoelectron spectroscopy (XPS), X-ray diffraction (XRD), Fourier transform infrared spectroscopy (FTIR) and thermogravimetric analysis (TGA).

For understanding more about NPs (NiOx and Co₃O₄), planning to make very good NPs (NiOx and Co₃O₄) and enhancing NPs properties, we will report the literatures about nanoparticles of NiO and Co₃O₄ and organic moiety (Na₂PA) as the following:

2.1 NiO Nanoparticle

Over the past two decades, bulk and nanoscale nickel oxide (NiO) have attracted attention for their high stability [64-71], low toxicity [67, 69], and anomalous chemical [71-74], electrochemical [54, 67-70, 75-81], electronic [65, 80, 82, 83], magnetic [64, 71, 84], catalytic [64, 85, 86] and optical [72, 75, 83, 86] properties. NiO nanoparticles (NiONPs), in particular, are used in a variety of fields as optochemical sensors [72], electrochemical sensors [77], biosensors [68, 69, 78, 79], electrochromic

windows [75] , gas sensors [73, 74] , batteries [67] , fuel cells [70, 78] , photovoltaic cell [80] , electrochemical water splitting[54, 81] , catalysis [64, 66, 71] , and photocatalysis [86]. The broad applicability of nanoscale NiO relies on the material's high surface area and interesting properties, including chemical, electrochemical, and catalytic properties, which are not present in the bulk material. To meet the high demand for this nanoscale material, several synthetic methods have been developed based on hydrothermal [68, 71, 73, 76-78, 87, 88] , sol-gel [66, 82, 84], hot-injection [75] , co-precipitation [69] , microwave [64, 67] , electrochemical [74] , pulsed laser ablation [89] and thermal decomposition techniques [72, 86, 90] , as well as techniques based on complex formation with an organic moieties and successively their thermal decomposition[85, 91-96]. Nanoscale NiO particles have been prepared to have a variety of sizes and shapes, including nanospheres[64, 66, 71, 75, 82, 84, 86, 91, 92, 94, 96] , nanoplates [76, 87] , nanosheets [86, 93] , nanoplatelets [90] , flaked like architectures [68, 93] , nanorings [88], nanoflowers[71, 74] , hollow nanostructures [97] , nanorods[78, 96] , and nanocubes [94, 96]. Numerous studies have examined the preparation of nanoscale NiO, and the development of novel synthetic methods that are simpler and provide smaller or more monodisperse product profiles remains a topic of interest. Small sizes monodisperse nanoparticles (NPs) are valuable because they provide a high surface area and homogeneous properties compared to larger polydisperse NPs samples.

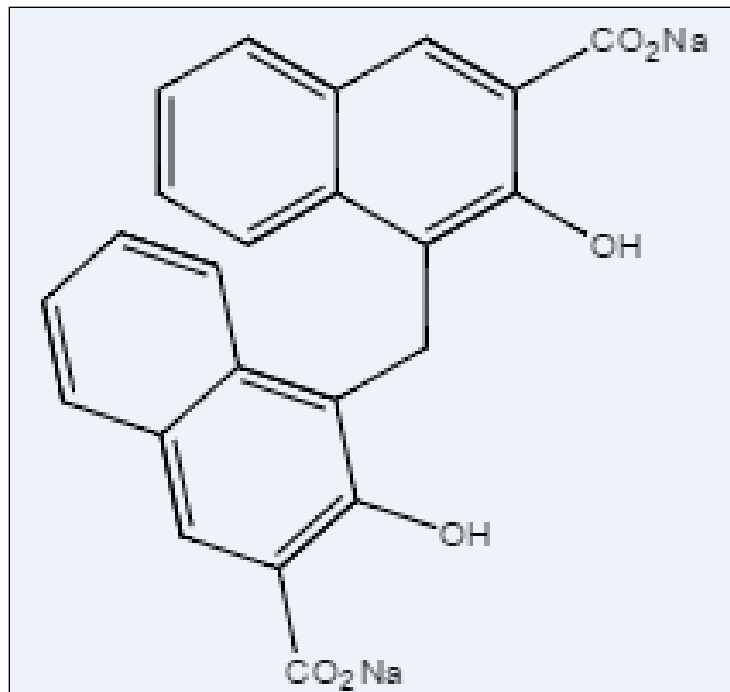


Figure 1: Structure-1 shows pamoic acid (Na₂PA)

Organic moieties that act as a surfactant, stabilizer, reductant, or ligand play an important role in determining the sizes and shapes of NPs. Recently, monodisperse 10.8 nm fluorescent gold NPs have been prepared using pamoic acid (PA) (structure 1 Fig. 1) as a reductant and stabilizer [98, 99]. Disodium salt pamoic acid (Na₂PA) provided monodisperse tin-doped indium oxide (ITO) NPs by acting as an organic additive and dehydrating agent [100]. The chemical structure of PA may facilitate the preparation of monodisperse NPs. PA includes two 3-hydroxy-2-naphthoic acid units bridged at the 1-position by a methylene (-CH₂-) group, as shown in structure 1(Fig 1). PA has been used for salt formation in pharmaceutical formulations [101], and PA and its monomer, 3-hydroxy-2-naphthoic acid, act as ligands in transition metal complexes[102-108] ; however, no studies have described the use of PA or its disodium salt as a complexing

agent for the thermal preparation of monodisperse NiONPs. We attempted to use Na₂PA in a simple thermal preparation of NiONPs for use as electrocatalysts in water oxidation. It should be noted that electrochemical water oxidation is important in renewable energy applications that convert solar energy into a usable fuel.

An electrocatalyst's cost, quality, and performance during water electrooxidation depend significantly on the substrate electrode. Glassy carbon electrodes (GCEs) are widely used to test electrocatalysts in a variety of electrochemical applications; however, they have a low surface area compared to porous electrodes, which limits the extent to which their surface modification can produce an efficient nanoelectrocatalyst. Moreover, the high cost of GCEs limits their applicability to the energy sector. Use of interconnected micro-nanostructured carbon is advantageous in that electrocatalysts are readily captured by the micro-nanostructured pores or adsorbed onto the side walls of the pores. Recently, scientists have pyrolyzed normal filter paper, a cheap source of carbon, to obtain highly conductive, low-cost, interconnected, micro-nanostructured carbon electrodes for a variety of electrochemical applications [109, 110]. The use of a filter paper derived carbon electrode (FPCE) as a base electrode is, therefore, quite reasonable.

Here, we report a simple preparation of relatively small monodisperse NiONPs via thermal decomposition of a Ni complex obtained by reacting Ni(NO₃)₂·6H₂O and Na₂PA in ethanol. The influence of Na₂PA was verified by preparing the NiO via the same protocol without adding Na₂PA. Field emission scanning electron microscopy (FESEM) images revealed that the NiONPs prepared in the presence of Na₂PA were smaller and monodisperse compared to those prepared without Na₂PA. The prepared NPs were characterized using X-ray diffraction (XRD) spectroscopy, X-ray photoelectron

spectroscopy (XPS), and transmission electron microscopy (TEM). The electrocatalytic properties of the NPs toward water electrooxidation in an alkaline medium were evaluated upon immobilization on the FPCE

2.2 Nano-Co₃O₄

Nano-Co₃O₄ has been recently attracting the attention of scientists due to its high stability, its anomalous chemical, electrochemical, electronic, magnetic and catalytic properties, and the relatively high abundance of cobalt in the earth. [111-125] Nano-Co₃O₄ have been used in various technological areas and applications such as electrochemical sensors, [118-120] electrochromic windows,[121] gas sensors,[122] batteries,[123] capacitors,[111, 113] solar cells,[124, 125] fuel cells,[126] electrochemical water splitting [117] and catalysis [112, 114, 124]. Due to its widespread application, several methods have been developed to prepare various types, including various sizes and shapes, of nano-Co₃O₄[111-113],[116-121],[123-146] Even though many efforts have been expended to prepare nano-Co₃O₄, the development of novel methods to prepare Co₃O₄ using simple processes and at low cost remain a topic of interest. Of the above-mentioned preparation methods, thermal decomposition is particularly advantageous in yielding phase-pure nano-Co₃O₄ and for its easy scale-up. Generally, the thermal decomposition method, when used for producing nano-Co₃O₄, requires a suitable cobalt precursor such as cobalt oxalate, [129] cobalt(II)-tartrate complex, [130] cobalt citrate, [131] cobalt ethylene glycol carboxylates, [132] N-N-bis(salicylaldehyde)-1,2-phenylenediimino cobalt(II), [133] [bis(salicylaldehydeato)cobalt(II)] ,[134] [bis(salicylaldehyde)ethylenediiminecobalt(II)],

[135] cobalt in complex with plant extract, [136] cobalt hydroxyl carbonates,[137] pentamminecobalt(III) complex,[138] hexamminecobalt(III) nitrate complex,[139] cobalt bis (4-pyridine carboxylate) tetrahydrate,[141] $\text{Co}(\text{cinnamate})_2(\text{N}_2\text{H}_4)_2$,[142] $\text{Co}_3[\text{Co}(\text{CN})_6]_2$,[143] cobalt hydroxide,[144] or a Co-based metal organic framework.[145] But these precursors themselves need to be prepared with tedious reactions between common simple inorganic salts like $\text{CoCl}_2 \cdot 6\text{H}_2\text{O}$ or $\text{Co}(\text{NO}_3)_2 \cdot 6\text{H}_2\text{O}$ and organic or inorganic molecules in solvents, and carrying out these reactions is time consuming and increases the overall cost of the final nano- Co_3O_4 products. Also note that, solvothermally prepared amorphous CoO_x from $\text{Co}(\text{NO}_3)_2 \cdot 6\text{H}_2\text{O}$ can be converted to Co_3O_4 upon thermal decomposition at various temperatures.[146] In addition, Yan et al. reported the preparation of nano- Co_3O_4 by a thermal decomposition of $\text{Co}(\text{NO}_3)_2 \cdot 6\text{H}_2\text{O}$ -loaded g- C_3N_4 , which was prepared by the mixing of $\text{Co}(\text{NO}_3)_2 \cdot 6\text{H}_2\text{O}$ and g- C_3N_4 in ethanol under stirring followed by the evaporation of the ethanol.[107] Clearly, it would be advantageous in terms simplicity, rapidity, and expense to be able to prepare pure nano- Co_3O_4 by a direct thermal decomposition of an inexpensive, simple and widely available cobalt inorganic precursor such as $\text{Co}(\text{NO}_3)_2 \cdot 6\text{H}_2\text{O}$ or $\text{CoCl}_2 \cdot 6\text{H}_2\text{O}$ without any type of pre-reaction or processing. Though it has been reported that $\text{Co}(\text{NO}_3)_2 \cdot 6\text{H}_2\text{O}$ can be decomposed to cobalt oxide,^[147] there has been no report of the preparation of pure nano- Co_3O_4 by a direct thermal decomposition of $\text{Co}(\text{NO}_3)_2 \cdot 6\text{H}_2\text{O}$ without any preprocessing or pre-reaction.

In this communication, we report a very simply preparation of nano- Co_3O_4 involving the direct thermal decomposition of $\text{Co}(\text{NO}_3)_2 \cdot 6\text{H}_2\text{O}$ at 520 °C in a normal aerial atmosphere. The prepared nanostructured materials were characterized by acquiring from

them field emission scanning electron microscopy (FESEM) and transmission electron microscopy (TEM) images and X-ray diffraction (XRD) data. The electrocatalytic properties of the prepared nano-Co₃O₄ toward water electrooxidation in alkaline medium were also evaluated, and done so by immobilizing them on a filter-paper-derived carbon electrode (FPCE) prepared by pyrolysis of normal filter paper

CHAPTER 3

INFLUENCE OF PAMOIC ACID AS A COMPLEXING

AGENT IN THE THERMAL PREPARATION OF NiO

NANOPARTICLES: APPLICATION TO

ELECTROCHEMICAL WATER OXIDATION

We developed a thermal decomposition method for preparing NiO nanoparticles (NiONPs) using disodium salt of pamoic acid (Na_2PA) as a complexing agent and $\text{Ni}(\text{NO}_3)_2 \cdot 6\text{H}_2\text{O}$ as a nickel precursor. Prior to thermal decomposition, a nickel precursor, $\text{Ni}(\text{NO}_3)_2 \cdot 6\text{H}_2\text{O}$, was mixed with Na_2PA in ethanol, and the ethanol was evaporated to obtain the dried reaction mass. The dried reaction mass was characterized using Fourier transform infrared spectroscopy, X-ray photoelectron spectroscopy, and thermal gravimetric analysis. Thermal decomposition was then performed in air to obtain the NiONPs. The role of Na_2PA in the synthesis of NiONP was evaluated by preparing the NiONPs according to the protocol described above without the addition of Na_2PA . The X-ray diffraction data indicated that crystalline NiO (bunsenite, cubic crystal system) formed with or without Na_2PA ; however, field emission scanning electron microscopy images showed that smaller monodisperse NiONPs formed only with the addition of

Na₂PA. Without Na₂PA, the obtained NPs were quite large and polydisperse. The sizes of the NiONPs prepared in the presence of Na₂PA were determined using transmission electron microscopy imaging to be 19.1 ± 3.2 nm. The crystallinity of the NiONPs prepared with Na₂PA was further confirmed using high-resolution transmission electron microscopy and the corresponding selected area diffraction patterns. The electrocatalytic activity of the NiONPs toward water oxidation under alkaline conditions was evaluated by immobilizing the NPs onto an in-house prepared filter paper derived carbon electrode, and compared.

3.1 Introduction

Over the past two decades, bulk and nanoscale nickel oxide (NiO) have attracted attention for their high stability [64-71], nontoxicity [67, 69], and anomalous chemical [71-74], electrochemical [54, 67-70, 75-81], electronic [65, 80, 82, 83], magnetic [64, 71, 84], catalytic [64, 85, 86] and optical [72, 75, 83, 86] properties. NiO nanoparticles (NiONPs), in particular, are used in a variety of fields as optochemical sensors [72], electrochemical sensors [77], biosensors [68, 69, 78, 79], electrochromic windows [75], gas sensors [73, 74], batteries [67], fuel cells [70, 78], photovoltaic cell [80], electrochemical water splitting [54, 81], catalysis [64, 66, 71], and photocatalysis [86]. The broad applicability of nanoscale NiO relies on the material's high surface area and interesting properties, including chemical, electrochemical, and catalytic properties, which are not present in the bulk material. To meet the high demand for this nanoscale material, several synthetic methods have been developed based on hydrothermal [68, 71, 73, 76-78, 87, 88], sol-gel [66, 82, 84], hot-injection [75], co-precipitation [69],

microwave [64, 67] , electrochemical [74] , pulsed laser ablation [89] and thermal decomposition techniques [72, 86, 90] , as well as techniques based on complex formation with an organic moieties and successively their thermal decomposition[85, 91-96]. Among the mentioned methods, the latest one is well known as scalable with high yield. To prepare NiONPs, thermal decomposition of nickel octanoate [91], aqua(2,9-dimethyl-1,10-phenanthroline)NiCl₂ complex [148], nickel oxalate [93, 96], dinuclear nickel(II) Schiff base complex [94] and nickel acetate [95] are reported. However, preparing the NiONPs by thermal decomposition of organometallic complex needs either numerous steps or surfactants or other toxic chemicals.

So far, nanoscale NiO particles have been prepared to have a variety of sizes and shapes, including nanospheres(NPs)[64, 66, 71, 75, 82, 84, 86, 91, 92, 94, 96] , nanoplates [76, 87] , nanosheets [86, 93] , nanoplatelets [90] , flaked like architectures [68, 93] , nanorings [88], nanoflowers[71, 74] , hollow nanostructures [97] , nanorods[78, 96] , and nanocubes [94, 96]. Numerous studies have examined the preparation of nanoscale NiO, and the development of novel synthetic methods that are simpler and provide smaller or more monodisperse product profiles remains a topic of interest. Small sizes monodisperse nanoparticles (NPs) are valuable because they provide a high surface area and homogeneous properties compared to larger polydisperse NPs samples.

Organic moieties that act as a surfactant, stabilizer, reductant, or ligand play an important role in determining the sizes and shapes of NPs. Recently, monodisperse 10.8 nm florescent gold NPs have been prepared using pamoic acid (PA) (structure 1 Fig. 1) as a reductant and stabilizer [98, 99]. Disodium salt pamoic acid (Na₂PA) provided monodisperse tin-doped indium oxide (ITO) NPs by acting as an organic additive and

dehydrating agent [100]. The chemical structure of PA may facilitate the preparation of monodisperse NPs. PA includes two 3-hydroxy-2-naphthoic acid units bridged at the 1-position by a methylene (-CH₂-) group, as shown in structure 1 (Fig 1). PA has been used for salt formation in pharmaceutical formulations [101], and PA and its monomer, 3-hydroxy-2-naphthoic acid, act as ligands in transition metal complexes [102-108]; however, no studies have described the use of PA or its disodium salt as a complexing agent for the thermal preparation of monodisperse NiONPs. We attempted to use Na₂PA in a simple thermal preparation of NiONPs for use as electrocatalysts in water oxidation. It should be noted that electrochemical water oxidation is important in renewable energy applications that convert solar energy into a usable fuel.

An electrocatalyst's cost, quality, and performance during water electrooxidation depend significantly on the substrate electrode. Glassy carbon electrodes (GCEs), indium tin oxide electrode and fluorine doped tin oxide (FTO) electrode are widely used to test electrocatalysts in a variety of electrochemical applications; however, they have a low surface area compared to porous electrodes, which limits the extent to which their surface modification can produce an efficient nanoelectrocatalyst. Along with the high cost and low surface area of commonly employed base electrodes, the complicated electrode modification method with electrocatalyst limits their applicability to the energy sector. As example, Singh et al. prepared NiONP- or NiO microball-modified FTO electrode for water electrooxidation application [54]. They prepared the NiO film on FTO by screen printing a mixture of NiO particles, ethyl cellulose, and terpineol, and successive sintering at 400 °C for 30 min and at 550 °C for 10 min. For reducing the complexity and cost in electrode modification step, using of numerous chemicals and sintering at high

temperature should be eliminated. Among the developed methods for electrode modification with nanoelectrocatalyst, drop-drying method is identified as simplest and straightforward one. However, aggregation of the nanomaterials on commonly employed bare electrode surface is severe obstacle of the drop-drying method, which reduces the electrocatalytic surface area. Therefore, it could be logical using alternative electrode materials which can reduce the severe aggregation of nanomaterials during immobilization them by drop-drying method. Use of interconnected micro-nanostructured carbon is advantageous in that electrocatalysts are readily captured by the micro-nanostructured pores or adsorbed onto the side walls of the pores. Recently, scientist have pyrolyzed normal filter paper, a cheap source of carbon, to obtain highly conductive, low-cost, interconnected, micro-nanostructured carbon electrodes for a variety of electrochemical applications [109, 110]. The use of a filter paper derived carbon electrode (FPCE) as a base electrode is, therefore, quite reasonable.

Here, we report a simple preparation of relatively small monodisperse NiONPs via thermal decomposition of a Ni complex obtained by reacting $\text{Ni}(\text{NO}_3)_2 \cdot 6\text{H}_2\text{O}$ and Na_2PA in ethanol. The influence of Na_2PA was verified by preparing the NiO via the same protocol without adding Na_2PA . Field emission scanning electron microscopy (FESEM) images revealed that the NiONPs prepared in the presence of Na_2PA were smaller and monodisperse compared to those prepared without Na_2PA . The prepared NPs were characterized using X-ray diffraction (XRD) spectroscopy, X-ray photoelectron spectroscopy (XPS), and transmission electron microscopy (TEM). The electrocatalytic properties of the NPs toward water electrooxidation in an alkaline medium were evaluated upon immobilization on the FPCE

3.2 Experimental

3.2.1 Materials

Nickel(II) nitrate hexahydrate ($\text{Ni}(\text{NO}_3)_2 \cdot 6\text{H}_2\text{O}$) was supplied by Merck. Pamoic acid disodium salt (Na_2PA), sodium hydroxide (NaOH) and filter papers were obtained from Sigma-Aldrich. Ethanol was purchased from Hayman Ltd., Eastways Park, UK. Copper tape (one-sided adhesive) and Scotch 898 premium-grade Filament Tape (one-sided adhesive) were obtained from 3M, United States.

3.2.2 Preparation of the FPCE

Initially, the filter papers were cut into pieces, 2 cm x 2 cm. The cut pieces were loaded onto a flat alumina crucible. The crucible was then transferred to the middle of the alumina tube in a tubular furnace. Both sides of the tube were locked, and the system was flushed with copious amounts of nitrogen (N_2) gas for five minutes to create an inert environment. We next purged the system with N_2 , drop by drop, and heated the system at a rate of $10^\circ\text{C}/\text{minute}$ until a temperature of 850°C was reached. After incubation at 850°C for 5 hr, the sample was cooled at a rate of $5^\circ\text{C}/\text{min}$ until reaching room temperature (RT). Finally the prepared FPCE was removed from the furnace. A useable working electrode was crafted by attaching one side of the prepared FPCE to the conducting copper tape and covering the FPCE with Scotch tape, leaving a 0.2 cm^2 area (working electrode area) and the end of the copper tape uncovered to allow connection to

a potentiostat (see reference Aziz et al. 2017 for details). The usable FPCE is illustrated in Fig. 2.

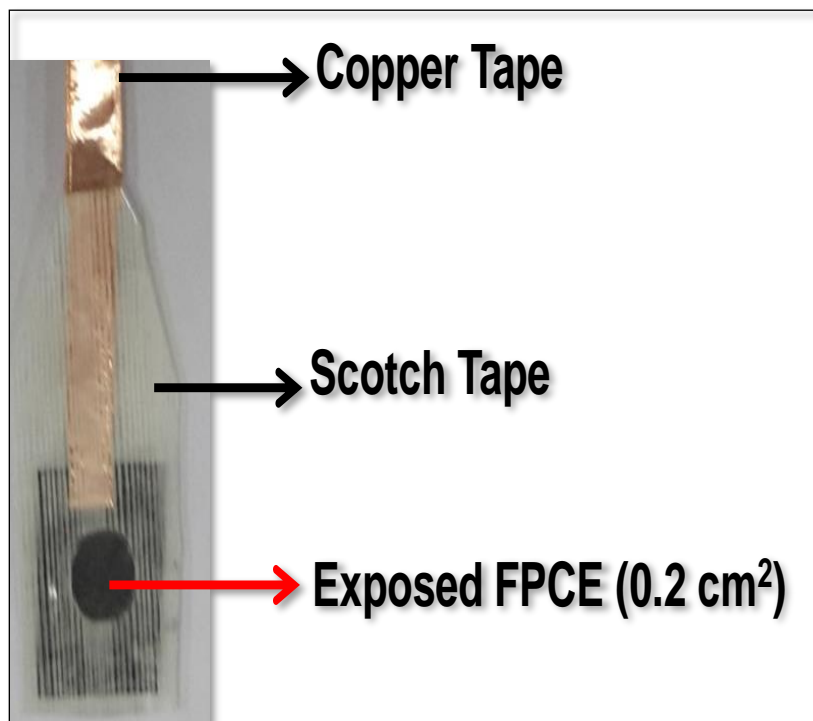


Figure 2: Photograph of the used FPCE.

3.2.3 Preparation of NiO NPs and the NiO NPs-Modified FPCE

Initially, we added 400 mg $\text{Ni}(\text{NO}_3)_2 \cdot 6\text{H}_2\text{O}$ to a glass beaker containing 50 mL ethanol, and successively sonicated the mixture for 10 minutes. We then added 350 mg of the Na_2PA to the reaction mass and sonicated for another 30 minutes. The beaker containing the reaction mass was transferred to a hot-plate and heated the sample at 65°C with stirring (300 rpm) to evaporate the ethanol. The obtained mass was dried overnight in an oven at 40°C . The dried mass was transferred to an alumina crucible and placed in the glass tube

of a tubular furnace. The position of the crucible in the middle of the tubular furnace was confirmed. We next heated the furnace under atmospheric conditions at 10°C/min until reaching 520°C, unless mentioned otherwise. This temperature was maintained for three hours, after which the sample was cooled at a rate of 5°C/min until reaching RT. Finally, we collected the NiONPs. Separately, NiONPs were prepared according to the same protocol without adding Na₂PA.

The NiONP prepared with Na₂PA were dispersed to a concentration of 1 mg/mL in water via ultrasonication. Thirty microliters of the dispersed of NiONPs were dropped onto the working electrode area of the FPCE (the exposed FPCE area shown in Fig. 1) and the assembly was dried at RT to obtain a NiONP-modified FPCE. Similarly, we prepared a NiONP-modified FPCE using the NiONPs prepared without Na₂PA.

3.3 Instrumentation

Electrochemical data were obtained using a CHI (760E) electrochemical workstation. The prepared bare FPCE and NiONP-modified FPCE were used as the working electrodes. A Pt wire and Ag/AgCl served as counter and reference electrodes, respectively. All electrochemical experiments were carried out at room temperature without deaeration. Fourier transform infrared spectra (FTIR) were recorded using a Nicolet 6700 spectrometer, Thermo Scientific, USA. TGA-DSC analysis was carried out using a Netzsch STA (Model STA 449 F3). FESEM images were recorded using a field emission scanning electron microscope (TESCAN LYRA 3, Czech Republic). TEM images were recorded using a high-resolution transmission electron microscope (HRTEM) (JEM-2011, Jeol Corp.) equipped with CCD camera 4k x 4k (Ultra Scan

400SP, gatan cop.). An XPS equipped with an Al-K α microfocusing X-ray monochromator (ESCALAB 250Xi XPS Microprobe, Thermo Scientific, USA) was used for the chemical analysis. X-ray diffraction patterns (XRD) of the NiONPs were obtained using a high-resolution Rigaku Ultima IV diffractometer equipped with Cu-K α radiation.

3.4 Results and discussion.

3.4.1 Interaction between the Na₂PA and Ni(NO₃)₂·6H₂O

Initially, Na₂PA and Ni(NO₃)₂·6H₂O were mixed in ethanol. The ethanol was evaporated away with heating. The interaction between Ni²⁺ and Na₂PA was explored using FTIR (Fig. 4A) and XPS (4B) analysis of the dried mass. The IR spectrum revealed characteristic peaks at 3610, 3410, 3060, 2940, 1640, 1580, 1520, 1460, 1400, 1360, 1240, 1200, and 820 cm⁻¹. The peaks at 3610, 3410, 3060, and 2940 cm⁻¹ indicated the presence of aromatic –OH groups, coordinated H₂O, aromatic H-C, and H-CH- functional groups, respectively. The peaks at 1640 and 1360 cm⁻¹ were attributed to ν_{as} (COO⁻) and ν_s (COO⁻), respectively. The $\Delta(\nu_{as} - \nu_s)$ value of 280 cm⁻¹ was assigned to the bis-monodentate chelation mode of carboxylate group to Ni, as shown in structure-2 [105]. These findings confirmed complex formation with the Ni transitional metal.

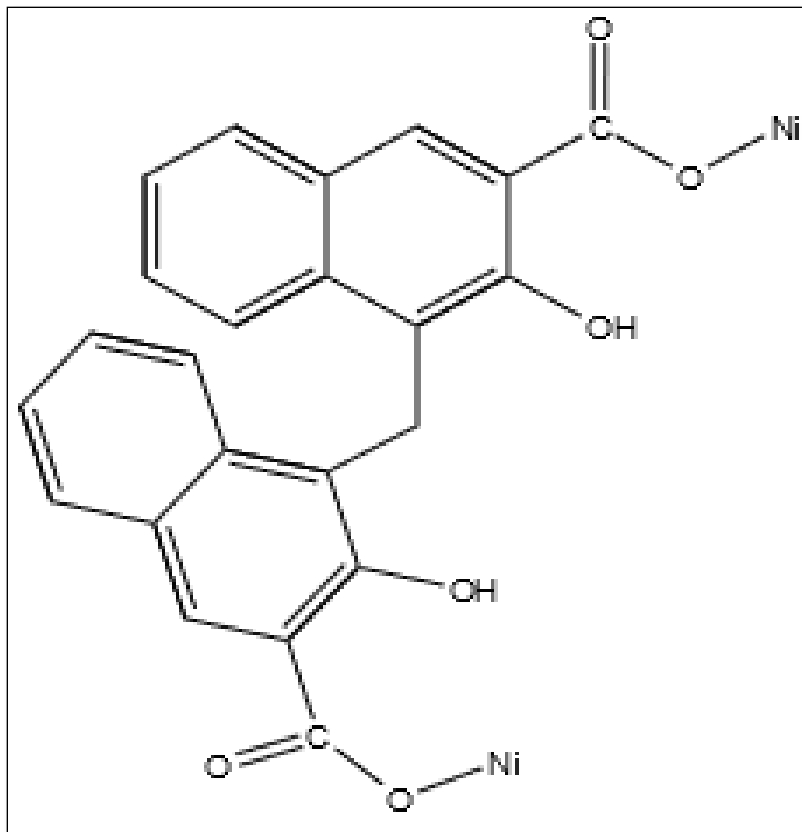


Figure 3: Structure-2 Plausible structure of the complex formed in the interaction with Ni(NO₃)₂ and Na₂PA.

The formation of the Ni-O bond was further confirmed by recording the XPS of the dried mass. The XPS spectrum revealed the binding energy peak positions at 856.0, 860.3, 873.5, and 879.4 eV, assigned to the Ni2p_{3/2}, Ni2p_{3/2(sat)}, Ni2p_{1/2}, Ni2p_{1/2(sat)} binding energies, which were comparable to the binding energies of Ni(acetate)₂·4H₂O and NiO [149-152]. That is, a Ni-O bond was present in the complex. A plausible structure of the complex is illustrated as structure-2(Fig. 3). The dried mass prepared by mixing Na₂PA and Ni(NO₃)₂·6H₂O was denoted the Ni-PA complex.

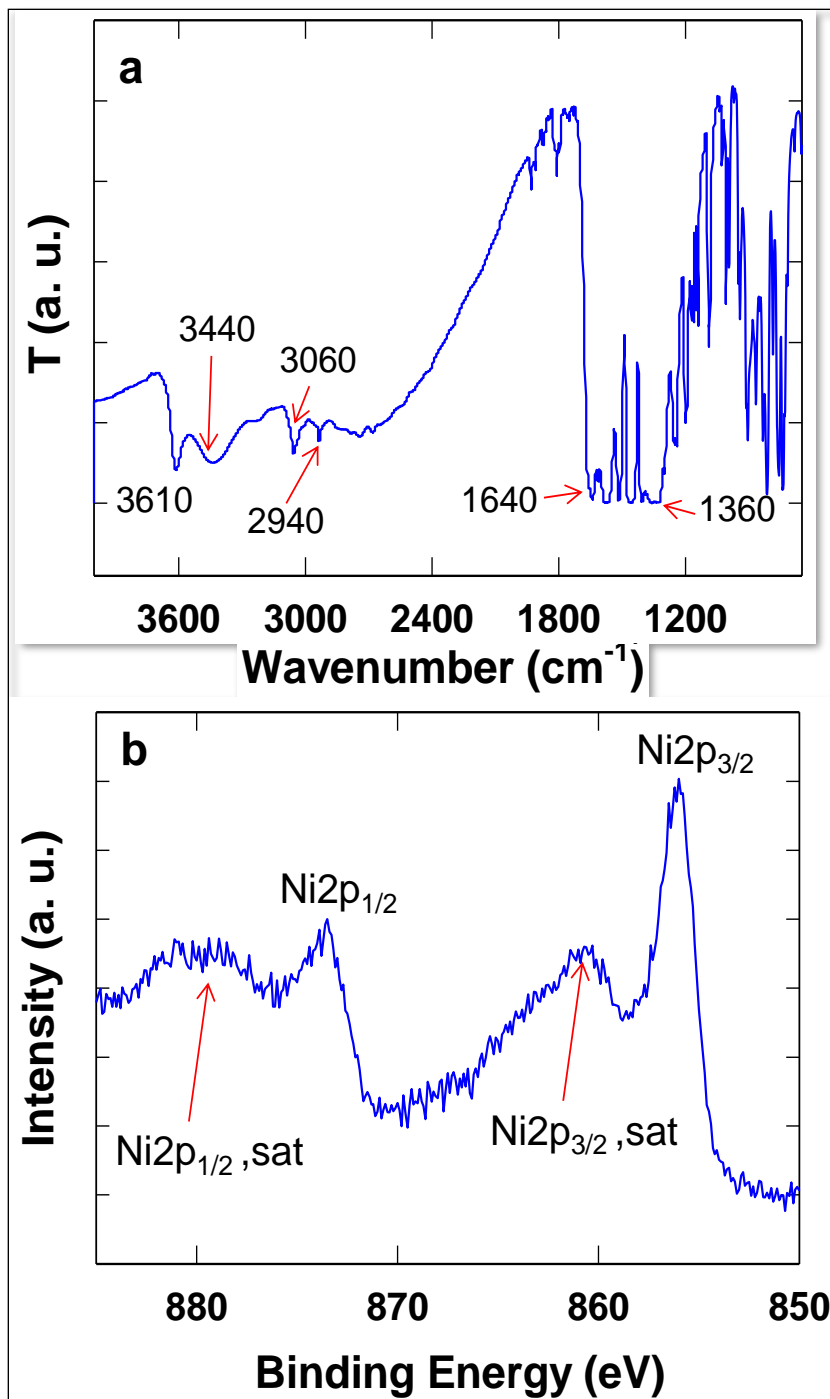


Figure 4: (A) FT-IR spectrum, and (B) XPS spectrum of the resultant dried reaction mass obtained after mixing Na₂PA and Ni(NO₃)₂·6H₂O in ethanol, followed by evaporation of the ethanol with heating.

3.4.2 TGA Analysis of the Ni-PA Complex.

Prior to the thermal decomposition of the of Ni-PA complex for NiO preparation, TGA analysis were performed to optimize the decomposition temperature. Slow weight losses were observed with increasing temperature up to 300°C (Fig. 5). This weight loss was attributed to the elimination of loosely bound solvent molecules, crystalline water, and the decomposition of some fraction of Na₂PA. Significant sharp weight losses observed in the range 300–420°C were attributed to the decomposition of the remaining parts of the Na₂PA and NO₃²⁻ structures. At temperatures exceeding 420°C, the weight remained nearly constant. The total weight loss at 420°C was ~25%. These findings indicated that the complete conversion of Ni-PA to NiO occurred at temperatures of 420°C and above. As a result, a temperature $\geq 420^\circ\text{C}$ were chosen for the thermal decomposition of the Ni-PA complex to prepare the NiONPs.

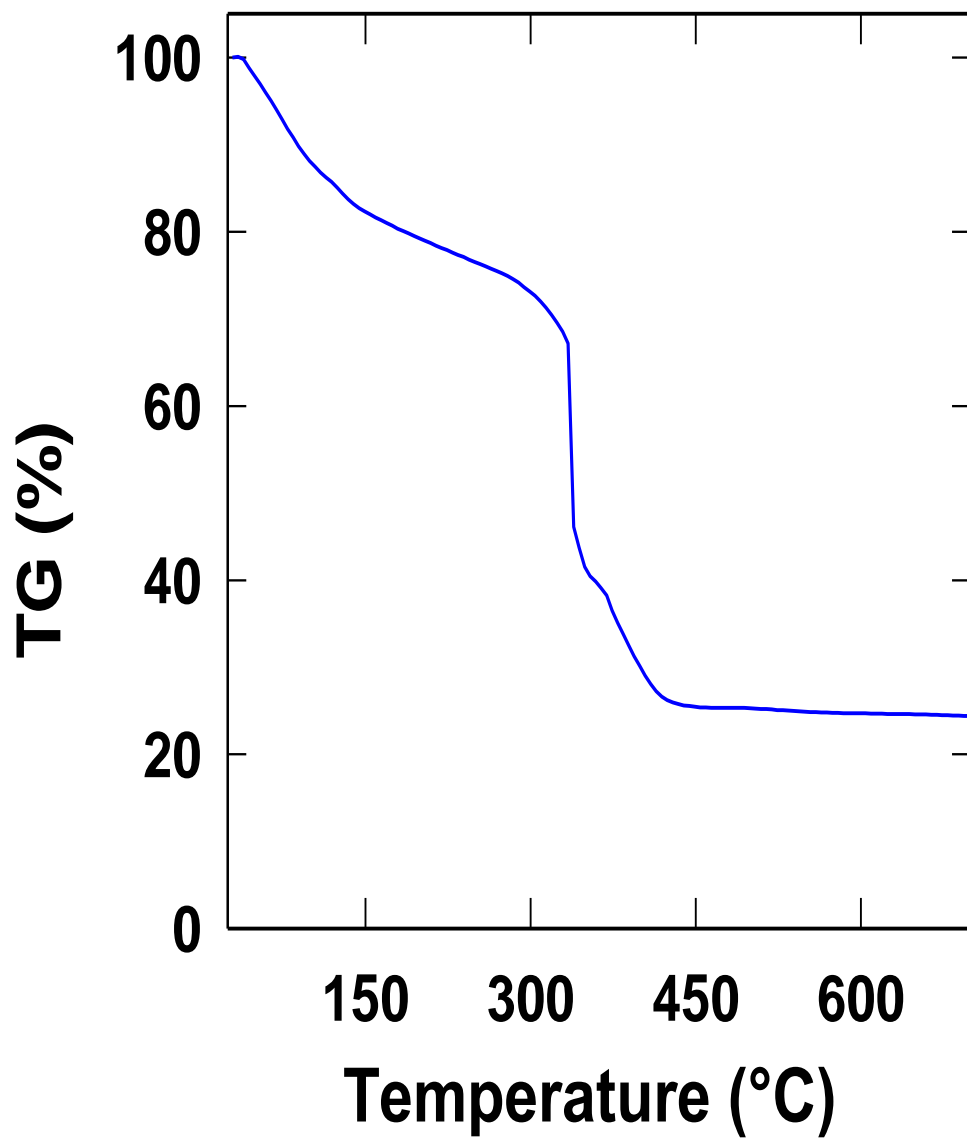


Figure 5: TGA curves of the resultant Ni-PA complex

3.4.3 Effect of the Extent of Heat Treatment on the Crystallinity of the NiONPs

The TGA analysis revealed that NiO formed upon decomposition of the Ni-PA complex at temperatures greater than or equal to 420°C; therefore, we heated the Ni-PA complex at a low temperature, 420°C, in air for three hours. After cooling, the product was subjected to XRD analysis. Figure 6a shows that the major peaks occurred at 2θ values of 37.25, 43.40, 62.20, 75.52, and 79.56°, corresponding to the 111, 200, 220, 311, and 322 crystal planes, indicating the formation of cubic NiO (bunsenite, NaCl-type structure) (JPCDS card No. 01-071-1179). As the heat treatment temperature was increased, the intensities of the peaks increased without changing the pattern; that is, the crystallinity and phase purity of the NiO increased with the extent of heat treatment within the temperature zone tested (Fig. 5a-c). By considering the extent of temperature and crystallinity, 520°C were chosen to form NiO in all subsequent experiments.

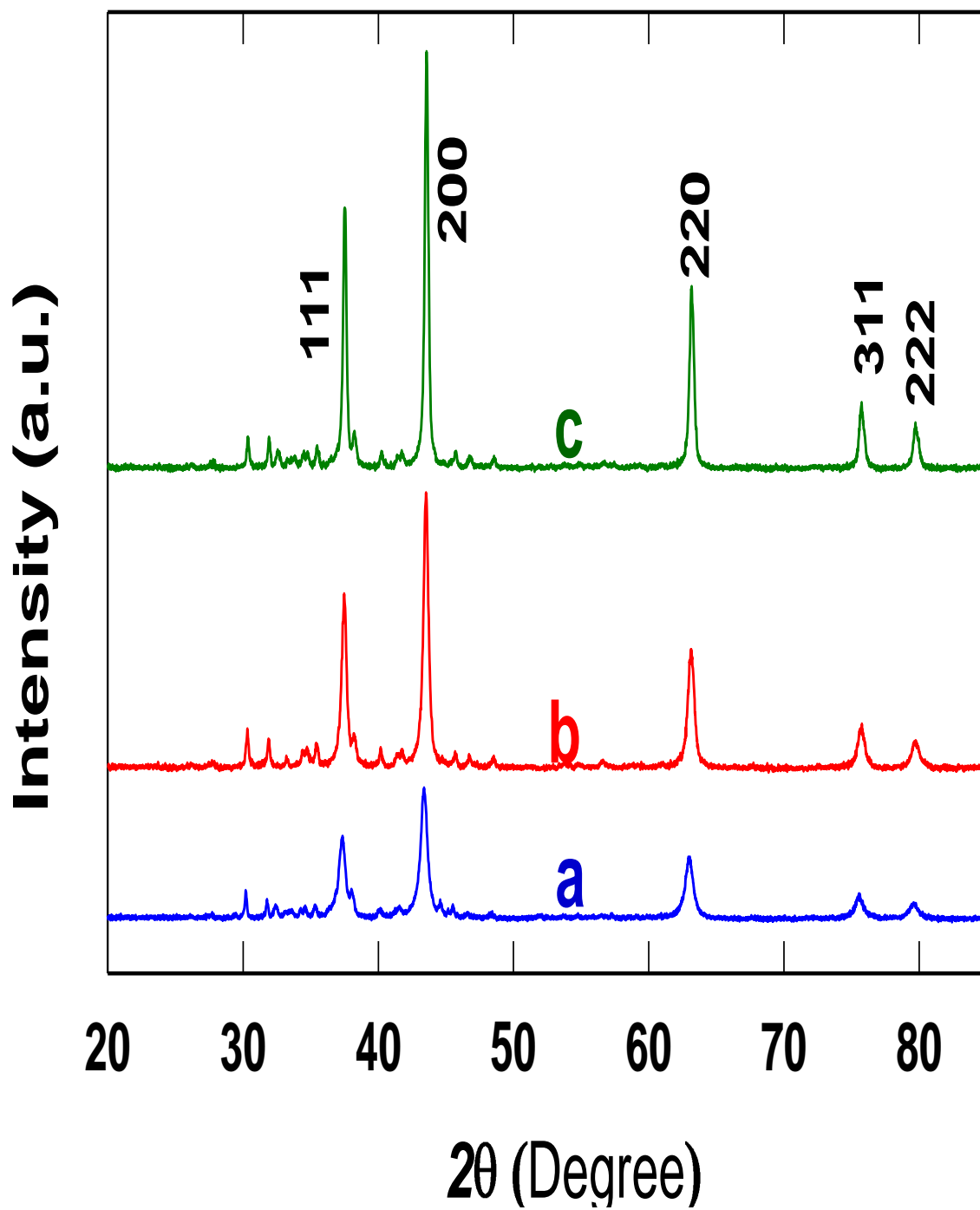


Figure 6: XRD patterns of NiO prepared by thermal decomposition of the Ni-PA complex at different temperatures: (a) 420°C, (b) 520°C, and (c) 620°C.

3.4.4 Morphological Characterization of the NiONPs Prepared at 520°C

Figure 7a shows an FESEM image of the NiO prepared using Na₂PA, and Fig. 7b shows a magnified view of Fig. 7a. These images show that the particles were nearly monodisperse NPs. The NiONP size was determined from the TEM images, discussed below. The effect of using Na₂PA was verified by following the fabrication protocol without adding Na₂PA. The solvent, ethanol, could form a complex and generate NiONPs upon thermal combustion with the divalent nickel salt in the absence of a ligand. Figure 7c shows an FESEM image of the NiO prepared without using Na₂PA. Figure 7d shows a magnified view of Fig. 7c. FESEM images revealed that the NiONPs formed without Na₂PA were much larger (Figs. 7c and 7d) than the NiONPs obtained in the presence of Na₂PA (Figs. 7a and 7b). It should be noted that the NiONPs formed without Na₂PA were polydisperse in terms of both shape and size. The phase of the NiONP prepared without using Na₂PA was confirmed by XRD experiments (data not shown). The XRD data revealed that the NiONPs prepared without Na₂PA were more crystalline than those prepared with Na₂PA. Although large polydisperse NiONPs (spherical, cubic, pentagonal shapes; 23–284 nm in size) were obtained without using Na₂PA, this approach provides a clue for a simple and cheap route to the formation of size- and shape-controlled metal oxide NPs. Optimization and the selection of the metal precursor could increase the monodispersity of the metal oxide NPs prepared using ethanol.

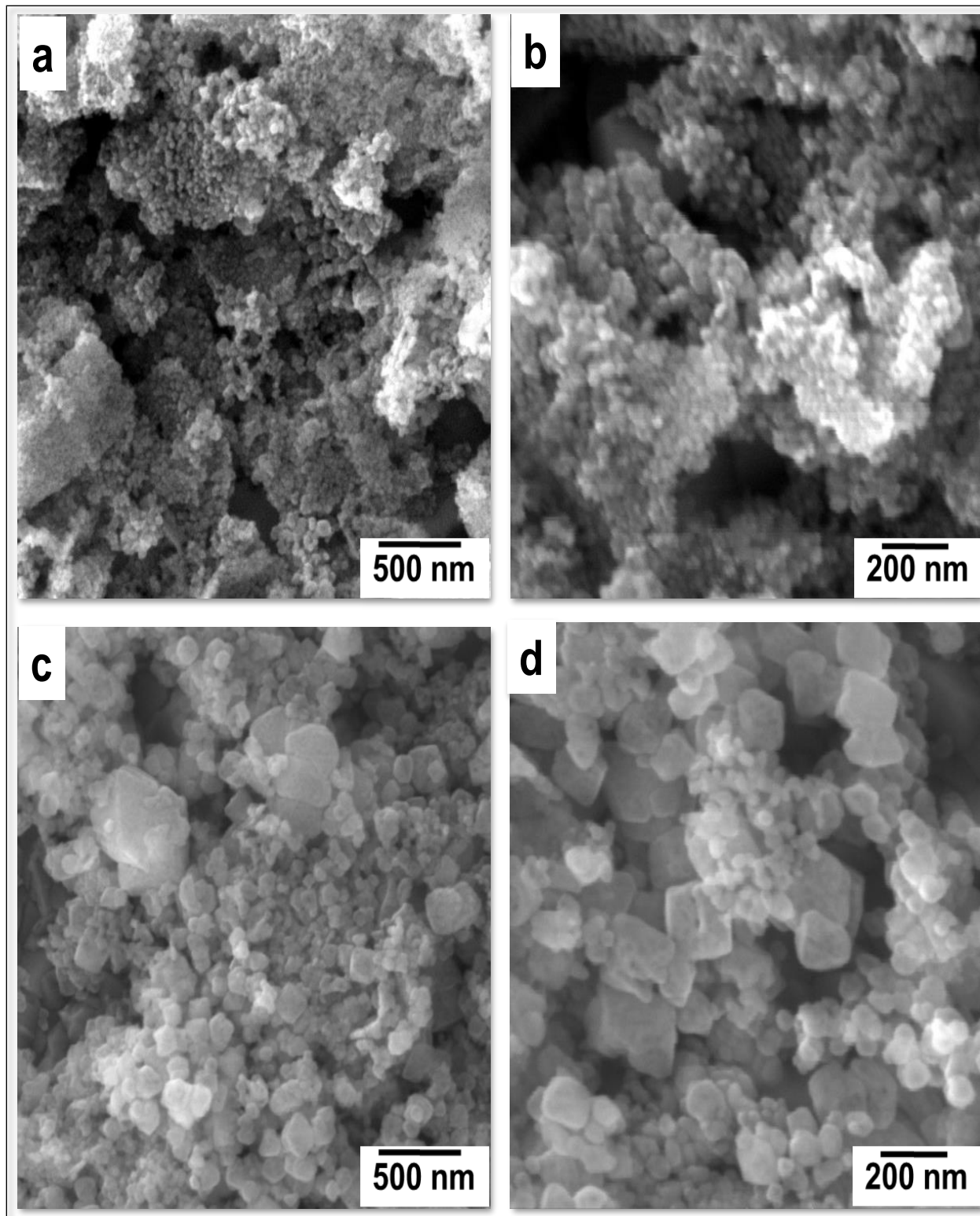


Figure 7: SEM images of NiO prepared by the thermal decomposition of a Ni-PA complex formed in the presence (a, b) or absence (c, d) of Na₂PA at 520°C.

The NP size could be estimated from the FESEM images shown in Figs. 7a and 7b. TEM images (Fig. 8a) permitted more precise particle size measurements. The average NiONP particle size prepared with Na₂PA, calculated from the TEM images, was 19.1 ± 3.2 nm. Figures 8b and 8c show, respectively, HRTEM images and selected area diffraction patterns (SAED) of the NiONPs prepared with Na₂PA. The interplanar distance was determined to be 0.2173 nm (Fig. 8b), which was close to the interplanar spacing (0.21 nm) measured over 200 planes of NiO (bunsenite) (Kwon et al. 2016). The SAED data also revealed higher-order crystallinity that was correlated with the XRD data (Fig. 5b).

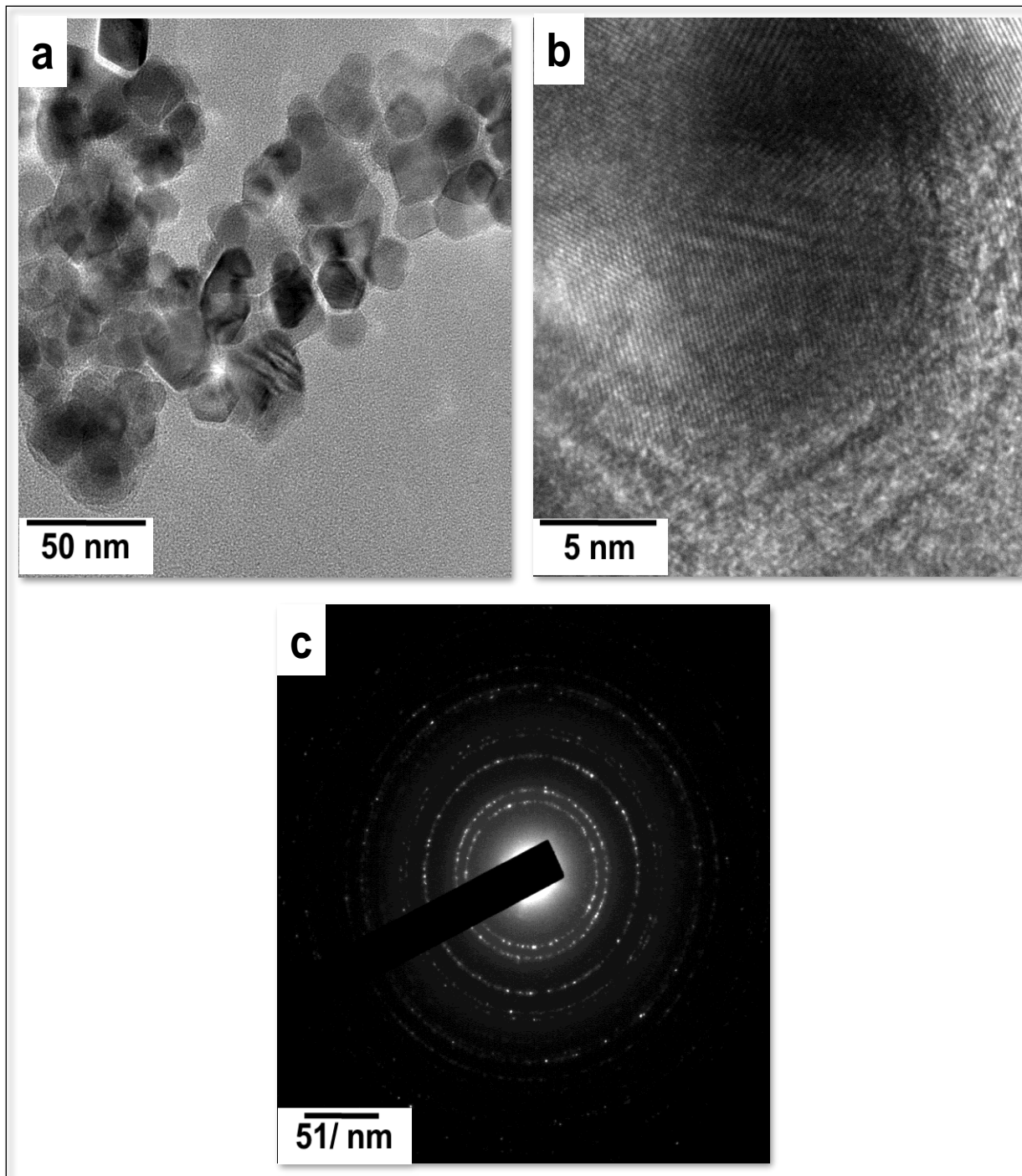


Figure 8: TEM image (a), HRTEM (b), and SAED (c) data collected from NiONPs prepared by thermal decomposition of a Ni-PA complex at 520°C.

3.4.5 Morphological Characterization of the NiONPs-Modified FPCE

We used FPCE as a substrate electrode rather than the commonly employed GCE because FPCE constitutes an interconnected micro-nanostructured carbon form with a high electroactive surface area (ECSA), as confirmed by FESEM images and surface area calculations by cyclic voltammetry techniques (data not shown). The characterization of the FPCE will be reported in detail elsewhere. The distribution of NiONPs on the FPCE surfaces was examined using FESEM imaging at low magnifications (Fig. 9) as the sizes of the synthesized NiONPs were described in details above. Figures 9a and 9b show FESEM images of the FPCE modified with NiONPs prepared with Na₂PA, and Figs. 9c and 9d show FESEM images of the FPCE modified with NiONPs prepared without Na₂PA. The white grains indicate NiONPs, and the background corresponds to the FPCE. The FESEM images revealed that both types of NiONPs were distributed as small cluster. Interestingly, the small clusters were distributed homogeneously across the surface (they did not aggregate as big cluster in certain areas). The big cluster formation of NPs in certain areas on a bare solid substrate during immobilization via drop-drying methods is very common and prohibits use of this method in many applications [100, 153, 154] . The homogenous distribution of NiONPs (as small cluster) on the FPCE may have resulted from the presence of the micro-nanostructured cavities on the FPCE. These cavities may have hindered NP to form big cluster during drying.

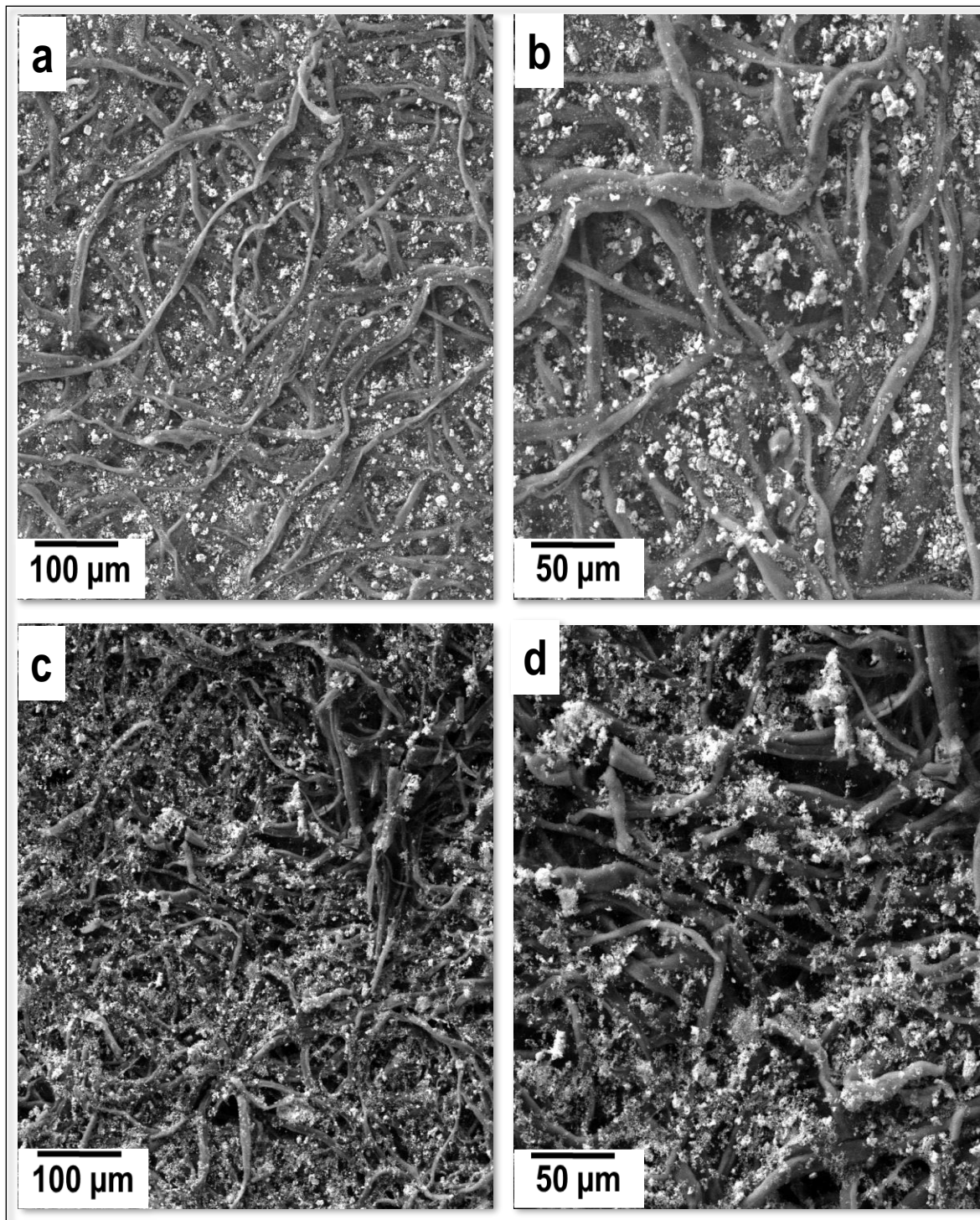


Figure 9: FESEM images of a FPCE modified with NiONPs prepared (a) with Na₂PA and (c) without Na₂PA. (b) and (d) show magnified views of (a) and (c), respectively.

3.4.6 Electrocatalytic Activities of NIO NPs Toward Water Oxidation in an Alkaline Medium

Figures 13a–13c show linear sweep voltammograms (LSVs) of the bare FPCE and the FPCEs modified with NiONPs prepared with or without Na₂PA. The three CVs reveal that the electrocatalytic activities toward water oxidation increased upon immobilization of NiONPs onto FPCE to a different extent, depending on whether the NiONPs were prepared with or without Na₂PA. The FPCE modified with NiONPs prepared with Na₂PA showed a higher electrooxidation current compared to that measured at the FPCE modified with NiONPs prepared without Na₂PA. The water electrooxidation current densities at 1.5 V were 8.80, 30.81 and 24.98 mAcm⁻¹ for the bare FPCE, FPCE modified with NiONPs prepared with Na₂PA, and FPCE modified with NiONPs prepared without Na₂PA, respectively. It should be noted that both modified FPCEs showed the same water electrooxidation potential, 0.5 V, which was 400 mV lower than the water electrooxidation potential of bare FPCE, 0.9 V. The higher electrocatalytic activity of the NiONP(with Na₂PA)-FPCE was expected because the NiONPs prepared with Na₂PA were smaller than those prepared without Na₂PA.

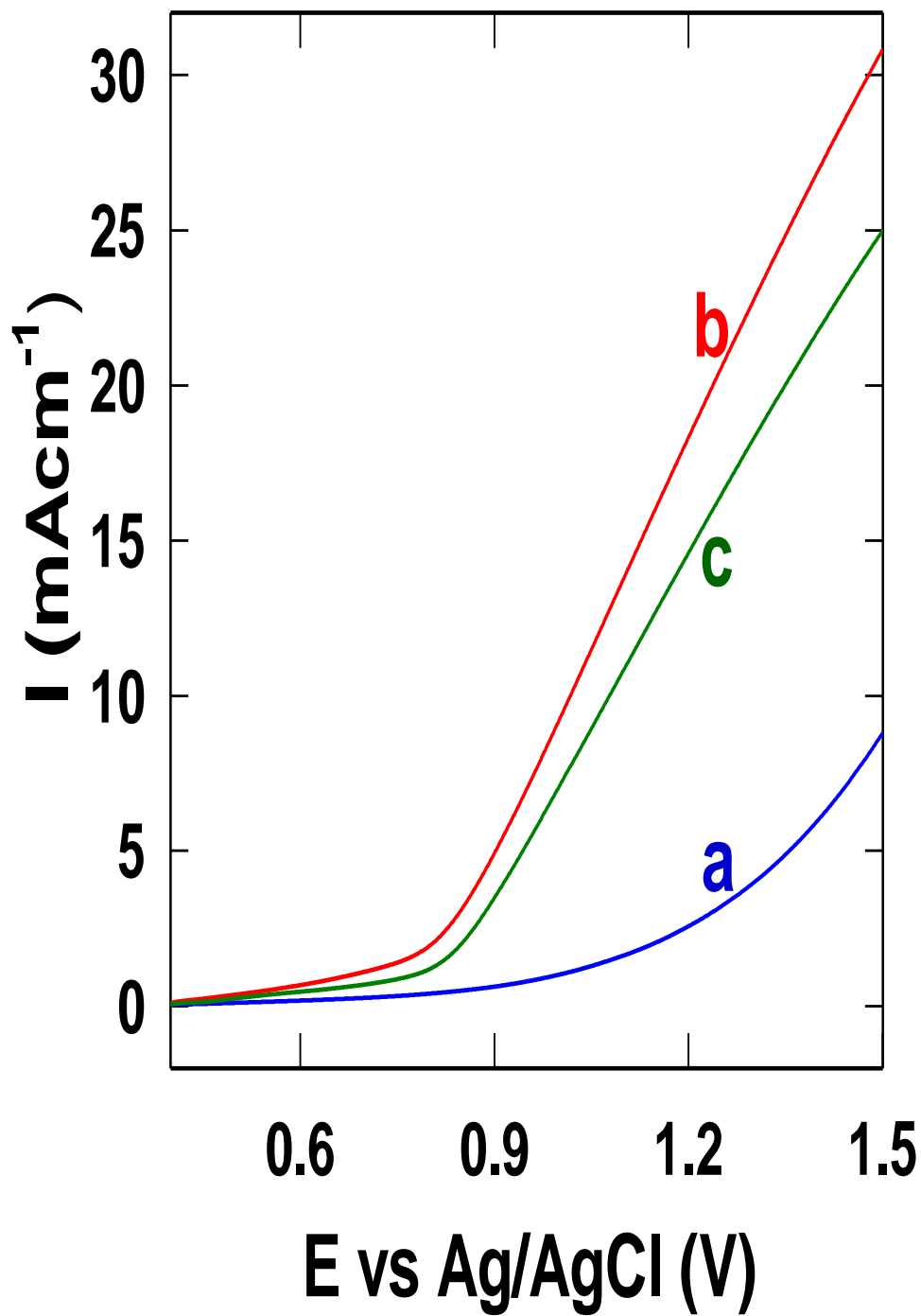


Figure 10: Linear sweep voltammogram of (a) the FPCE, and an FPCE modified with NiONPs prepared (b) with and (c) without Na₂PA, in 0.1 NaOH (aq). Scan rate: 100 mVs⁻¹.

3.5 Conclusions

In summary, we developed a thermal decomposition method for preparing monodisperse NiONPs using $\text{Ni}(\text{NO}_3)_2 \cdot 6\text{H}_2\text{O}$ as a nickel precursor and Na_2PA as a complexing agent. We also verified the influence of Na_2PA by preparing nanoparticles using a common procedure conducted with or without Na_2PA addition. The NiONPs prepared without Na_2PA were highly polydisperse. The average NP size was much larger than that obtained with the addition of Na_2PA . The electrocatalytic activities of both NiONPs toward electrooxidation in an alkaline medium were evaluated after immobilization on an FPCE using a simple drop-drying method. The NiONP(with Na_2PA)-FPCE showed a much higher electrocatalytic activity toward water electrooxidation than the NiONP(without Na_2PA)-FPCE or bare FPCE. The superior electrocatalytic properties of the NiONP(with Na_2PA)-FPCE were expected because these NPs were small and monodisperse. The monodisperse small NPs described here could play an important role in catalysis, electronics, optoelectrical device, and electrochemical applications, including electrochemical sensors, biosensors, gas sensors, batteries, capacitors, solar cells, fuel cells, and water splitting cells.

CHAPTER 4

PREPARATION OF NANO-CO₃O₄ BY DIRECT

THERMAL DECOMPOSITION OF CO(NO₃)₂·6H₂O FOR

ELECTROCHEMICAL WATER OXIDATION

BACKGROUND: Nano-Co₃O₄ has been used in various technological areas and applications such as electrochemical sensors and electrochemical water splitting. Even though many efforts have been expended to prepare nano-Co₃O₄, the development of novel methods to prepare Co₃O₄ using simple processes and at low cost remain a topic of interest. Besides, it could be economic and useful if the synthesized nanoparticle could be applied as efficient electrocatalyst upon its immobilization on a cheap base electrode material by very simple method for various practical applications including renewable energy.

METHOD: We prepared nano-Co₃O₄ by a direct thermal decomposition of an inexpensive, simple and widely available cobalt inorganic precursor such as Co(NO₃)₂·6H₂O without any type of pre-reaction or processing. The nano-Co₃O₄ was immobilized on filter-paper-derived carbon electrode by drop-drying method for applying as electrode materials toward water electrooxidation.

RESULTS: The X-ray diffraction, field emission scanning electron microscopy, and transmission electron microscopy analysis confirmed the formation of short nanorods of

single-phase Co_3O_4 upon thermal decomposition of $\text{Co}(\text{NO}_3)_2 \cdot 6\text{H}_2\text{O}$ at $520\text{ }^\circ\text{C}$. The electrocatalytic properties of the nano- Co_3O_4 were evaluated after immobilizing it on a cheap carbon electrode derived from normal filter paper. The modified electrode showed good electrocatalytic properties toward water oxidation in an alkaline solution.

CONCLUSION: In conclusion, we developed a very simple, straight-forward and economic method for preparation of nano- Co_3O_4 and immobilized it on very cheap carbon electrode for evaluating its electrocatalytic properties. Due to the high electrocatalytic properties, the prepared nano- Co_3O_4 could potentially play an important role in various practical fields.

4.1 Introduction

Nano- Co_3O_4 has been recently attracting the attention of scientists due to its high stability, its anomalous chemical, electrochemical, electronic, magnetic and catalytic properties, and the relatively high abundance of cobalt in the earth. [111-125] Nano- Co_3O_4 have been used in various technological areas and applications such as electrochemical sensors, [118-120] electrochromic windows,[121] gas sensors,[122] batteries,[123] capacitors,[111, 113] solar cells,[124, 125] fuel cells,[126] electrochemical water splitting [117] and catalysis [112, 114, 124]. Due to its widespread application, several methods have been developed to prepare various types, including various sizes and shapes, of nano- Co_3O_4 [111-113],[116-121],[123-146] Even though many efforts have been expended to prepare nano- Co_3O_4 , the development of novel methods to prepare Co_3O_4 using simple processes and at low cost remain a topic of interest. Of the above-mentioned preparation methods, thermal decomposition is

particularly advantageous in yielding phase-pure nano-Co₃O₄ and for its easy scale-up. Generally, the thermal decomposition method, when used for producing nano-Co₃O₄, requires a suitable cobalt precursor such as cobalt oxalate, [129] cobalt(II)-tartrate complex, [130] cobalt citrate, [131] cobalt ethylene glycol carboxylates, [132] N-N-bis(salicylaldehyde)-1,2-phenylenediimino cobalt(II), [133] [bis(salicylaldehydeato)cobalt(II)] , [134] [bis(salicylaldehyde)ethylenediiminecobalt(II)], [135] cobalt in complex with plant extract, [136] cobalt hydroxyl carbonates, [137] pentamminecobalt(III) complex, [138] hexamminecobalt(III) nitrate complex, [139] cobalt bis (4-pyridine carboxylate) tetrahydrate, [141] Co(cinnamate)₂(N₂H₄)₂, [142] Co₃[Co(CN)₆]₂, [143] cobalt hydroxide, [144] or a Co-based metal organic framework. [145] But these precursors themselves need to be prepared with tedious reactions between common simple inorganic salts like CoCl₂·6H₂O or Co(NO₃)₂·6H₂O and organic or inorganic molecules in solvents, and carrying out these reactions is time consuming and increases the overall cost of the final nano-Co₃O₄ products. Also note that, solvothermally prepared amorphous CoO_x from Co(NO₃)₂·6H₂O can be converted to Co₃O₄ upon thermal decomposition at various temperatures. [146] In addition, Yan et al. reported the preparation of nano-Co₃O₄ by a thermal decomposition of Co(NO₃)₂·6H₂O-loaded g-C₃N₄, which was prepared by the mixing of Co(NO₃)₂·6H₂O and g-C₃N₄ in ethanol under stirring followed by the evaporation of the ethanol. [107] Clearly, it would be advantageous in terms simplicity, rapidity, and expense to be able to prepare pure nano-Co₃O₄ by a direct thermal decomposition of an inexpensive, simple and widely available cobalt inorganic precursor such as Co(NO₃)₂·6H₂O or CoCl₂·6H₂O without any type of pre-reaction or processing. Though it has been reported that Co(NO₃)₂·6H₂O can

be decomposed to cobalt oxide,^[147] there has been no report of the preparation of pure nano-Co₃O₄ by a direct thermal decomposition of Co(NO₃)₂·6H₂O without any preprocessing or pre-reaction.

In this communication, we report a very simply preparation of nano-Co₃O₄ involving the direct thermal decomposition of Co(NO₃)₂·6H₂O at 520 °C in a normal aerial atmosphere. The prepared nanostructured materials were characterized by acquiring from them field emission scanning electron microscopy (FESEM) and transmission electron microscopy (TEM) images and X-ray diffraction (XRD) data. The electrocatalytic properties of the prepared nano-Co₃O₄ toward water electrooxidation in alkaline medium were also evaluated, and done so by immobilizing them on a filter-paper-derived carbon electrode (FPCE) prepared by pyrolysis of normal filter paper

4.2 Experimental

To prepare the nano-Co₃O₄, initially we transferred 400 mg of Co(NO₃)₂·6H₂O (obtained from Sigma-Aldrich) into an alumina crucible, which was then placed into a Pyrex glass tube of a tubular furnace. Next, we heated the mass at 520 °C for three hours in a normal aerial atmosphere to obtain nano-Co₃O₄. Finally, we collected the nano-Co₃O₄ and characterized it with XRD (using a Rigaku Ultima IV diffractometer equipped with Cu K-alpha radiation), FESEM (using a TESCAN LYRA 3, Czech Republic), energy dispersive spectroscopy (EDS) (using an Xmass detector, Oxford Instruments, equipped with the TESCAN LYRA 3) and TEM (using a JEOL JEM-2100F).

As mentioned above, we immobilized prepared nano-Co₃O₄ on an FPCE, and to do so we first dispersed it at a concentration of 1 mg/ml in water via ultrasonication. A volume of 30 μ L of this dispersion was then dropped on the working electrode area (0.2 cm²) of the FPCE, and dried at room temperature to obtain a Co₃O₄/FPCE. Note that FPCE was prepared by carrying out a pyrolysis of cut pieces (2 cm x 2 cm) of filter paper (purchased from WhatmanTM; <http://www.capitolscientific.com/>) under nitrogen atmosphere at 850 °C for five hours, and a photograph of the used form of the FPCE, which was prepared according to our earlier report^[155], is shown in Fig. 2. Bare FPCE or Co₃O₄/FPCE was used as the working electrode, and a Pt wire and Ag/AgCl served as the counter and reference electrodes, respectively. Electrochemical data were obtained in 0.1 M sodium hydroxide (NaOH) (aq.) using a CHI 760E (<http://www.chinstruments.com>) electrochemical workstation. The used NaOH was received from Sigma-Aldrich (<http://www.sigmaaldrich.com>).

4.3 Results and discussion

Figure 10a shows a thermal gravimetric analysis (TGA) of Co(NO₃)₂·6H₂O; this TGA experiment was carried out at a scanning rate of 10 °C/min from 35 °C to 640 °C in air. The TGA curve indicated that a sharp weight loss occurred upon heating the sample from 65 °C to 270 °C, at which point only 30% of the original weight of Co(NO₃)₂·6H₂O remained. Further increasing the temperature to 640 °C did not yield any additional weight loss. The weight loss that occurred from 65 °C to 270 °C was attributed to the loss of water molecules and decomposition of Co(NO₃)₂ to cobalt oxide.[147] Even though applying a relatively low temperature of \geq 270 °C converted Co(NO₃)₂·6H₂O to cobalt

oxide, we chose 520 °C for this conversion in subsequent experiments. A detailed study of the temperature dependence of the formation of cobalt oxide from $\text{Co}(\text{NO}_3)_2 \cdot 6\text{H}_2\text{O}$ is in progress. Figure 10b shows the XRD pattern of the product of heating the $\text{Co}(\text{NO}_3)_2 \cdot 6\text{H}_2\text{O}$ at 520 °C for three hours in a normal aerial atmosphere. The obtained peaks were very sharp, indicating the product to be highly crystalline. The peak positions at 2θ values of 19.13, 31.40, 37.0, 38.63, 44.91, 55.71, 59.43 and 65.29 were attributed to the 111, 220, 311, 222, 400, 422, 511 and 440 crystal planes of cubic Co_3O_4 based on JCPDS 42-1467. This result clearly indicated the formation of pure single-phase cubic Co_3O_4 upon carrying out a heat treatment of $\text{Co}(\text{NO}_3)_2 \cdot 6\text{H}_2\text{O}$ at 520 °C for three hours in normal aerial conditions.

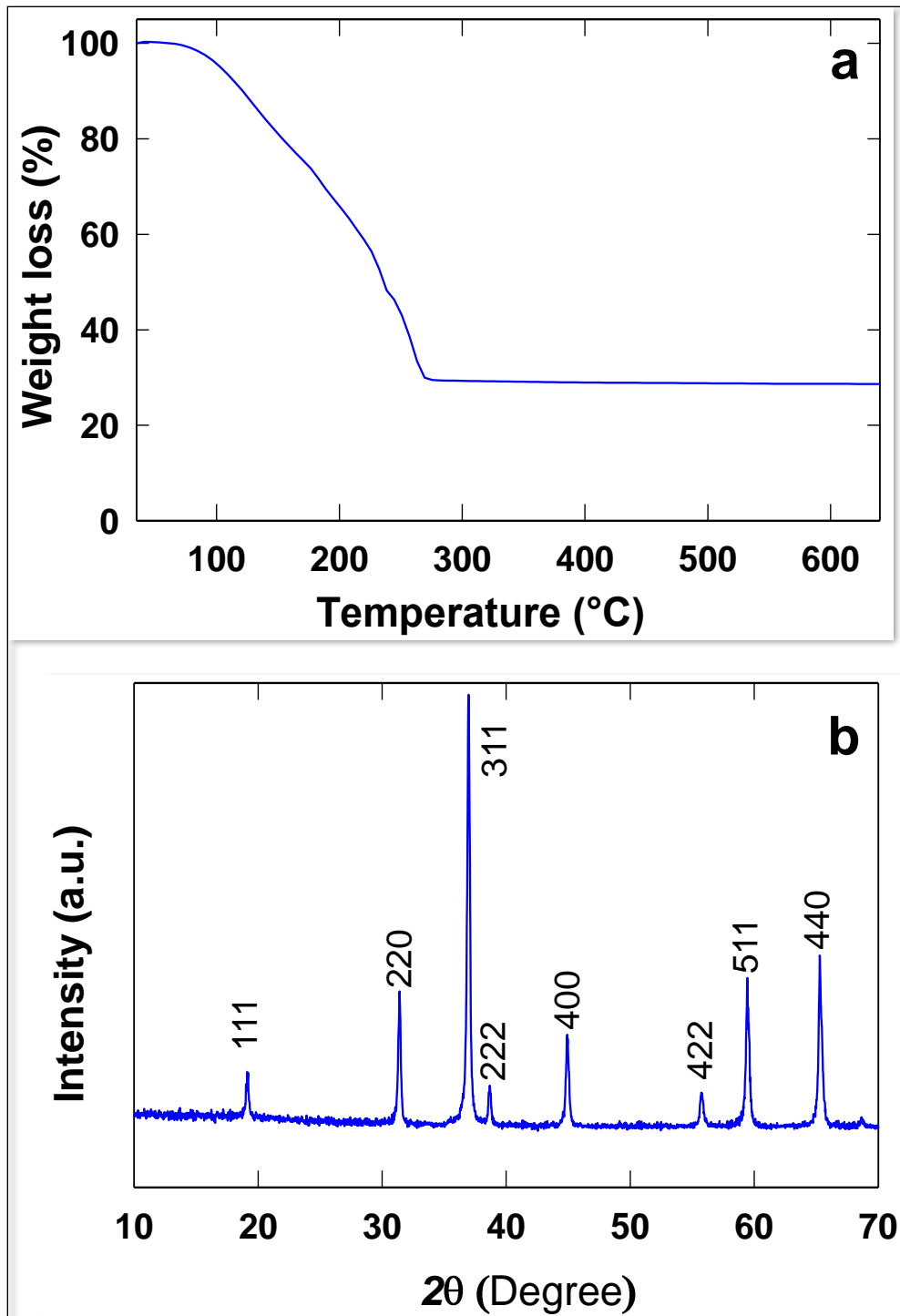


Figure 11: (a) TGA curve of $\text{Co}(\text{NO}_3)_2 \cdot 6\text{H}_2\text{O}$ at the selected temperature zone. (b) XRD pattern of the product of subjecting $\text{Co}(\text{NO}_3)_2 \cdot 6\text{H}_2\text{O}$ to a temperature of 520 °C for three hours.

Next, we carried out morphological studies of the prepared Co_3O_4 . Figures 11a and 11c show the FESEM and TEM images of the prepared nano- Co_3O_4 . Figures 11b and 11d are magnified views of Figures 11a and 11c, respectively. The initial FESEM image (Figure 11a) indicated the presence of homogeneously dispersed nano- Co_3O_4 . The magnified view of this image (Figure 11b) and the TEM images (Figure 11c, d) clearly showed that shape of the nano- Co_3O_4 is very short rod. The diameters and lengths of the Co_3O_4 nanorods were measured to range from 20.5 to 45.9 nm and from 28.3 to 69.4 nm, respectively, with their average diameter being 32.0 nm. The distances between the planes observed in the HRTEM image were 0.25 nm (marked in Figure 11e), corresponding to the 311 planes of cubic Co_3O_4 , which yielded the strongest peak in its XRD pattern (Figure 10b).[123] The selected area electron diffraction (SAED) image of the obtained Co_3O_4 nanorod (Figure 11f) revealed its high-order crystallinity.

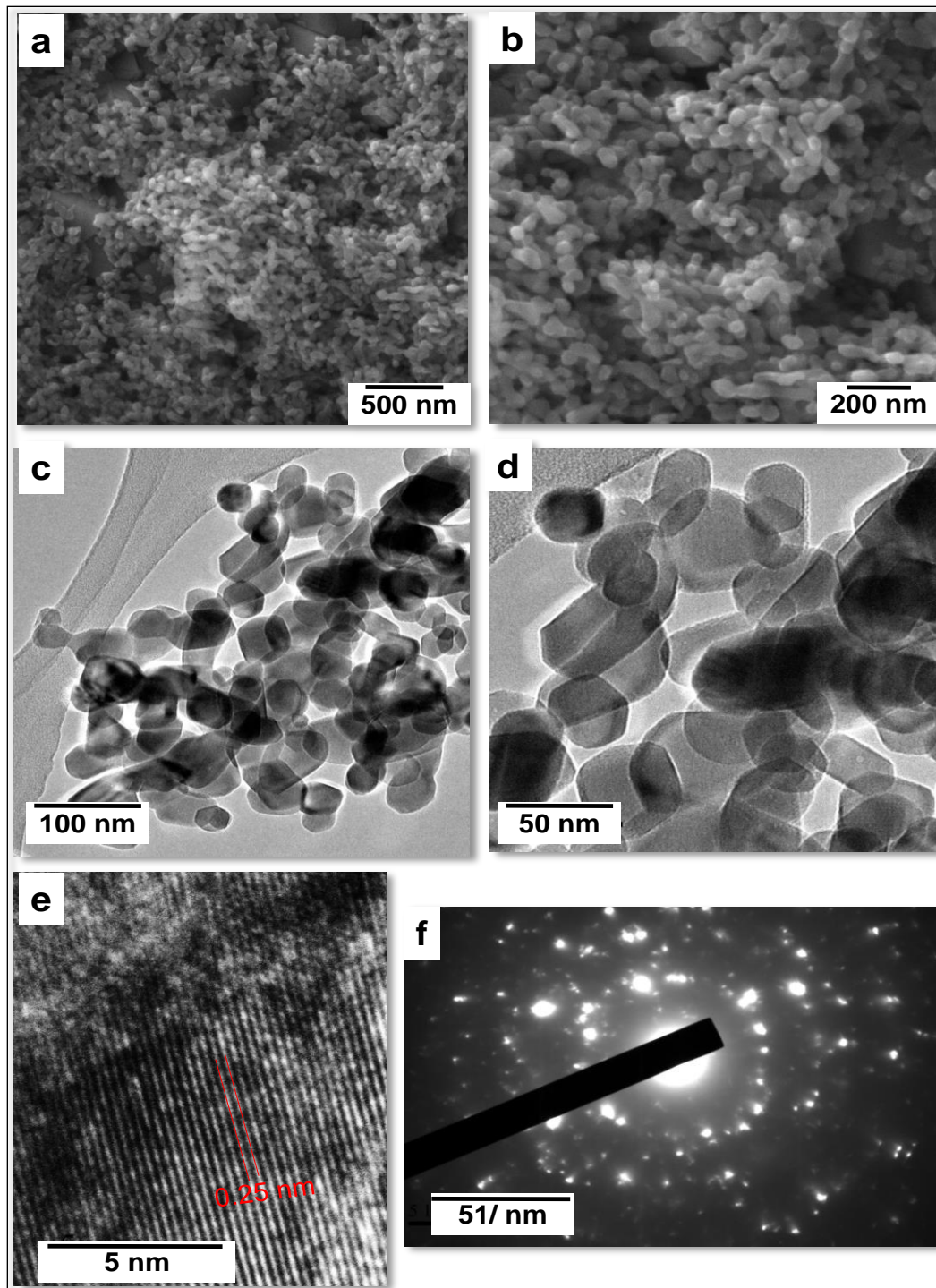


Figure 12: (a, b) FESEM images, (c, d) TEM images, (e) HRTEM image, and (f) SAED pattern of the nano-Co₃O₄ prepared by heating Co(NO₃)₂·6H₂O at 520 °C for three hours in an aerial atmosphere.

In order to evaluate the electrocatalytic properties of nano- Co_3O_4 , we immobilized it on FPCE as the substrate electrode (Fig. 2) rather than on the commonly employed glassy carbon electrode because FPCE is micro-nanoporous in nature and has a high electroactive surface area. The micro-nanoporous cavities of FPCE were expected to be helpful in creating a homogeneous distribution of immobilized nano-structured materials, rather than aggregates only in certain locations, when using the drop-drying method. Fig. 12a shows an FESEM image of a nano- Co_3O_4 /FPCE, which was prepared by drop-drying of an aqueous solution of the prepared nano- Co_3O_4 . To visualize the distribution of the nano- Co_3O_4 on a comparatively large surface of FPCE, we also recorded FESEM images at comparatively low magnifications. The FESEM image showed the nano- Co_3O_4 to form aggregates (clusters), but these aggregates were observed to be distributed homogeneously throughout the surface (i.e., not gathering only in certain areas). Note that the gathering of immobilized nanostructured materials in only certain places on bare solid substrate materials is very commonly observed when carrying out drop-drying, and such gathering limits a wide practical application of the drop-drying method. [100, 153, 154] We attributed the relatively homogenous distribution of the nano- Co_3O_4 on the FPCE to the micro-nanostructured cavities of the FPCE. These cavities perhaps hindered the gathering of nano- Co_3O_4 in certain places during the drying of the nano- Co_3O_4 solution. Fig. 12b shows the corresponding EDS spectrum of the FPCE modified with nano- Co_3O_4 ; this spectrum indicated the presence of the expected elements, i.e., C, O, and Co.

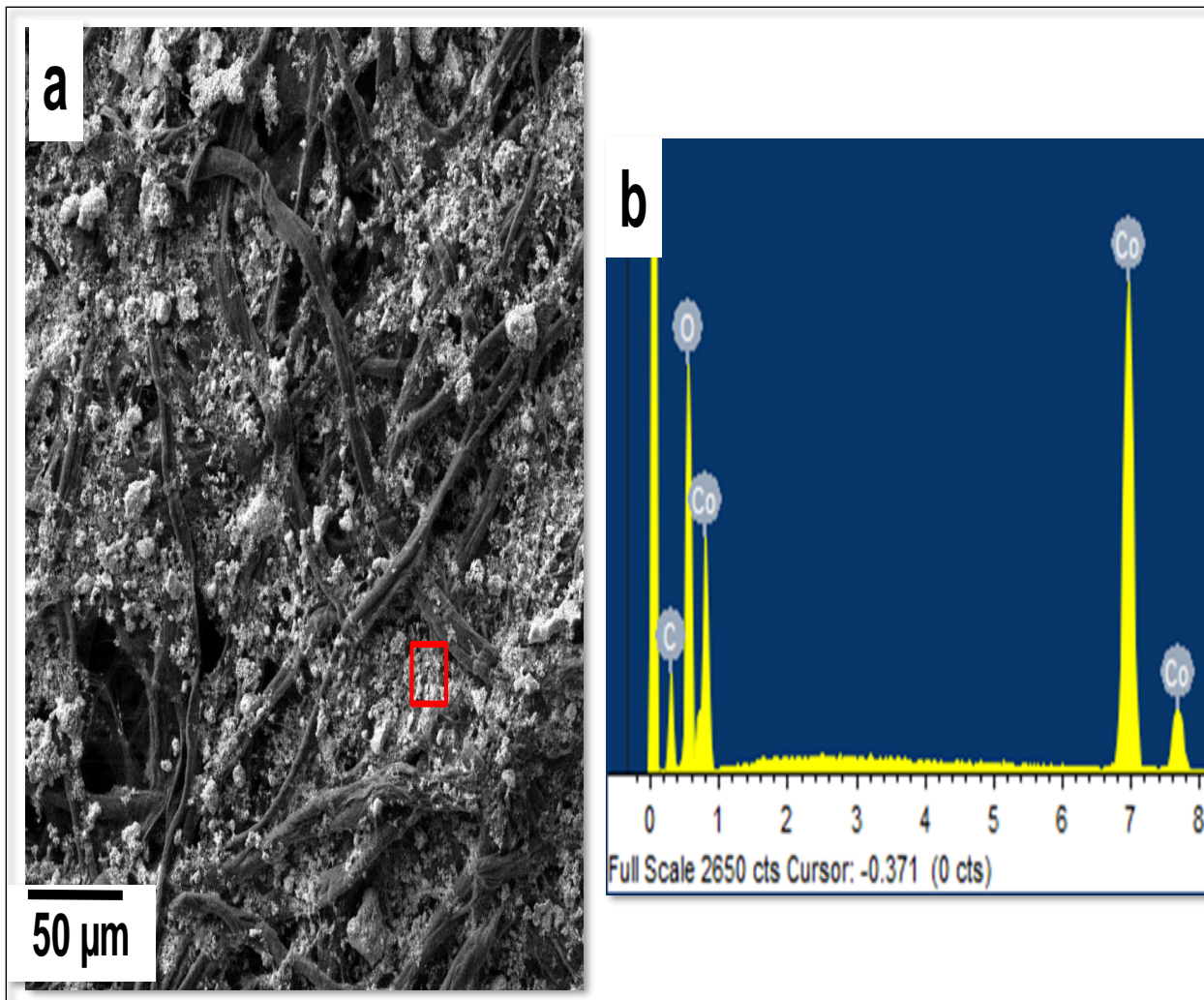


Figure 13: (a) FESEM image of a nano-Co₃O₄/FPCE. (b) Corresponding EDS spectrum of red boxed area of (a).

Figs. 14a and 14b show linear sweep voltammograms (LSVs) of the bare FPCE and nano-Co₃O₄/FPCE in 0.1 M NaOH, respectively. Comparison of these two CVs readily showed a significant improvement in the electrocatalytic properties toward water oxidation upon immobilization of Co₃O₄ nanorods on the FPCE. The achieved water electrooxidation current densities at 1.5 V were 37.89 mAcm⁻² and 8.80 mAcm⁻² for nano-Co₃O₄ /FPCE and FPCE, respectively. Also note that nano-Co₃O₄ /FPCE started

water oxidation at low potential, 0.7 V. These results taken together revealed the good electrocatalytic properties of the prepared Co₃O₄ nanorods toward water oxidation.

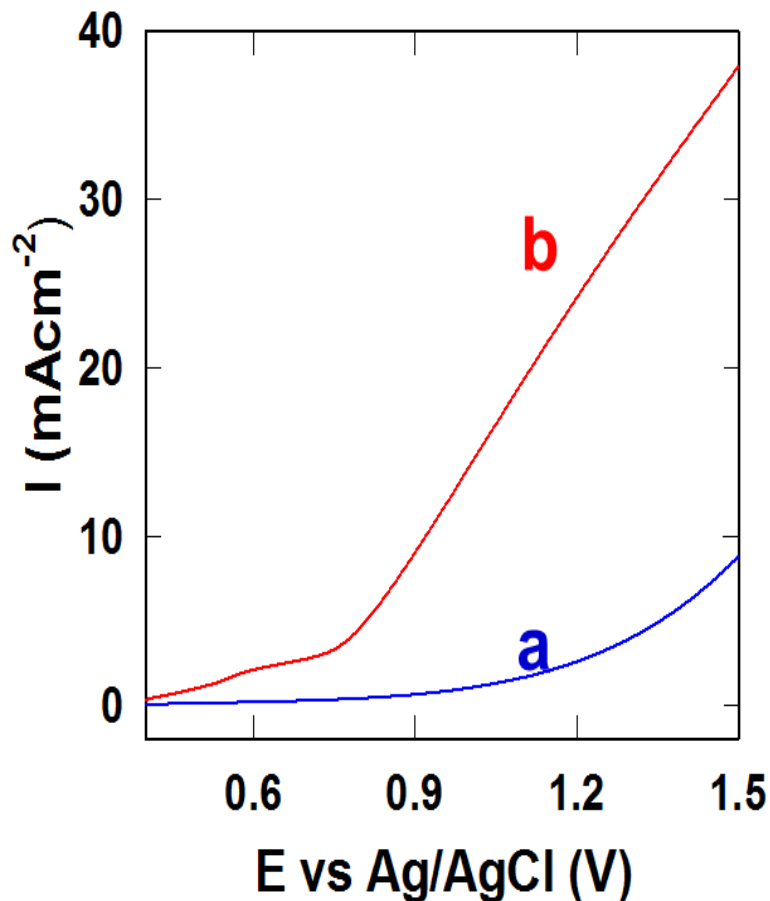


Figure 14: Linear sweep voltammograms of FPCE (a) and nano-Co₃O₄/FPCE (b) in 0.1 M NaOH (aq.).

4.4 Conclusion

Here, nano-Co₃O₄ was prepared by carrying out a direct thermal decomposition of Co(NO₃)₂·6H₂O at 520 °C in an aerial atmosphere. The prepared nano-Co₃O₄ was characterized in detail by using XRD, FESEM and TEM, and HRTEM. These analyses confirmed the formation of highly crystalline Co₃O₄ nanorods with an average diameter

of 32 nm. The nanorods were immobilized on an FPCE to evaluate their electrocatalytic properties. The FPCE modified with nano-Co₃O₄ showed good electrocatalytic properties toward water oxidation in an alkaline medium. This simply and straightforwardly prepared nano-Co₃O₄ could potentially play an important role in various practical fields and applications such as catalysis, electronics, opto-electrical devices, and electrochemical applications including electrochemical sensors, biosensors, gas sensors, batteries, capacitors, solar cells, fuel cells, and water splitting.

CHAPTER 5

EFFECTS OF CALCINATION TEMPERATURE ON

THE OXYGEN EVOLUTION REACTION

PERFORMANCE OF Co_3O_4 NP/FPCE CATALYSTS

Tricobalt tetraoxide nanoparticles (Co_3O_4 NPs) catalysts have been widely studied for water oxidation (oxygen evolution reaction). However, few researchers have investigated the effects of calcination temperatures on the Co_3O_4 nanoparticles for water splitting. For preparing Co_3O_4 nanoparticles, the catalysts of Co_3O_4 NPs/FPCE (Co_3O_4 NPs -modified filter paper derived carbon electrode (as substrate)) were utilized by thermal decomposition method. Also, it was confirmed that there was a good activity for Co_3O_4 nanoparticles at a calcination temperature of 520°C toward oxygen evolution reaction. The effects of different annealing temperatures of $320, 420, 520$ and 620°C on the activity and stability of Co_3O_4 nanoparticles for oxygen evolution reaction were studied. The electrochemical measurements resulted from the experimental electrodes were recorded by cyclic voltammograms and chronoamperometry techniques. The electrochemical findings have revealed that Co_3O_4 NPs/FPCE catalyst with the calcination temperature of 420°C has highest activity while the highest stability was at 320°C . Increasing the efficiency of nanoparticles catalyst (Co_3O_4 NPs) at a calcination temperature of 420°C resulted from their well-distribution, smaller nanorods sizes, and higher

electrochemically active surface area. In addition, the properties of catalysts prepared at different calcination temperatures have been characterized by X-Ray diffraction (XRD), scanning, and transmission electron microscopy (SEM, TEM) , high -resolution transmission electron microscopy (HRTEM) and Fourier transform infrared spectra (FT-IR).

5.1 Introduction.

The advantages of technology in the renewable energy field attracts the research and industrial community to devote a tremendous effort to make a breakthrough in this area. Currently, most available energy sources are not sustainable, and they are considered as a source of pollution. As a result, develop a new generation of energy sources that are environmentally friendly, clean and sustainable are urgent. As an example of cheap renewable energy sources is water oxidation(WO) including oxygen evolution reaction(OER). However, this technique encounters many challenges such as low kinetics, short activity and large overpotential [2]. In other words, obtaining efficient stable catalyst capable of splitting water is one of the most challenges in conversion the chemical energy to electrical energy. This is because of the poor kinetics of OER [31].Furthermore, the ultimate dissociation of water-oxidizing complexes (WOCs) into soluble species is mainly one of the most limitation in this process (OER)[156, 157].Therefore, enhancing and controlling the structure of catalysts are imperatively needed for optimizing the activity of these catalysts [31].This means to achieve a high activity of water oxidation(WO),active catalysts should be utilized. Many categories of catalysts such as electrochemical, photoelectrochemical and chemicals have been studied

and developed to get a high catalytic activity toward oxygen evolution reaction. Where a lot of researchers have reported the synthesis of many electrochemical [3-15] and photochemical [16-18] catalysts. In the current study, the focused was on the electrochemical catalysts because of their simpler preparation.

One of these electrocatalysts is cobalt oxides over a substrate (like carbon which work as an electrode). Specifically, Co_3O_4 , which is one of the spinel oxides, has been significantly and recently investigated because of its own unique physical and chemical properties, applications in interconversion between chemical and electrical energies as well as storage [55-58]. Moreover, in regard to its applications, it can be used in supercapacitors, water splitting, and batteries of lithium-ion [55-58]. Therefore, various researchers have developed different methods to synthesis Co_3O_4 with 2D nanostructure to electrothermally improve the performance [25, 49, 50, 52, 158-160]. In our last work, we have used the simple way of preparation []. With respect to the substrate, numerous substrates have been used in published papers as electrodes. However, most of them were not cheap. Thus, in the previous work, we have used a cheap substrate (the carbon derived from the filter paper carbon) as an electrode. Where the current densities were 37.89 and 8.80 mA cm^{-2} at 1.5V for Co_3O_4 NPs/FPCE and FPCE at a temperature of 520 $^{\circ}\text{C}$, respectively. However, the problems with this catalyst (Co_3O_4 NPs/FPCE) are the non-stability and the less activity as well. This is may be attributed to the dissolution of the complex catalyst, the weak contact between the NPs and electrode substrate, the bigger NPs formed at a temperature of 520 $^{\circ}\text{C}$ and the dropping method used for depositing NPs over FPCE. As it is known, the fabricated conditions for preparation of NPs play a significant role in determining the basic characteristics of synthesized

nanoparticle including shape, size, size of the distribution, crystals and mutual alignment. Thus, using various conditions in the fabrication of nanoparticles results in different findings. Therefore, in this work, the method of thermal decomposition for preparation NPs will be considered, so the activity and stability of NPs can be improved by studying the effects of different annealing temperatures on Co_3O_4 NPs for oxygen evolution reaction application. This method will be used because it is easy to prepare the raw material and controlling the prepared nanoparticles.

Up to this moment, a few researchers reported the effects of calcination temperature on the catalyst performance for water oxidation. In previous work, Co_3O_4 NPs nanoparticles were prepared using only nitrate cobalt precursor without adding any chemical by thermal decomposition at a temperature of 520 °C. It revealed that Co_3O_4 NPs/FPCE catalyst had a good activity toward water oxidation while the stability was not quite well. However, no body studied the effect of calcination temperature on the Co_3O_4 NPs- which were prepared directly from thermal decomposition of only nitrate cobalt precursor- performance for water oxidation. Therefore, it is necessary to study the synthesis conditions for optimizing them, so the activity and stability of Co_3O_4 NPs/FPCE catalyst can be improved. In this work, the effect of the calcination temperature was investigated on the performance of Co_3O_4 NPs/FPCE catalyst toward water oxidation. The calcination temperature: 420 °C is the best temperature to prepare Co_3O_4 NPs/FPCE catalyst for oxygen evolution reaction during the zone (320-620°C) of testing.

5.2 Experimental.

5.2.1 Materials and Instruments.

Both Cobalt(II) nitrate Hexahydrate ($\text{Co}(\text{NO}_3)_2 \cdot 6\text{H}_2\text{O}$) and Sodium Hydroxide (NaOH) were obtained from Sigma-Aldrich while filter Papers were purchased from Whatman.

The electrochemical workstation (CHI 760E) was used for obtaining Electrochemical data. The working, counter and reference electrodes were represented by Co_3O_4 -modified FPCE, Pt wire, and Ag/AgCl , respectively. All electrochemical measurements were recorded at the room temperature and atmospheric pressure. Fourier transform infrared spectra (FTIR) was carried out by a Nicolet 6700 spectrometer, Thermo Scientific, USA. FESEM images were carried out via a field emission scanning electron microscope (TESCAN LYRA 3, Czech Republic). TEM images were carried out by a high-resolution transmission electron microscope (HRTEM) (JEM-2011, Joel Corp.) supplied with CCD camera 4k x 4k (Ultra Scan 400SP, gatan cop.). X-ray diffraction patterns (XRD) for the Co_3O_4 NPs were recorded by a high-resolution Rigaku Ultima IV diffractometer supplied with $\text{Cu-K}\alpha$ radiation.

5.2.2 Preparation of Filter Paper Derived Carbon Electrode(FPCE)

At the beginning, many pieces were obtained by cutting filter papers to with dimensions of 1.4 cm x 1.8 cm. These pieces were inserted in a flat alumina crucible. Next, the crucible was taken to the center of the alumina tube, which is in a tubular furnace. The two sides of the tube were sealed. Then, the system was fed with full amounts of nitrogen gas for a period of five minutes for evacuating the environment from air and water. Then,

the system was fed with N₂ in slow flow rate and heated at a temperature rate of 10°C every minute until reaching the temperature of 850°C. Then, after constant heating for 5 hours at 850°C, the temperature was decreased at a rate of 5°C per min till the room temperature. Finally, the obtained FPCE was ready to take out from the furnace. For preparing working electrode, one side of the obtained FPCE was attached to the scotch tape and the other side was connected with conducting copper tape. Then, the other side was covered with scotch tape excluding the area of 0.2 cm² of FPCE and the copper tape end. Where the area of 0.2 cm² was worked as working electrode and the uncovered end of the copper tape was connected to a potentiostat (see reference [161]). The prepared FPCE is shown in Fig. 1.

5.2.3 Preparation of Co₃O₄ NPs and Co₃O₄ NPs-Modified FPCE Catalyst

Initially, 400 mg of Ni(NO₃)₂.6H₂O was transferred to an alumina crucible. The crucible was placed in the glass tube, which was positioned in a tubular furnace. We confirmed that the crucible containing the sample was positioned in the center of the tubular furnace. Then, the furnace was heated at a rate of 10°C per min till reaching 320°C. Next, the temperature of 320°C was constant for three hours. After that, the product was cooled at a temperature rate of 5°C/ min until the room temperature was reached. Finally, the Co₃O₄ NPs were collected. Separately, Co₃O₄ NPs was prepared at temperatures of 420, 520 and 620°C were prepared according to the same protocol with temperature of 320°C

The prepared Co₃O₄ NPs prepared at temperatures of 320, 420, 520 and 620 °C were dispersed in water with a concentration of 3mg/3mL using ultrasonication. 30 μL of the

dispersed Co_3O_4 NPs were deposited on the exposed working electrode area of 0.2 cm^2 of FPCE by dropping cast method as illustrated in Fig. 1. After that, the complex was dried at room temperature overnight. At the end, a Co_3O_4 NPs -modified FPCE was obtained. Following the same procedures, a Co_3O_4 NPs -modified FPCE at temperatures of 420, 520 and $620 \text{ }^\circ\text{C}$ were prepared.

5.3 Electrochemical Measurements

The electrochemical measurements were recorded via CHI (760E) electrochemical workstation in the solution of 0.1 M NaOH at atmospheric conditions. The Co_3O_4 NPs (prepared at $320, 420, 520 \& 620^\circ\text{C}$)-modified FPCE, Ag/AgCl and Pt wire were used as working, reference and counter electrodes, respectively as mentioned above. The cyclic voltammograms (CVs) for the catalysts of Co_3O_4 NPs (at $320, 420, 520 \& 620^\circ\text{C}$)-modified FPCE were recorded for showing water oxidation and redox reactions in the potential ranges of $0.7\text{-}1.5 \text{ V}$ and $0.4\text{-}0.75 \text{ V}$, respectively. Furthermore, the chronoamperometry curves were recorded for showing the stability of the catalysts in the time range of $0.0\text{-}5000 \text{ s}$. Also, the electrochemical active surface area was calculated using electrochemical double layer capacitance of the catalytic surface. All these electrochemical measurements will be illustrated in detail in the next the section of results and discussion.

5.4 Results and Discussions

Figure 2 shows a simple photograph of the FPCE which was modified with the prepared nano- Co_3O_4 . Where the Co_3O_4 NPs catalysts and the filter paper carbon electrode (FPCE) have been successfully prepared by thermal decomposition method at different

temperatures (320,420,520 and 620°C) and pyrolysis process at a temperature of 850 °C ,respectively. Then, the NPs have deposited on the FPCE by dropping cast method for oxygen evolution reaction

5.4.1 Characterizations of Co₃O₄ NPs Formed at Different Calcinations Temperatures

Figure 15 shows the XRD patterns of the product (Co₃O₄ NPs) formed from the calcination process at various temperatures of 320, 420, 520 and 620°C. The rise of calcination temperatures resulted in sharp peaks where the crystallinity of nanoparticles was the lowest at 320°C and it increased until 620 °C. Thus, it can be deduced that there was a linear relationship between the sintering temperature and the crystallized particles. However, the diffraction peaks positions of four samples are similar. Furthermore, it can be observed that there are only obvious eight peaks diffractions between $2\theta=10^\circ$ and $2\theta=70^\circ$, so no detectable peaks for impurities were found. Therefore, the product of Co₃O₄ NPs has high purity. All the diffractions peaks at 2θ values of 19.13, 31.40, 37.0, 38.63, 44.91, 55.71, 59.43 and 65.29° can be indexed to planes of 111, 220, 311, 222, 400, 422, 511 and 440, respectively, indicating that cubic crystalline planes of Co₃O₄ (pure phase) were formed. This is in consistent agreement with the standard JCPDS (card No. 42-1467) of cubic Co₃O₄ crystals.

Figure 16 shows the spectra of FTIR for Co₃O₄ NPs catalysts at different temperatures (320,420,520 and 620°C). The investigation of the region (400-1370cm⁻¹) indicated the existence of two obvious absorption bands all above the tested temperatures. Where they had different transmittances (intensities) but they had approximately the same bands. The

first one at around $\nu_1(576) \text{ cm}^{-1}$ and the other at nearly $\nu_2(661) \text{ cm}^{-1}$. where these two bands originate from extended vibrations of bonds connecting the metal and oxygen. This confirms the formation of Co_3O_4 oxide [162-164]. The band of ν_1 shows OA_3 vibration where A denotes Co^{3+} in the tetrahedron hole of the lattice. On the other hand, the band of ν_2 shows BAO_3 vibration where B denotes the Co^{+2} in the tetrahedron hole of the lattice, too [164]. The obtained FTIR results match with the results of XRD, both confirming the existence of only a pure phase of Co_3O_4 detected in the temperature range of 320-620°C.

Figure 17 shows the SEM images of Co_3O_4 over ITO substrate at different temperatures: (a) 320, (b)420, (c)520 and (d) 620°C . Overall, as the temperature increase till 620°C , the short nanorods(NRs) were clearly observed. Although enormous nanorods and few nanosheets(NSs) of Co_3O_4 began forming at 320°C, NRs and NSs were not completely formed in this temperature (320°C). Regarding the nanosheets, they nearly disappeared above or equal to 420°C. However, the NRs sizes significantly increased through the temperature range of 420-620°C .In other words, the NRs became bigger when the sintering temperature was increasing from 420 °C to 620 °C ,so the smallest NRs appeared at 420°C as shown in figure 17 where the average diameters and lengths of nanorods were 31.592,51.592 and 66.929 nm and 61.014,55.734 and 95.24 nm at temperatures of 420, 520 and 620 °C ,respectively. The lengths of NRs ranged from 39.508 to 88.112 nm, 24.485 nm to 118.145 nm and 52.341 to 132.91 nm at temperatures of 420, 520 and 620°C ,respectively. In addition, it can be observed that the nanoparticles were very well

homogenously monodispersed at 420°C as shown in part b of the same figure. overall, the Co₃O₄ nanoparticles sizes increased as the temperature increased through the temperature zone (320-620°C). Where the NPs at temperature of 420°C had the lowest size compared to NPs at two temperatures of 520 and 620°C. Furthermore, the shapes of Nano particles were short rods and the NPs had the best distribution at 420°C as illustrated in part b of figure 4. Because of the above-mentioned NPs features, the electrochemical properties were optimized at temperature of 420°C.

Figure 18 shows TEM images of short rod nanoparticles of Co₃O₄. Where these nanorods sizes become bigger as the calcination temperature increases through the tested zone (320-620°C). The nanorods diameters range from 5.979 to 9.371, 12.005 to 22.022, 26.118 to 50.018 and 47.584 to 103.372 nm while the lengths range from 7.187 to 27.002, 15.165 to 33.835, 29.61 to 62.846 and 53.265 to 140.711 nm for calcination temperatures of 320, 420, 520 and 620°C, respectively. The diameters averages of Co₃O₄ NPs at 320, 420, 520 and 620°C were 7.753, 15.852, 37.137 and 62 nm whilst the average lengths were 16.052, 23.753, 44.937 and 71.928 nm, respectively. From the figure 18, it can also be observed that the sheet and rod nanoparticles were found at calcination temperature of 320°C. However, the NPs at the temperature of 420 °C are more obvious and more independent than those at 320°C where the rod nanoparticles are mostly found more than the sheets, which were nearly disappeared. Although particles became bigger (as mentioned above) as the calcination temperatures rose from 320 to 620°C, they became significantly agglomerated above 420°C, too, as shown in fig. 18c and d. In addition, the polycrystalline formations are shown in the insets of figures 18c and d for calcination temperature of 520 and 620°C while monocrystalline formations are shown in

the two insets of two parts of 18a and b of the same figure, respectively. Furthermore, at calcination temperature of 420, the nanorods particles were closer to the spherical shapes compared to the others through the same test zone. Also, the distribution of NPs at this calcination temperature (420°C) was better than others as shown in the fig.18b. These results are consistent with the results of XRD and SEM. Because of the above discussed reasons, the calcination temperature of 420°C was selected as the optimized choice for investigating the activity and stability of the nanoparticles.

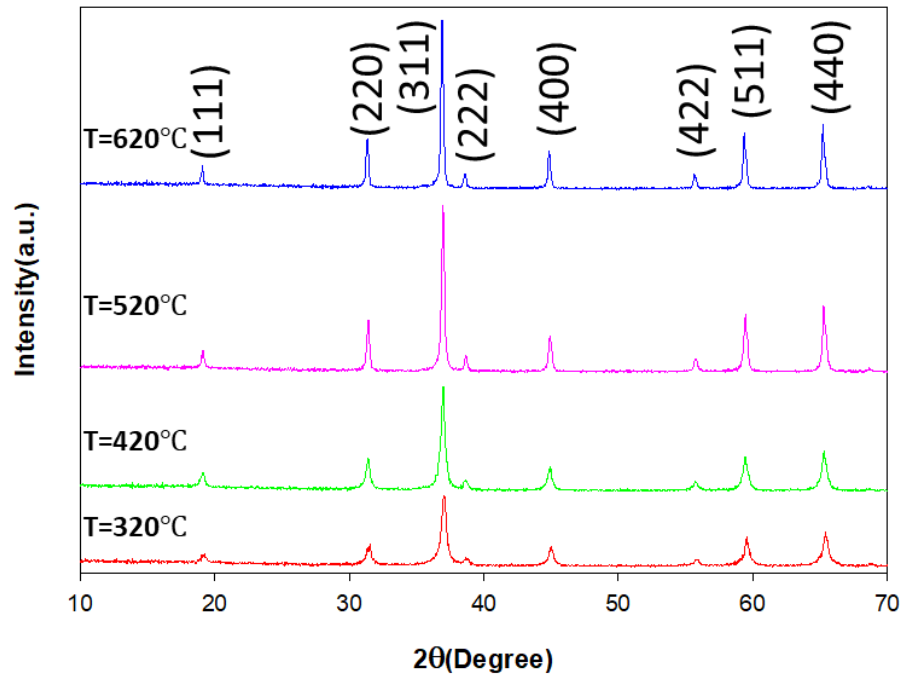


Figure 15: XRD patterns for CO₃O₄ NPs at different temperatures (320,420,520, and 620°C)

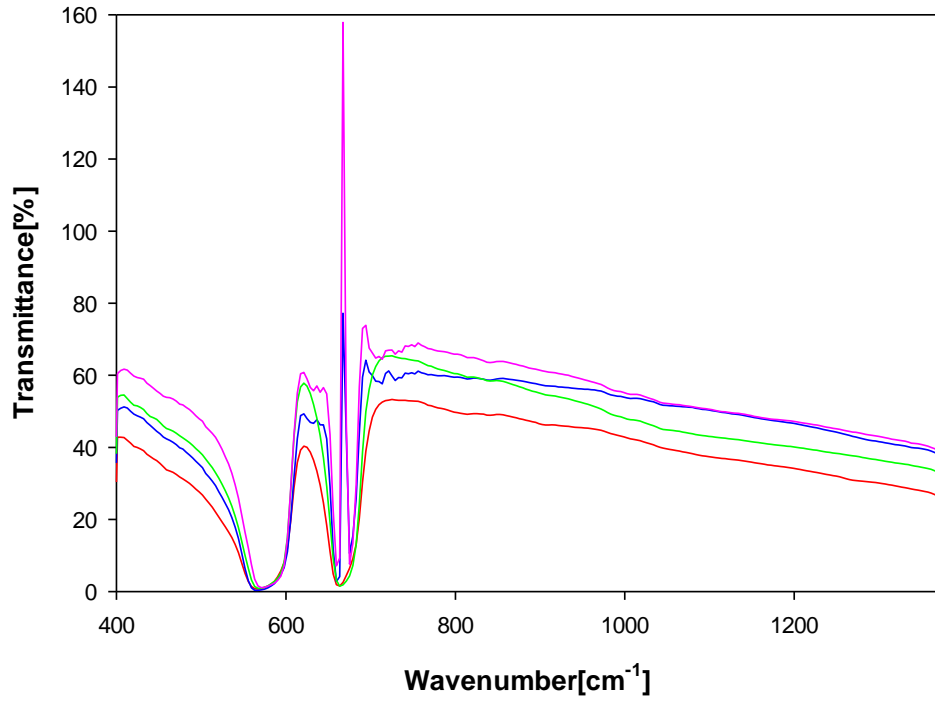


Figure 16: FTIR spectra of prepared Co₃O₄ NPs sintered at 320-620°C.

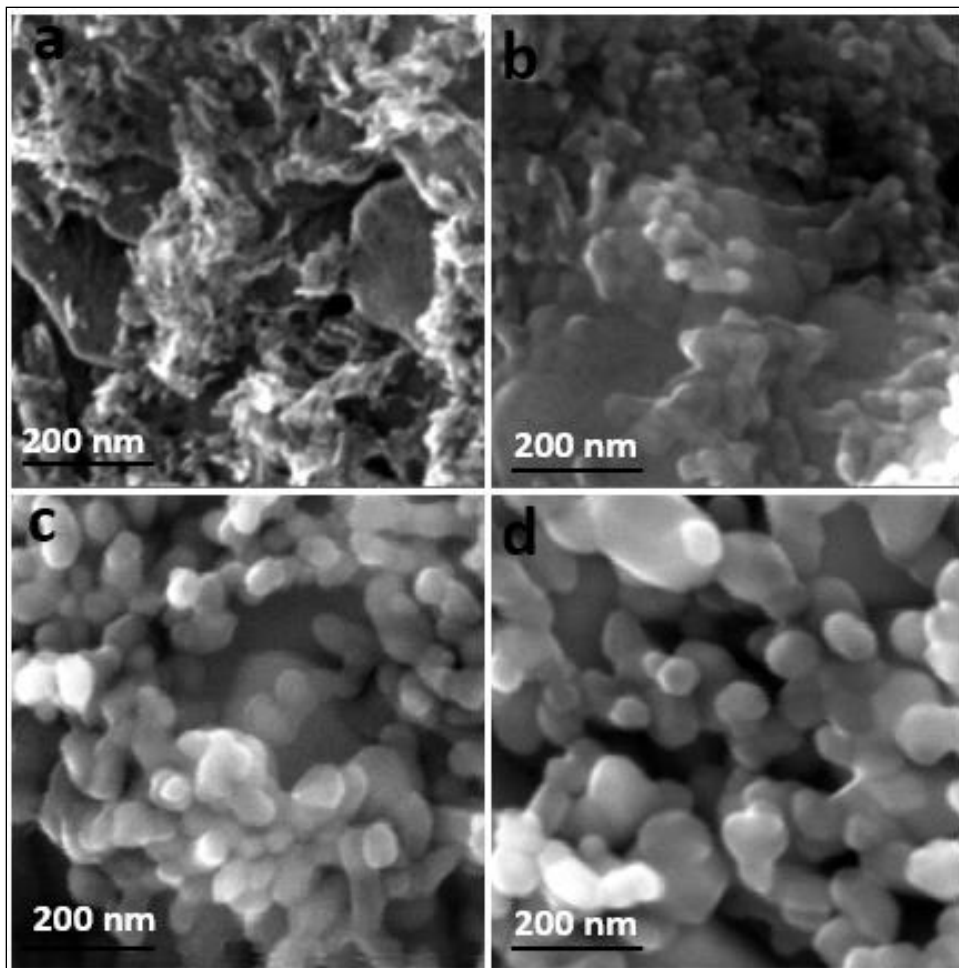


Figure 17: SEM images of CO₃O₄ NPs on ITO substrate at magnification of 400KX for various calcination temperature of (a)320, (b)420, (c)520, and (d) 620 °C.

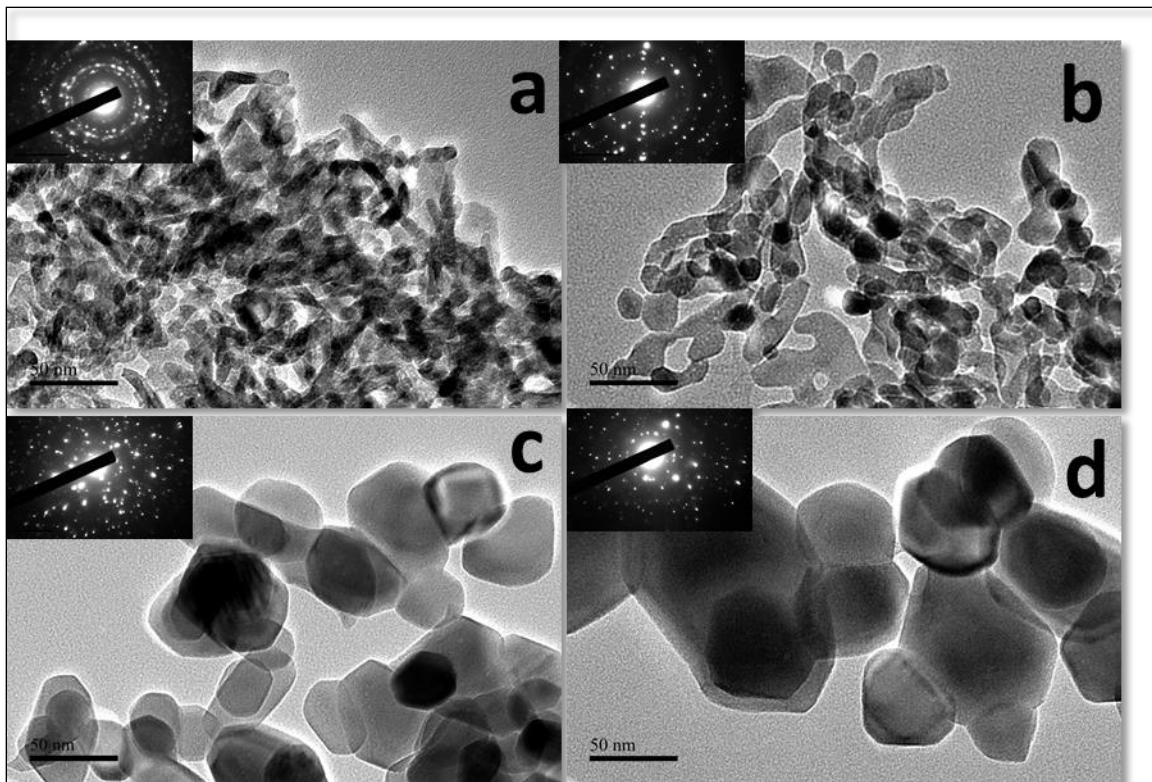


Figure 18: TEM images of as-prepared Co_3O_4 NPs at different calcination temperatures of (a)320, (b)420, (c)520 and (d)620 °C and the insets show XRD diffraction for every temperature.

5.4.2 Electrochemical measurements

Figure 19 shows water oxidation by recording cyclic voltammograms (CVs) for Co_3O_4 NPs/FPCE at various temperatures: 320, 420, 520 and 620 °C. The water oxidation for all the tested temperatures were approximately starting at the same potential of 0.7 V. However, it was clear that the highest current density reached 41 mA cm^{-2} at temperature of 420 °C as shown in the same figure. The lowest current density of 27 mA cm^{-2} was at 620 °C. Also, the current density of 38 mA cm^{-2} was at the calcination temperature of 520 °C while it was 32 mA cm^{-2} at 320 °C. It can be observed that the highest and the lowest stability of Co_3O_4 NPs catalysts for water oxidation was at 420 °C and 620 °C, respectively.

From these results, we can confirm that the optimized temperature for water oxidation over Co₃O₄ NPs /FPCE is 420 °C. These results are significantly consistent with previous results obtained by characterizing the surface of catalyst via above mentioned instruments.

The CVs of redox reactions at the four calcination temperatures for electro catalyst (Co₃O₄ NPs /FPCE) were shown in the inset of the parts a of figure 19. where the two highest peaks oxidation (0.65 V) and reduction (0.44 V) were achieved at the temperature of 420 °C at current densities of 4.5 and -3.2 mA cm⁻², respectively. In addition, at temperature of 620 °C ,the lowest two peaks of oxidation and reduction were reached. This is because the sizes of particles were changing from small sizes to big sizes, thus they became agglomerated (at 620C) as the temperature was increasing from 320°C to 620 °C . With respect to the temperature of 520°C, the redox reaction was better than that at 620C. However, the redox reaction at 320°C was better than both at 520 and 620 C. This may contribute to the morphologies of NPs. Thus, this is consistent with the results of SEM and TEM. Consequently, this confirms that the calcination temperature of 420 °C is the best optimized temperature through the zone of 320-620°C for making very active Co₃O₄ NPs /FPCE.

Figure 21 shows time responses vs. current density using technique of Chronoamperometry curves for water oxidation of the Co₃O₄ NPs /FPCE catalyst in 0.1M NaOH solution at different calcination temperatures (320,420,520 and 620°C). In the same figure, at the initial point (at t=0) and the final point (after 5000 s), the two values of current densities measured for Co₃O₄ NPs /FPCE at temperatures of 420 °C were higher than those at other temperatures (320,520 and 620°C). However, the stability

order of electro catalysts Co_3O_4 NPs /FPCE was as the following: $320 > 420 > 520 > 620$ °C . Although the current density difference between the final and the initial point at 320°C was the lowest (this means: the best stability), the current density at temperature of 420°C at the final point (at $t=5000\text{s}$) was still the highest. This finding is attributed to the morphologies, which change through increasing the calcination temperature as mentioned in SEM and TEM analysis, of Co_3O_4 NPs. This result shows that the catalyst of Co_3O_4 NPs formed at temperature of 420°C has a better activity and stability. This is consistent with CVs results for water oxidation.

The insets in parts of a, b, c and d in figure 20 show that the oxidation peak current of Co_3O_4 NPs-modified FPCE in 0.1MNaOH depends on the square root of scan rates, which was ranging from 10 to 60 mV s^{-1} . Overall, all NPs deposited on FPCE are proportional to square root of scan rate. However, the best linear relationship was at temperature of 420°C as shown in the inset of figure 21b.

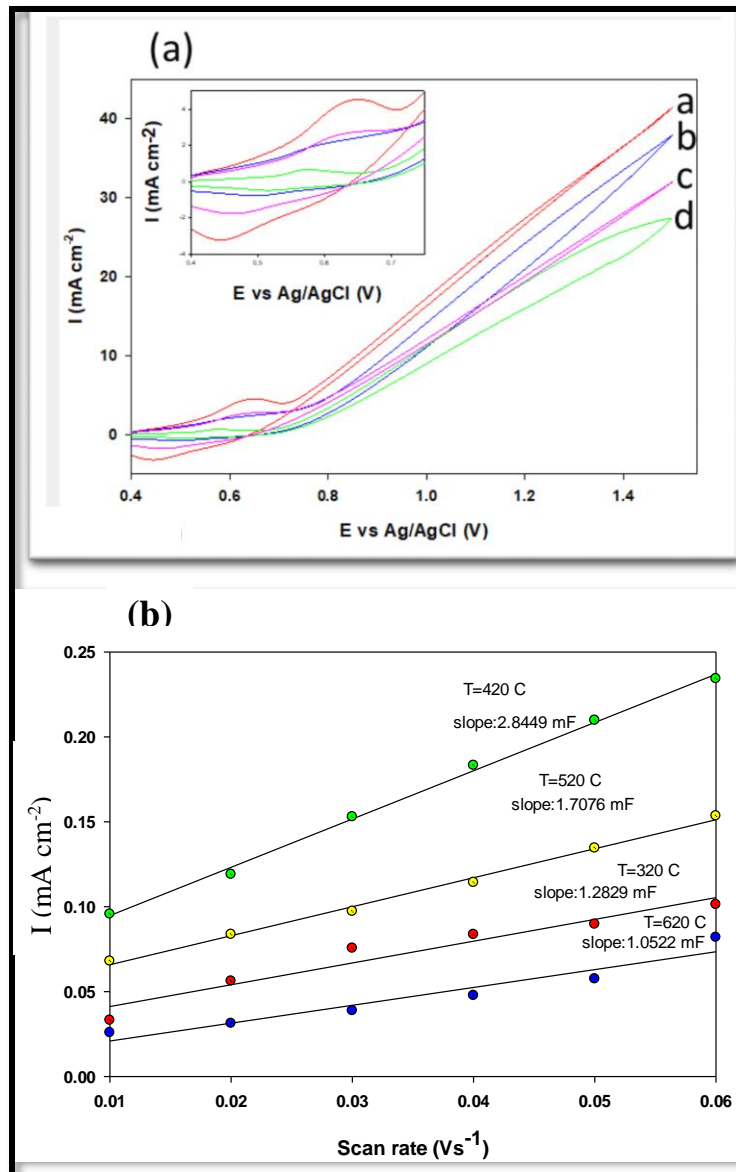


Figure 19: (a) Cycles of Linear sweep voltammograms of prepared CO₃O₄NPs on FCE at (a) 420 °C, (b) 520 °C, (c) 320 °C and (d) 620 °C in 0.1 M NaOH (aq.), the inset in the same part (a) shows the redox reactions at the four different temperatures and (b) scan rates versus current density using CO₃O₄NPs/ FCE prepared at different temperatures :320,420,520 and 620 °C in 0.1 M NaOH (aq.), too.

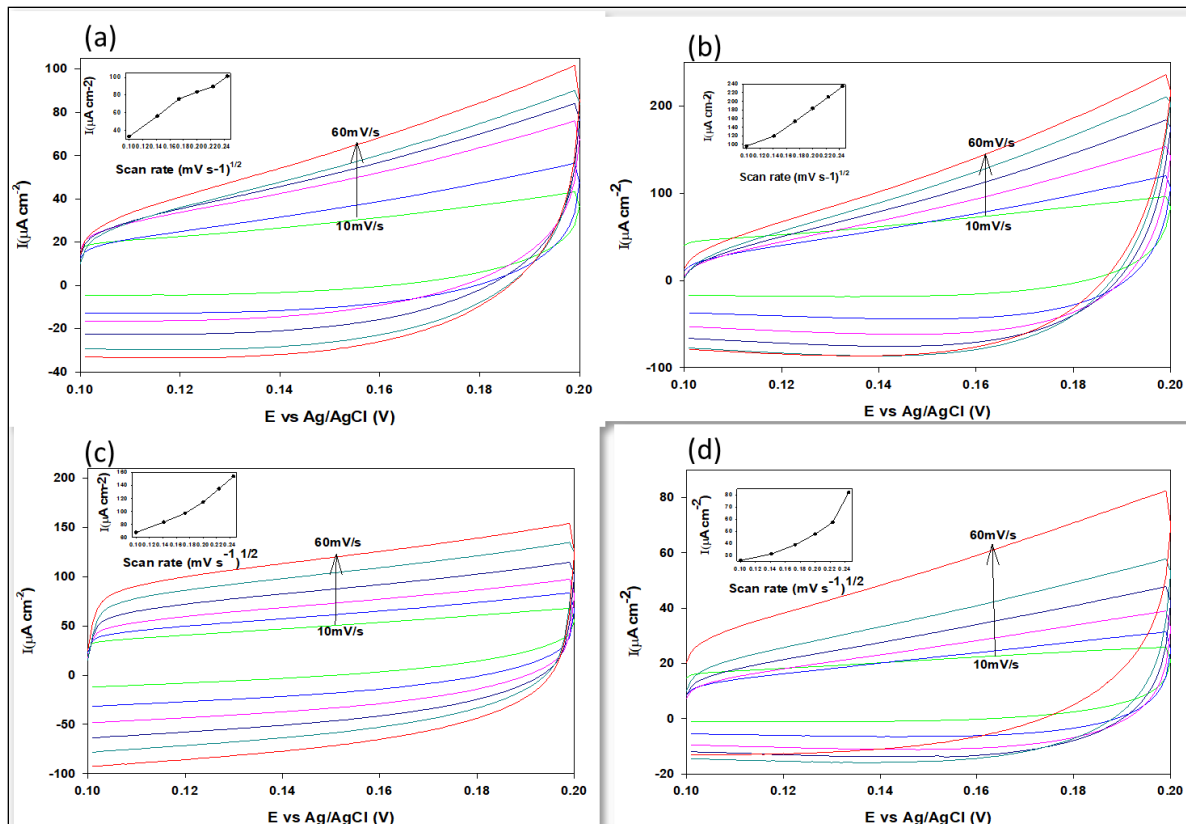


Figure 20: Cyclic voltammograms of Co₃O₄ NPs- modified FPCE at sintered temperatures of (a)320, (b)420, (c)520, and (d) 620°C with different scan rates started from 10 to 60mvs⁻¹ in 0.1 M NaOH (aq.) .insets in plots are the relative anodic peaks current densities vs. the square roots of scan rates.

5.4.3 Calculation of Electrochemically Active Surface Area(ECSA)

Obtaining ECSAs of Co₃O₄ NPs at different temperatures of 320,420,520 and 620°C was performed by electrochemical double layer capacitance for the catalytic surface as reported by Md. et al. [161]. The capacitances of Co₃O₄ NPs were measured via recording CVs in an aqueous solution of 0.1M NaOH within the limited zone of potential. This potential zone ranges from 0.1 to 0.2 V at various scan rates of 10,20,30,40,50 and 60 mV/S for the following temperatures: 320,420,520 and 620°C as shown in figure 20 d,

b, c, and d, respectively. In this non-faradic potential zone, all measured current was attributed to the double layer charging current (I_C) [5.1]. This can be expressed mathematically by the following equations:

$$I_C = C_{DL} * Y \quad (5.1)$$

Where Y is scan rate and C_{DL} is double layer capacitance. When I_C vs. Y were plotted, the straight line will be yielded with a slope of C_{DL} . The values of C_{DLs} for CO_3O_4 NPs obtained from drawing scan rate versus charging current at various temperatures of 320,420,520 and 620 °C were 1.2829, 2.8449, 1.7076 and 1.0522, respectively, as shown in figure 19b. After that, the ECSAs of CO_3O_4 NPs at temperatures of 320,420,520 and 620 °C were calculated from the slope (C_{DL}) as shown in the equation (5.2)

$$ECSA = C_{DL}/C_S \quad (5.2)$$

Where C_S is the area specific capacitance of CO_3O_4 NPs. The value of the C_S is 0.040 mF/cm^2 for the metal electrode as reported by Suho et al.[165]. Therefore, ECSAs of CO_3O_4 NPs were calculated at various temperatures: 320,420,520 and 620 °C for 1 cm^2 by dividing the capacitance of double -layer(C_{DL}) by the specific capacitance ($C_S=0.040$ mF/cm^2), which is a typical value for an electrode of metal in an aqueous solution of NaOH. Consequently, ECSAs were 32.0725, 71.1225, 42.69 and 26.305 cm^2 for temperatures of 320,420,520 and 620°C, respectively. This means that ECSAs were significantly higher than those of geometric surfaces areas. It was clear that the highest ECSA was 71.1225 cm^2 at the temperature of 420 °C, so the best temperature for preparing well active CO_3O_4 NPs is 420°C in this tested zone.

It was found that the activity and stability of the catalysts were affected by changing the calcination temperature. Thus, the optimized temperature for the nanoparticles catalysts activity and stability was 420°C. This is can be explained by crystallinity shape and the size of particles, which both affect directly on ECSA and interactions between the prepared FPCE and the Co₃O₄ NPs at temperatures: 320,420,520 and 620°C . As the calcination temperature increases up, the crystallinity and the size of nanoparticles increase significantly. Furthermore, at a temperature of 320°C ,there were nanosheets and nanorods. However, at a temperature of 420°C ,the nanosheets were approximately disappeared and the nanorods were mostly observed. This was confirmed by TEM and SEM images. In addition, the size of nanoparticles at a temperature of 420°C were smaller compared to others at temperatures of 520 and 620 °C.Thus , the ECSA was the highest at a temperature of 420 °C ,the well-distributed nanoparticles on ECSA inhibits the dissolution of Co₃O₄ NPs /FPCE. Therefore, the best temperature for preparing the active and stable catalyst of Co₃O₄ NPs /FPCE was at 420 °C.

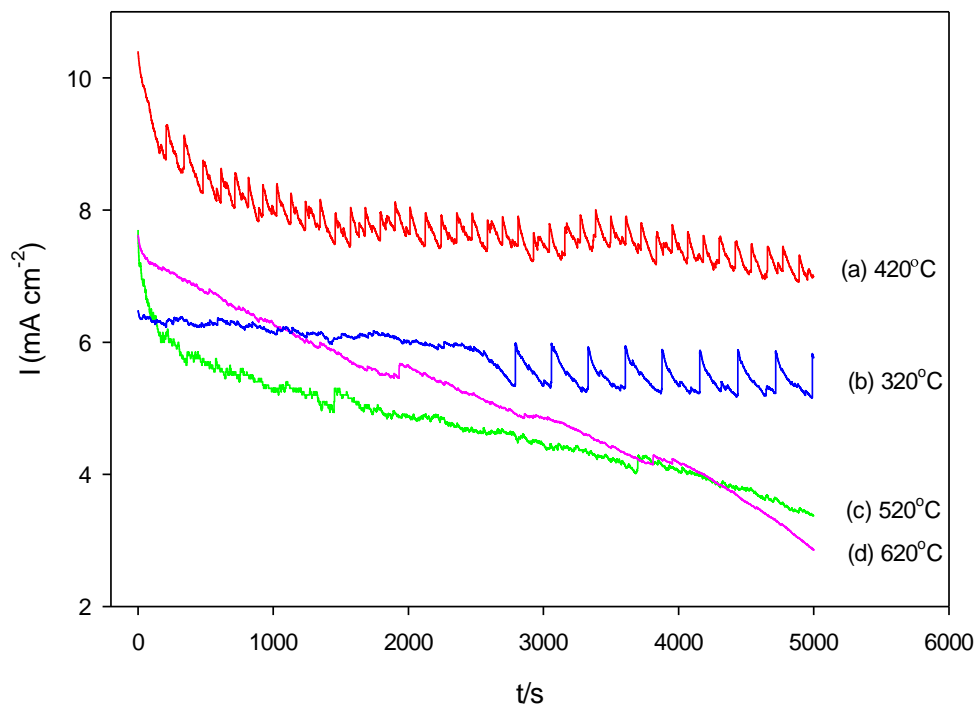


Figure 21: Chronoamperometry curves of Co₃O₄ NPs /FPCE CVs in 0.1M NaOH at various sintering temperatures: 320,420,520 and 620 °C

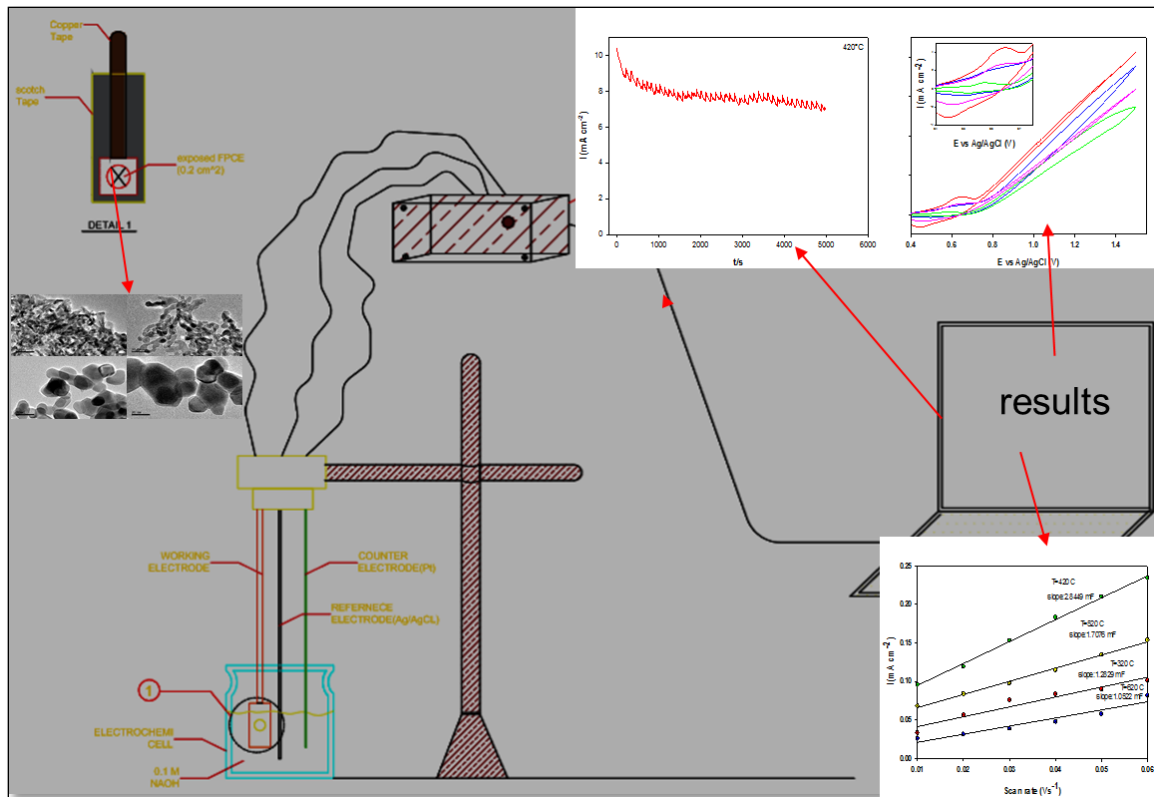


Figure 22: The schematic diagram of electrochemical cell setup for oxygen evolution reaction(OER).

5.5 Conclusion

A Co_3O_4 NPs /FPCE catalyst has been prepared and then investigated at different calcination temperatures (320,420,520 and 620 °C). The activity of the catalysts was affected by the calcination temperature. Initially, the activity was enhanced with the increase of temperature from 320 to 420°C and then decreased at further increase of the temperature. However, the stability at 320 was the most stable. Overall, 420°C is still the optimum temperature.

CHAPTER 6

CONCLUSIONS AND RECOMMENDATIONS

Conclusion:

In summary, we developed a thermal decomposition method for preparing monodisperse NiO NPS and Co₃O₄ NPS. Then, we used them as the catalysts for oxygen evolution reaction. The separate conclusions for NiO NPS and Co₃O₄ NPS are as follows:

For preparation of NiONPs, Ni(NO₃)₂·6H₂O as a nickel precursor and Na₂PA as a complexing agent were used. We also verified the influence of Na₂PA by preparing nanoparticles using a common procedure conducted with or without Na₂PA addition. The NiONPs prepared without Na₂PA were highly polydisperse. The average NP size was much larger than that obtained with the addition of Na₂PA. The electrocatalytic activities of both NiONPs toward electrooxidation in an alkaline medium were evaluated after immobilization on an FPCE using a simple drop-drying method. The NiONP(with Na₂PA)-FPCE showed a much higher electrocatalytic activity toward water electrooxidation than the NiONP(without Na₂PA)-FPCE or bare FPCE. The superior electrocatalytic properties of the NiONP(with Na₂PA)-FPCE were expected because these NPs were small and monodisperse. The monodisperse small NPs described here could play an important role in catalysis, electronics, optoelectrical device, and electrochemical applications, including electrochemical sensors, biosensors, gas sensors, batteries, capacitors, solar cells, fuel cells, and water splitting cells.

On the other hand, nano-Co₃O₄ was prepared by carrying out a direct thermal decomposition of Co(NO₃)₂·6H₂O at 520 °C in an aerial atmosphere, too. The prepared nano-Co₃O₄ was characterized in detail by using XRD, FESEM and TEM, and HRTEM. These analyses confirmed the formation of highly crystalline Co₃O₄ nanorods with an average diameter of 32 nm. The nanorods were immobilized on an FPCE to evaluate their electrocatalytic properties. The FPCE modified with nano-Co₃O₄ showed good electrocatalytic properties toward water oxidation in an alkaline medium. This simply and straight-forwardly prepared nano-Co₃O₄ could potentially play an important role in various practical fields and applications such as catalysis, electronics, opto-electrical devices, and electrochemical applications including electrochemical sensors, biosensors, gas sensors batteries, capacitors, solar cells, fuel cells, and water splitting.

A Co₃O₄ NPs /FPCE catalyst has been prepared and then investigated at different calcination temperatures (320,420,520 and 620 °C). The activity of the catalysts was affected by the calcination temperature. Initially, the activity was enhanced with the increase of temperature from 320 to 420°C and then decreased at further increase of the temperature. However, the stability at 320 was the most stable. Overall, 420°C is still the optimum temperature.

Recommendation:

Our recommendation is to use NiO NPs and Co₃O₄ NPs in other applications such as: electrochemical sensors, gas sensors, batteries, capacitors, solar cells and fuel cells.

REFERENCES

- [1] N. Naseri, A. Esfandiar, M. Qorbani, and A. Z. Moshfegh, "Selecting Support Layer for Electrodeposited Efficient Cobalt Oxide/Hydroxide Nanoflakes to Split Water," *ACS Sustainable Chemistry & Engineering*, vol. 4, pp. 3151-3159, 2016.
- [2] L. Han, S. Dong, and E. Wang, "Transition-Metal (Co, Ni, and Fe)-Based Electrocatalysts for the Water Oxidation Reaction," *Adv Mater*, vol. 28, pp. 9266-9291, Nov 2016.
- [3] Y. Zhao, N. M. Vargas-Barbosa, E. A. Hernandez-Pagan, and T. E. Mallouk, "Anodic deposition of colloidal iridium oxide thin films from hexahydroxyiridate(IV) solutions," *Small*, vol. 7, pp. 2087-93, Jul 18 2011.
- [4] Y. Zhao, E. A. Hernandez-Pagan, N. M. Vargas-Barbosa, J. L. Dysart, and T. E. Mallouk, "A High Yield Synthesis of Ligand-Free Iridium Oxide Nanoparticles with High Electrocatalytic Activity," *The Journal of Physical Chemistry Letters*, vol. 2, pp. 402-406, 2011.
- [5] T. Kuwabara, E. Tomita, S. Sakita, D. Hasegawa, K. Sone, and M. Yagi, "Characterization and analysis of self-assembly of a highly active colloidal catalyst for water oxidation onto transparent conducting oxide substrates," *The Journal of Physical Chemistry C*, vol. 112, pp. 3774-3779, 2008.
- [6] M. Yagi, E. Tomita, S. Sakita, T. Kuwabara, and K. Nagai, "Self-assembly of active IrO₂ colloid catalyst on an ITO electrode for efficient electrochemical water oxidation," *The Journal of Physical Chemistry B*, vol. 109, pp. 21489-21491, 2005.
- [7] M.-C. Chuang and J.-a. A. Ho, "Efficient electrocatalytic oxidation of water: minimization of catalyst loading by an electrostatic assembly of hydrous iridium oxide colloids," *RSC Advances*, vol. 2, pp. 4092-4096, 2012.
- [8] T. Nakagawa, N. S. Bjorge, and R. W. Murray, "Electrogenerated IrO_x nanoparticles as dissolved redox catalysts for water oxidation," *Journal of the American Chemical Society*, vol. 131, pp. 15578-15579, 2009.
- [9] Y. Lee, J. Suntivich, K. J. May, E. E. Perry, and Y. Shao-Horn, "Synthesis and activities of rutile IrO₂ and RuO₂ nanoparticles for oxygen evolution in acid and alkaline solutions," *The journal of physical chemistry letters*, vol. 3, pp. 399-404, 2012.
- [10] T. Nakagawa, C. A. Beasley, and R. W. Murray, "Efficient electro-oxidation of water near its reversible potential by a mesoporous IrO_x nanoparticle film," *The Journal of Physical Chemistry C*, vol. 113, pp. 12958-12961, 2009.
- [11] E. N. El Sawy and V. I. Birss, "Nano-porous iridium and iridium oxide thin films formed by high efficiency electrodeposition," *Journal of Materials Chemistry*, vol. 19, p. 8244, 2009.
- [12] G. Li, H. Yu, W. Song, M. Dou, Y. Li, Z. Shao, *et al.*, "A hard-template method for the preparation of IrO(2) , and its performance in a solid-polymer-electrolyte water electrolyzer," *ChemSusChem*, vol. 5, pp. 858-61, May 2012.

- [13] W. Hu, Y. Wang, X. Hu, Y. Zhou, and S. Chen, "Three-dimensional ordered macroporous IrO₂ as electrocatalyst for oxygen evolution reaction in acidic medium," *Journal of Materials Chemistry*, vol. 22, pp. 6010-6016, 2012.
- [14] E. Ortel, T. Reier, P. Strasser, and R. Kraehnert, "Mesoporous IrO₂ Films Templated by PEO-PB-PEO Block-Copolymers: Self-Assembly, Crystallization Behavior, and Electrocatalytic Performance," *Chemistry of Materials*, vol. 23, pp. 3201-3209, 2011.
- [15] D. Chandra, N. Abe, D. Takama, K. Saito, T. Yui, and M. Yagi, "Open pore architecture of an ordered mesoporous IrO₂ thin film for highly efficient electrocatalytic water oxidation," *ChemSusChem*, vol. 8, pp. 795-9, Mar 2015.
- [16] W. J. Youngblood, S. H. Lee, Y. Kobayashi, E. A. Hernandez-Pagan, P. G. Hoertz, T. A. Moore, *et al.*, "Photoassisted overall water splitting in a visible light-absorbing dye-sensitized photoelectrochemical cell," *J Am Chem Soc*, vol. 131, pp. 926-7, Jan 28 2009.
- [17] S. D. Tilley, M. Cornuz, K. Sivula, and M. Gratzel, "Light-induced water splitting with hematite: improved nanostructure and iridium oxide catalysis," *Angew Chem Int Ed Engl*, vol. 49, pp. 6405-8, Aug 23 2010.
- [18] M. Hara and T. E. Mallouk, "Photocatalytic water oxidation by Nafion-stabilized iridium oxide colloids," *Chemical Communications*, pp. 1903-1904, 2000.
- [19] A. P. Harriman, I. J.; Thomas, J. M.; Christensen, P. A., *J. Chem. Soc, Faraday Trans.*, vol. 84, 1988
- [20] A. Mills and N. McMurray, "Characterisation of an RuO₂ · x H₂O colloid and evaluation of its ability to mediate the oxidation of water," *Journal of the Chemical Society, Faraday Transactions 1: Physical Chemistry in Condensed Phases*, vol. 84, pp. 379-390, 1988.
- [21] G. Beni, L. Schiavone, J. Shay, W. Dautremont-Smith, and B. Schneider, "Electrocatalytic oxygen evolution on reactively sputtered electrochromic iridium oxide films," *Nature*, vol. 282, pp. 281-283, 1979.
- [22] J. Kiwi and M. Grätzel, "Colloidal Redox Catalysts for Evolution of Oxygen and for Light-Induced Evolution of Hydrogen from Water," *Angewandte Chemie International Edition in English*, vol. 18, pp. 624-626, 1979.
- [23] J. Kiwi and M. Grätzel, "Oxygen evolution from water via redox catalysis," *Angewandte Chemie International Edition in English*, vol. 17, pp. 860-861, 1978.
- [24] J. Rosen, G. S. Hutchings, and F. Jiao, "Ordered mesoporous cobalt oxide as highly efficient oxygen evolution catalyst," *J Am Chem Soc*, vol. 135, pp. 4516-21, Mar 20 2013.
- [25] Y. Fan, N. Zhang, L. Zhang, H. Shao, J. Wang, J. Zhang, *et al.*, "Synthesis of Small-Sized Freestanding Co₃O₄ Nanosheets with Improved Activity for H₂O₂ Sensing and Oxygen Evolution," *Journal of the Electrochemical Society*, vol. 160, pp. F218-F223, 2013.
- [26] M. Fayette, A. Nelson, and R. D. Robinson, "Electrophoretic deposition improves catalytic performance of Co₃O₄ nanoparticles for oxygen reduction/oxygen evolution reactions," *J. Mater. Chem. A*, vol. 3, pp. 4274-4283, 2015.

- [27] Y. Li, B. Tan, and Y. Wu, "Freestanding mesoporous quasi-single-crystalline Co₃O₄ nanowire arrays," *Journal of the American Chemical Society*, vol. 128, pp. 14258-14259, 2006.
- [28] X. Chen, C. Li, M. Grätzel, R. Kostecki, and S. S. Mao, "Nanomaterials for renewable energy production and storage," *Chemical Society Reviews*, vol. 41, pp. 7909-7937, 2012.
- [29] S. Y. Reece, J. A. Hamel, K. Sung, T. D. Jarvi, A. J. Esswein, J. J. Pijpers, *et al.*, "Wireless solar water splitting using silicon-based semiconductors and earth-abundant catalysts," *Science*, vol. 334, pp. 645-648, 2011.
- [30] T. Audichon, S. Morisset, T. W. Napporn, K. B. Kokoh, C. Comminges, and C. Morais, "Effect of Adding CeO₂ to RuO₂-IrO₂ Mixed Nanocatalysts: Activity towards the Oxygen Evolution Reaction and Stability in Acidic Media," *ChemElectroChem*, vol. 2, pp. 1128-1137, 2015.
- [31] H. B. Aiyappa, J. Thote, D. B. Shinde, R. Banerjee, and S. Kurungot, "Cobalt-Modified Covalent Organic Framework as a Robust Water Oxidation Electrocatalyst," *Chemistry of Materials*, vol. 28, pp. 4375-4379, 2016.
- [32] Q. Lu, M. W. Lattanzi, Y. Chen, X. Kou, W. Li, X. Fan, *et al.*, "Supercapacitor Electrodes with High-Energy and Power Densities Prepared from Monolithic NiO/Ni Nanocomposites," *Angewandte Chemie*, vol. 123, pp. 6979-6982, 2011.
- [33] K. M. Dooley, S. Y. Chen, and J. R. H. Ross, "Stable Nickel-Containing Catalysts for the Oxidative Coupling of Methane," *Journal of Catalysis*, vol. 145, pp. 402-408, 1994/02/01 1994.
- [34] H. Kuhlenbeck, S. Shaikhutdinov, and H. J. Freund, "Well-ordered transition metal oxide layers in model catalysis--a series of case studies," *Chem Rev*, vol. 113, pp. 3986-4034, Jun 12 2013.
- [35] G. Wang, X. Lu, T. Zhai, Y. Ling, H. Wang, Y. Tong, *et al.*, "Free-standing nickel oxide nanoflake arrays: synthesis and application for highly sensitive non-enzymatic glucose sensors," *Nanoscale*, vol. 4, pp. 3123-3127, 2012.
- [36] D. T. Gillaspie, R. C. Tenent, and A. C. Dillon, "Metal-oxide films for electrochromic applications: present technology and future directions," *Journal of Materials Chemistry*, vol. 20, p. 9585, 2010.
- [37] E. L. Miller and R. E. Rocheleau, "Electrochemical behavior of reactively sputtered iron-doped nickel oxide," *Journal of the Electrochemical Society*, vol. 144, pp. 3072-3077, 1997.
- [38] H. X. Yang, Q. F. Dong, X. H. Hu, X. P. Ai, and S. X. Li, "Preparation and characterization of LiNiO₂ synthesized from Ni(OH)₂ and LiOH·H₂O," *Journal of Power Sources*, vol. 79, pp. 256-261, 6// 1999.
- [39] I. Hotový, J. Huran, L. Spiess, R. Čapkovic, and Š. Haščík, "Preparation and characterization of NiO thin films for gas sensor applications," *Vacuum*, vol. 58, pp. 300-307, 8// 2000.
- [40] H. Liu, G. Wang, J. Liu, S. Qiao, and H. Ahn, "Highly ordered mesoporous NiO anode material for lithium ion batteries with an excellent electrochemical performance," *Journal of Materials Chemistry*, vol. 21, pp. 3046-3052, 2011.
- [41] Y. Ichiyangi, "Magnetic properties of NiO nanoparticles," *Physica B: Condensed Matter*, vol. 329-333, pp. 862-863, 2003.

- [42] S. A. Makhlof, F. T. Parker, F. E. Spada, and A. E. Berkowitz, "Magnetic anomalies in NiO nanoparticles," *Journal of Applied Physics*, vol. 81, pp. 5561-5563, 1997.
- [43] Z. C. X. Y. Deng, *Materials Letters* 58, vol. 276–290., 2004.
- [44] J. Wang, H. X. Zhong, Y. L. Qin, and X. B. Zhang, "An efficient three-dimensional oxygen evolution electrode," *Angew Chem Int Ed Engl*, vol. 52, pp. 5248-53, May 10 2013.
- [45] F. Lin and S. W. Boettcher, "Adaptive semiconductor/electrocatalyst junctions in water-splitting photoanodes," *Nat Mater*, vol. 13, pp. 81-6, Jan 2014.
- [46] M. J. Kenney, M. Gong, Y. Li, J. Z. Wu, J. Feng, M. Lanza, *et al.*, "High-performance silicon photoanodes passivated with ultrathin nickel films for water oxidation," *Science*, vol. 342, pp. 836-840, 2013.
- [47] A. Singh, S. L. Y. Chang, R. K. Hocking, U. Bach, and L. Spiccia, "Highly active nickel oxide water oxidation catalysts deposited from molecular complexes," *Energy Environ. Sci.*, vol. 6, pp. 579-586, 2013.
- [48] K. Fominykh, J. M. Feckl, J. Sicklinger, M. Döblinger, S. Böcklein, J. Ziegler, *et al.*, "Ultrasmall Dispersible Crystalline Nickel Oxide Nanoparticles as High-Performance Catalysts for Electrochemical Water Splitting," *Advanced Functional Materials*, vol. 24, pp. 3123-3129, 2014.
- [49] N. Zhang, Y. Fan, H. Fan, H. Shao, J. Wang, J. Zhang, *et al.*, "Cross-Linked Co₃O₄ Nanowalls Synthesized by Electrochemical Oxidation of Metallic Cobalt Layer for Oxygen Evolution," *ECS Electrochemistry Letters*, vol. 1, pp. H8-H10, 2012.
- [50] X. Zhou, Z. Xia, Z. Tian, Y. Ma, and Y. Qu, "Ultrathin porous Co₃O₄ nanoplates as highly efficient oxygen evolution catalysts," *J. Mater. Chem. A*, vol. 3, pp. 8107-8114, 2015.
- [51] N. Shi, W. Cheng, H. Zhou, T. Fan, and M. Niederberger, "Facile synthesis of monodisperse Co₃O₄ quantum dots with efficient oxygen evolution activity," *Chem Commun (Camb)*, vol. 51, pp. 1338-40, Jan 25 2015.
- [52] S. Chen, Y. Zhao, B. Sun, Z. Ao, X. Xie, Y. Wei, *et al.*, "Microwave-assisted synthesis of mesoporous Co₃O₄ nanoflakes for applications in lithium ion batteries and oxygen evolution reactions," *ACS Appl Mater Interfaces*, vol. 7, pp. 3306-13, Feb 11 2015.
- [53] L. Han, X. Y. Yu, and X. W. Lou, "Formation of Prussian-Blue-Analog Nanocages via a Direct Etching Method and their Conversion into Ni-Co-Mixed Oxide for Enhanced Oxygen Evolution," *Adv Mater*, vol. 28, pp. 4601-5, Jun 2016.
- [54] A. Singh, M. Fekete, T. Gengenbach, A. N. Simonov, R. K. Hocking, S. L. Chang, *et al.*, "Catalytic Activity and Impedance Behavior of Screen-Printed Nickel Oxide as Efficient Water Oxidation Catalysts," *ChemSusChem*, vol. 8, pp. 4266-74, Dec 21 2015.
- [55] M. Hamdani, R. Singh, and P. Chartier, "Co₃O₄ and Co-based spinel oxides bifunctional oxygen electrodes," *Int. J. Electrochem. Sci*, vol. 5, p. 556, 2010.
- [56] W.-Y. Li, L.-N. Xu, and J. Chen, "Co₃O₄ nanomaterials in lithium-ion batteries and gas sensors," *Advanced Functional Materials*, vol. 15, pp. 851-857, 2005.

- [57] Y. Wang, T. Zhou, K. Jiang, P. Da, Z. Peng, J. Tang, *et al.*, "Reduced mesoporous Co₃O₄ nanowires as efficient water oxidation electrocatalysts and supercapacitor electrodes," *Advanced Energy Materials*, vol. 4, 2014.
- [58] T. Y. Ma, S. Dai, M. Jaroniec, and S. Z. Qiao, "Metal–organic framework derived hybrid Co₃O₄-carbon porous nanowire arrays as reversible oxygen evolution electrodes," *Journal of the American Chemical Society*, vol. 136, pp. 13925-13931, 2014.
- [59] Y. Cheng, P. K. Shen, and S. P. Jiang, "NiO x nanoparticles supported on polyethylenimine functionalized CNTs as efficient electrocatalysts for supercapacitor and oxygen evolution reaction," *International Journal of Hydrogen Energy*, vol. 39, pp. 20662-20670, 2014.
- [60] S. Chen, J. Duan, J. Ran, M. Jaroniec, and S. Z. Qiao, "N-doped graphene film-confined nickel nanoparticles as a highly efficient three-dimensional oxygen evolution electrocatalyst," *Energy & Environmental Science*, vol. 6, pp. 3693-3699, 2013.
- [61] Z. Pu, Q. Liu, A. M. Asiri, and X. Sun, "Ni nanoparticles-graphene hybrid film: one-step electrodeposition preparation and application as highly efficient oxygen evolution reaction electrocatalyst," *Journal of Applied Electrochemistry*, vol. 44, pp. 1165-1170, 2014.
- [62] X. Yu, T. Hua, X. Liu, Z. Yan, P. Xu, and P. Du, "Nickel-based thin film on multiwalled carbon nanotubes as an efficient bifunctional electrocatalyst for water splitting," *ACS applied materials & interfaces*, vol. 6, pp. 15395-15402, 2014.
- [63] V. M. Dhavale, S. S. Gaikwad, L. George, R. N. Devi, and S. Kurungot, "Nitrogen-doped graphene interpenetrated 3D Ni-nanocages: efficient and stable water-to-dioxygen electrocatalysts," *Nanoscale*, vol. 6, pp. 13179-87, Nov 07 2014.
- [64] R. Azhagu Raj, M. S. AlSalhi, and S. Devanesan, "Microwave-Assisted Synthesis of Nickel Oxide Nanoparticles Using Coriandrum sativum Leaf Extract and Their Structural-Magnetic Catalytic Properties," *Materials (Basel)*, vol. 10, Apr 26 2017.
- [65] Y. Chen, Y. Sun, X. Dai, B. Zhang, Z. Ye, M. Wang, *et al.*, "Tunable electrical properties of NiO thin films and p-type thin-film transistors," *Thin Solid Films*, vol. 592, pp. 195-199, 2015.
- [66] J. A. Tanna, R. G. Chaudhary, N. V. Gandhare, A. Rai, and H. D. Juneja, "Nickel oxide nanoparticles: synthesis, characterization and recyclable catalyst. ," *International Journal of Scientific & Engineering Research*, vol. 6 pp. 93-99, 2015.
- [67] A. Kumar Rai, L. Tuan Anh, C.-J. Park, and J. Kim, "Electrochemical study of NiO nanoparticles electrode for application in rechargeable lithium-ion batteries," *Ceramics International*, vol. 39, pp. 6611-6618, 2013.
- [68] S. R. K. Kumar, K. Y. Kumar, G. P. Mamatha, H. B. Muralidhara, M. S. Anantha, S. Archana, *et al.*, " Synthesis and characterization of hierarchical nickel oxide (NiO) nanoparticles and its application in modified carbon paste electrode for electrochemical detection of biomolecules. ," *Journal of Chemical and Pharmaceutical Research* . vol. 8, pp. 633-639, 2016.

- [69] M. Tyagi, M. Tomar, and V. Gupta, "NiO nanoparticle-based urea biosensor," *Biosens Bioelectron*, vol. 41, pp. 110-5, Mar 15 2013.
- [70] G. Yang, W. Zhou, M. Liu, and Z. Shao, "Enhancing Electrode Performance by Exsolved Nanoparticles: A Superior Cobalt-Free Perovskite Electrocatalyst for Solid Oxide Fuel Cells," *ACS Appl Mater Interfaces*, vol. 8, pp. 35308-35314, Dec 28 2016.
- [71] M. Khairy, S. A. El-Safty, M. Ismael, and H. Kawarada, "Mesoporous NiO nanomagnets as catalysts and separators of chemical agents," *Applied Catalysis B: Environmental*, vol. 127, pp. 1-10, 2012.
- [72] M. El-Kemary, N. Nagy, and I. El-Mehasseb, "Nickel oxide nanoparticles: Synthesis and spectral studies of interactions with glucose," *Materials Science in Semiconductor Processing*, vol. 16, pp. 1747-1752, 2013.
- [73] D. Ahire, G. Patil, G. Jain, and V. Gaikwad, "Synthesis of nanostructured NiO by hydrothermal route and its gas sensing properties," in *Sensing Technology (ICST), 2012 Sixth International Conference on*, 2012, pp. 136-141.
- [74] Y. Zhang, L.-z. Xie, C.-x. Yuan, C.-l. Zhang, S. Liu, Y.-q. Peng, *et al.*, "Preparation of 3D rose-like nickel oxide nanoparticles by electrodeposition method and application in gas sensors," *Journal of Materials Science: Materials in Electronics*, vol. 27, pp. 1817-1827, 2016.
- [75] D.-L. Sun, B.-W. Zhao, J.-B. Liu, H. Wang, and H. Yan, "Application of nickel oxide nanoparticles in electrochromic materials," *Ionics*, vol. 23, pp. 1509-1515, 2017.
- [76] M. Albalawi and R. K. Gupta, "Effect of Surfactant on Structural and Electrochemical Properties of Nickel Oxide," Pittsburg State University, 2016.
- [77] L. A. Saghatfroush, M. Hasanzadeh, S. Sanati, and R. Mehdizadeh, "Ni(OH)₂ and NiO Nanostructures: Synthesis, Characterization and Electrochemical Performance," *Bulletin of the Korean Chemical Society*, vol. 33, pp. 2613-2618, 2012.
- [78] G. Zeng, W. Li, S. Ci, J. Jia, and Z. Wen, "Highly Dispersed NiO Nanoparticles Decorating graphene Nanosheets for Non-enzymatic Glucose Sensor and Biofuel Cell," *Sci Rep*, vol. 6, p. 36454, Nov 02 2016.
- [79] O. E. Fayemi, A. S. Adekunle, and E. E. Ebenso, "Electrochemical determination of serotonin in urine samples based on metal oxide nanoparticles/MWCNT on modified glassy carbon electrode," *Sensing and Bio-Sensing Research*, vol. 13, pp. 17-27, 2017.
- [80] U. Kwon, B. G. Kim, D. C. Nguyen, J. H. Park, N. Y. Ha, S. J. Kim, *et al.*, "Solution-Processible Crystalline NiO Nanoparticles for High-Performance Planar Perovskite Photovoltaic Cells," *Sci Rep*, vol. 6, p. 30759, Jul 28 2016.
- [81] D. Wang, F. Watanabe, and W. Zhao, "Reduced Graphene Oxide-NiO/Ni Nanomembranes as Oxygen Evolution Reaction Electrocatalysts," *ECS Journal of Solid State Science and Technology*, vol. 6, pp. M3049-M3054, 2017.
- [82] B. Kavitha, M. Nirmala, and A. Pavithra, "Annealing effect on nickel oxide nanoparticles synthesized by sol-gel method.," *World Scientific News*, vol. 52, pp. 118-129, 2016.

- [83] S. Sriram and A. Thayumanavan, "Structural, Optical and Electrical Properties of NiO Thin Films Prepared by Low Cost Spray Pyrolysis Technique," *International Journal of Materials Science and Engineering*, 2014.
- [84] M. Tadic, D. Nikolic, M. Panjan, and G. R. Blake, "Magnetic properties of NiO (nickel oxide) nanoparticles: Blocking temperature and Neel temperature," *Journal of Alloys and Compounds*, vol. 647, pp. 1061-1068, 2015.
- [85] M. Imran Din and A. Rani, "Recent Advances in the Synthesis and Stabilization of Nickel and Nickel Oxide Nanoparticles: A Green Adeptness," *Int J Anal Chem*, vol. 2016, p. 3512145, 2016.
- [86] F. Motahari, M. R. Mozdianfard, F. Soofivand, and M. Salavati-Niasari, "NiO nanostructures: synthesis, characterization and photocatalyst application in dye wastewater treatment," *RSC Advances*, vol. 4, p. 27654, 2014.
- [87] X. Zhang, W. Shi, J. Zhu, W. Zhao, J. Ma, S. Mhaisalkar, *et al.*, "Synthesis of porous NiO nanocrystals with controllable surface area and their application as supercapacitor electrodes," *Nano Research*, vol. 3, pp. 643-652, 2010.
- [88] D. Wang, R. Xu, X. Wang, and Y. Li, "NiO nanorings and their unexpected catalytic property for CO oxidation," *Nanotechnology*, vol. 17, pp. 979-83, Feb 28 2006.
- [89] S. Z. Khan, Y. Yuan, A. Abdolvand, M. Schmidt, P. Crouse, L. Li, *et al.*, "Generation and characterization of NiO nanoparticles by continuous wave fiber laser ablation in liquid," *Journal of Nanoparticle Research*, vol. 11, pp. 1421-1427, 2009.
- [90] X. Wang, L. Li, Y. g. Zhang, S. Wang, Z. Zhang, L. Fei, *et al.*, "High-yield synthesis of NiO nanoplatelets and their excellent electrochemical performance," *Crystal growth & design*, vol. 6, pp. 2163-2165, 2006.
- [91] Z. Fereshteh, M. Salavati-Niasari, K. Saberyan, S. M. Hosseinpour-Mashkani, and F. Tavakoli, "Synthesis of Nickel Oxide Nanoparticles from Thermal Decomposition of a New Precursor," *Journal of Cluster Science*, vol. 23, pp. 577-583, 2012.
- [92] A. Barakat, M. Al-Noaimi, M. Suleiman, A. S. Aldwayyan, B. Hammouti, T. Ben Hadda, *et al.*, "One step synthesis of NiO nanoparticles via solid-state thermal decomposition at low-temperature of novel aqua(2,9-dimethyl-1,10-phenanthroline)NiCl₂ complex," *Int J Mol Sci*, vol. 14, pp. 23941-54, Dec 09 2013.
- [93] S. Rakshit, S. Chall, S. S. Mati, A. Roychowdhury, S. P. Moulik, and S. C. Bhattacharya, "Morphology control of nickel oxalate by soft chemistry and conversion to nickel oxide for application in photocatalysis," *RSC Advances*, vol. 3, p. 6106, 2013.
- [94] A. D. Khalaji, M. Nikookar, and D. Das, "Preparation and characterization of nickel oxide nanoparticles via solid state thermal decomposition of dinuclear nickel(II) Schiff base complex [Ni₂(Brsal-1,3-ph)₂] as a new precursor," *Research on Chemical Intermediates*, vol. 41, pp. 357-363, 2015.
- [95] N. Dharmaraj, P. Prabu, S. Nagarajan, C. H. Kim, J. H. Park, and H. Y. Kim, "Synthesis of nickel oxide nanoparticles using nickel acetate and poly(vinyl acetate) precursor," *Materials Science and Engineering: B*, vol. 128, pp. 111-114, 2006.

- [96] S. Vaidya, P. Rastogi, S. Agarwal, S. K. Gupta, T. Ahmad, A. M. Antonelli Jr, *et al.*, "Nanospheres, nanocubes, and nanorods of nickel oxalate: control of shape and size by surfactant and solvent," *The Journal of Physical Chemistry C*, vol. 112, pp. 12610-12615, 2008.
- [97] N. Chopra, L. Claypoole, and L. G. Bachas, "Morphological control of Ni/NiO core/shell nanoparticles and production of hollow NiO nanostructures," *Journal of Nanoparticle Research*, vol. 12, pp. 2883-2893, 2010.
- [98] M. A. Aziz, J.-P. Kim, and M. Oyama, "Preparation of monodispersed carboxylate-functionalized gold nanoparticles using pamoic acid as a reducing and capping reagent," *Gold Bulletin*, vol. 47, pp. 127-132, 2014.
- [99] M. A. Aziz, J.-P. Kim, M. N. Shaikh, M. Oyama, F. O. Bakare, and Z. H. Yamani, "Size-controlled preparation of fluorescent gold nanoparticles using pamoic acid," *Gold Bulletin*, vol. 48, pp. 85-92, 2015.
- [100] M. A. Aziz, W. Mahfoz, M. Nasiruzzaman Shaikh, M. H. Zahir, A.-R. Al-Betar, M. Oyama, *et al.*, "Preparation of Indium Tin Oxide Nanoparticle-modified 3-Aminopropyltrimethoxysilane-functionalized Indium Tin Oxide Electrode for Electrochemical Sulfide Detection," *Electroanalysis*, vol. 29, pp. 1683-1690, 2017.
- [101] M. Jørgensen, " Quantitative determination of pamoic acid in dog and rat serum by automated ion-pair solid-phase extraction and reversed-phase highperformance liquid chromatography.," *Journal of Chromatography B* vol. 716, pp. 315–323, 1998.
- [102] G. S. Baghel and C. P. Rao, "Pamoic acid in forming metallo-organic framework: Synthesis, characterization and first crystal structure of a dimeric Ti(IV) complex," *Polyhedron*, vol. 28, pp. 3507-3514, 2009.
- [103] N. Li, L. Gou, H.-M. Hu, S.-H. Chen, X.-L. Chen, B.-C. Wang, *et al.*, "The effect of organic acid on self-assembly process: Syntheses and characterizations of six novel cadmium(II)/zinc(II) complexes derived from mixed ligands," *Inorganica Chimica Acta*, vol. 362, pp. 3475-3483, 2009.
- [104] M. Chandra and A. Dey " Ternary complexes of copper(II), nickel(II) and zinc(II) with nitrilotriacetic acid as a primary ligand and some phenolic acids as secondary ligands. ," *Transition Met. Chem.* , vol. 5, pp. 1-3., 1980.
- [105] X.-M. Shi, M.-X. Li, X. He, H.-J. Liu, and M. Shao, "Crystal structures and properties of four coordination polymers constructed from flexible pamoic acid," *Polyhedron*, vol. 29, pp. 2075-2080, 2010.
- [106] H. Oda and T. Kitao, "Photostabilisation of colorants for imaging and data recording systems: Effect of metal carboxylates on the lightfastness of colour formers. ," *Dyes and Pigments*, vol. 16, pp. 1-10, 1991.
- [107] S. Wang, R. Yun, Y. Peng, Q. Zhang, J. Lu, J. Dou, *et al.*, "A Series of Four-Connected Entangled Metal–Organic Frameworks Assembled from Pamoic Acid and Pyridine-Containing Ligands: Interpenetrating, Self-Penetrating, and Supramolecular Isomerism," *Crystal Growth & Design*, vol. 12, pp. 79-92, 2012.
- [108] N. Arunadevi and S. Vairam, "3-hydroxy-2-naphthoate complexes of transition metals with hydrazine-preparation, spectroscopic and thermal studies," *Journal of Chemistry*, vol. 6, pp. S413-S421, 2009.

- [109] L. Jiang, G. W. Nelson, H. Kim, I. N. Sim, S. O. Han, and J. S. Foord, "Cellulose-Derived Supercapacitors from the Carbonisation of Filter Paper," *ChemistryOpen*, vol. 4, pp. 586-9, Oct 2015.
- [110] M. Liu, S. He, W. Fan, Y.-E. Miao, and T. Liu, "Filter paper-derived carbon fiber/polyaniline composite paper for high energy storage applications," *Composites Science and Technology*, vol. 101, pp. 152-158, 2014.
- [111] X. Wang, X. Wu, B. Xu, and T. Hua, "Coralloid and hierarchical Co₃O₄ nanostructures used as supercapacitors with good cycling stability," *Journal of solid state electrochemistry*, vol. 20, pp. 1303-1309, 2016.
- [112] Y. Teng, L. X. Song, L. B. Wang, and J. Xia, "Face-raised octahedral Co₃O₄ nanocrystals and their catalytic activity in the selective oxidation of alcohols," *The Journal of Physical Chemistry C*, vol. 118, pp. 4767-4773, 2014.
- [113] S. K. Meher and G. R. Rao, "Ultralayered Co₃O₄ for high-performance supercapacitor applications," *The Journal of Physical Chemistry C*, vol. 115, pp. 15646-15654, 2011.
- [114] Z. Ma, "Cobalt oxide catalysts for environmental remediation," *Current Catalysis*, vol. 3, pp. 15-26, 2014.
- [115] G. Godillot, L. Guerlou-Demourgues, L. Croguennec, K. M. Shaju, and C. Delmas, "Effect of Temperature on Structure and Electronic Properties of Nanometric Spinel-Type Cobalt Oxides," *The Journal of Physical Chemistry C*, vol. 117, pp. 9065-9075, 2013.
- [116] S. Thota, A. Kumar, and J. Kumar, "Optical, electrical and magnetic properties of Co₃O₄ nanocrystallites obtained by thermal decomposition of sol-gel derived oxalates," *Materials Science and Engineering: B*, vol. 164, pp. 30-37, 2009.
- [117] Z. Chen, C. X. Kronawitter, and B. E. Koel, "Facet-dependent activity and stability of Co(3)O(4) nanocrystals towards the oxygen evolution reaction," *Phys Chem Chem Phys*, vol. 17, pp. 29387-93, Nov 21 2015.
- [118] W. Jia, M. Guo, Z. Zheng, T. Yu, E. G. Rodriguez, Y. Wang, *et al.*, "Electrocatalytic oxidation and reduction of H₂O₂ on vertically aligned Co₃O₄ nanowalls electrode: Toward H₂O₂ detection," *Journal of Electroanalytical Chemistry*, vol. 625, pp. 27-32, 2009.
- [119] C. Guo, X. Zhang, H. Huo, C. Xu, and X. Han, "Co(3)O(4) microspheres with free-standing nanofibers for high performance non-enzymatic glucose sensor," *Analyst*, vol. 138, pp. 6727-31, Nov 21 2013.
- [120] C. Hou, Q. Xu, L. Yin, and X. Hu, "Metal-organic framework templated synthesis of Co₃O₄ nanoparticles for direct glucose and H₂O₂ detection," *Analyst*, vol. 137, pp. 5803-8, Dec 21 2012.
- [121] A. Louardi, A. Rmili, T. Chtouki, B. Elidrissi, H. Erguig, A. El Bachiri, *et al.*, "Effect of annealing treatment on Co₃O₄ thin films properties prepared by spray pyrolysis," 2017.
- [122] J. M. Xu and J. P. Cheng, "The advances of Co₃O₄ as gas sensing materials: A review," *Journal of Alloys and Compounds*, vol. 686, pp. 753-768, 2016.
- [123] D. Su, X. Xie, P. Munroe, S. Dou, and G. Wang, "Mesoporous hexagonal Co₃O₄ for high performance lithium ion batteries," *Sci Rep*, vol. 4, p. 6519, Oct 06 2014.
- [124] J. K. Sharma, P. Srivastava, G. Singh, M. S. Akhtar, and S. Ameen, "Green synthesis of Co₃O₄ nanoparticles and their applications in thermal decomposition

- of ammonium perchlorate and dye-sensitized solar cells," *Materials Science and Engineering: B*, vol. 193, pp. 181-188, 2015.
- [125] T. S. Kabre, "Co₃O₄ Thin Films: Sol-Gel Synthesis, Electrocatalytic Properties & Photoelectrochemistry," The Ohio State University, 2011.
- [126] M. M. Shahid, A. Pandikumar, A. M. Golsheikh, N. M. Huang, and H. N. Lim, "Enhanced electrocatalytic performance of cobalt oxide nanocubes incorporating reduced graphene oxide as a modified platinum electrode for methanol oxidation," *RSC Adv.*, vol. 4, pp. 62793-62801, 2014.
- [127] S. Hu, C. Melton, and D. Mukherjee, "A facile route for the synthesis of nanostructured oxides and hydroxides of cobalt using laser ablation synthesis in solution (LASIS)," *Physical Chemistry Chemical Physics*, vol. 16, pp. 24034-24044, 2014.
- [128] Y. V. Shmatok, N. I. Globa, and S. A. Kirillov, "Microwave-assisted citric acid aided synthesis and electrochemical performance of nanosized Co₃O₄," *Electrochimica Acta*, vol. 245, pp. 88-98, 2017.
- [129] J. Ahmed, T. Ahmad, K. V. Ramanujachary, S. E. Lofland, and A. K. Ganguli, "Development of a microemulsion-based process for synthesis of cobalt (Co) and cobalt oxide (Co₃O₄) nanoparticles from submicrometer rods of cobalt oxalate," *J Colloid Interface Sci*, vol. 321, pp. 434-41, May 15 2008.
- [130] C. R. Bhattacharjee, D. D. Purkayastha, and N. Das, "Surfactant-free thermal decomposition route to phase pure tricobalt tetraoxide nanoparticles from cobalt(II)-tartrate complex," *Journal of Sol-Gel Science and Technology*, vol. 65, pp. 296-300, 2012.
- [131] V. Raman, S. Suresh, P. A. Savarimuthu, T. Raman, A. M. Tsatsakis, K. S. Golokhvast, *et al.*, "Synthesis of Co₃O₄ nanoparticles with block and sphere morphology, and investigation into the influence of morphology on biological toxicity," *Exp Ther Med*, vol. 11, pp. 553-560, Feb 2016.
- [132] K. Assim, S. Schulze, M. Pügner, M. Uhlemann, T. Gemming, L. Giebel, *et al.*, "Co(II) ethylene glycol carboxylates for Co₃O₄ nanoparticle and nanocomposite formation," *Journal of Materials Science*, vol. 52, pp. 6697-6711, 2017.
- [133] M. Salavati-Niasari, A. Khansari, and F. Davar, "Synthesis and characterization of cobalt oxide nanoparticles by thermal treatment process," *Inorganica Chimica Acta*, vol. 362, pp. 4937-4942, 2009.
- [134] A. Khansari, M. Salavati-Niasari, and A. K. Babaheydari, "Synthesis and Characterization of Co₃O₄ Nanoparticles by Thermal Treatment Process," *Journal of Cluster Science*, vol. 23, pp. 557-565, 2012.
- [135] M. Salavati-Niasari and A. Khansari, "Synthesis and characterization of Co₃O₄ nanoparticles by a simple method," *Comptes Rendus Chimie*, vol. 17, pp. 352-358, 2014.
- [136] A. Diallo, A. C. Beye, T. B. Doyle, E. Park, and M. Maaza, "Green synthesis of Co₃O₄ nanoparticles via *Aspalathus linearis*: Physical properties," *Green Chemistry Letters and Reviews*, vol. 8, pp. 30-36, 2015.
- [137] R. Xu and H. C. Zeng, "Dimensional control of cobalt-hydroxide-carbonate nanorods and their thermal conversion to one-dimensional arrays of Co₃O₄ nanoparticles," *The Journal of Physical Chemistry B*, vol. 107, pp. 12643-12649, 2003.

- [138] S. Farhadi, M. Javanmard, and G. Nadri, "Characterization of Cobalt Oxide Nanoparticles Prepared by the Thermal Decomposition," *Acta Chimica Slovenica*, pp. 335-343, 2016.
- [139] S. Farhadi and K. Pourzare, "Simple and low-temperature preparation of Co₃O₄ sphere-like nanoparticles via solid-state thermolysis of the [Co(NH₃)₆](NO₃)₃ complex," *Materials Research Bulletin*, vol. 47, pp. 1550-1556, 2012.
- [140] Z. H. Ibupoto, S. Elhag, M. S. AlSalhi, O. Nur, and M. Willander, "Effect of Urea on the Morphology of Co₃O₄ Nanostructures and Their Application for Potentiometric Glucose Biosensor," *Electroanalysis*, vol. 26, pp. 1773-1781, 2014.
- [141] Y. Huang, C. Chen, C. An, C. Xu, Y. Xu, Y. Wang, *et al.*, "Synthesis of Cobalt based Complexes and conversion to Co₃O₄ nanoparticles as a high performance anode for lithium ion battery," *Electrochimica Acta*, vol. 145, pp. 34-39, 2014.
- [142] K. Kalpanadevi, C. R. Sinduja, and R. Manimekalai, "Characterisation of Nanostructured Co₃O₄ Synthesised by the Thermal Decomposition of an Inorganic Precursor," *Australian Journal of Chemistry*, vol. 67, pp. 1671-1674, 2014.
- [143] S. Harish, K. Silambarasan, G. Kalaiyarasan, A. V. Narendra Kumar, and J. Joseph, "Nanostructured porous cobalt oxide synthesis from Co₃[Co(CN)₆]₂ and its possible applications in Lithium battery," *Materials Letters*, vol. 165, pp. 115-118, 2016.
- [144] W. E. Mahmoud and F. A. Al-Agel, "A novel strategy to synthesize cobalt hydroxide and Co₃O₄ nanowires," *Journal of Physics and Chemistry of Solids*, vol. 72, pp. 904-907, 2011.
- [145] J.-y. Pu, J.-q. Wan, Y. Wang, and Y.-w. Ma, "Different Co-based MOFs templated synthesis of Co₃O₄ nanoparticles to degrade RhB by activation of oxone," *RSC Adv.*, vol. 6, pp. 91791-91797, 2016.
- [146] R. K. Gupta, A. K. Sinha, B. N. Raja Sekhar, A. K. Srivastava, G. Singh, and S. K. Deb, "Synthesis and characterization of various phases of cobalt oxide nanoparticles using inorganic precursor," *Applied Physics A*, vol. 103, pp. 13-19, 2011.
- [147] Ž. Živković, D. Živković, and D. Grujičić, "Kinetics and mechanism of the thermal decomposition of M(NO₃)₂·nH₂O (M= Cu, Co, Ni)," *Journal of thermal analysis and calorimetry*, vol. 53, pp. 617-623, 1998.
- [148] A. Barakat, M. Al-Noaimi, M. Suleiman, A. S. Aldwayyan, B. Hammouti, T. B. Hadda, *et al.*, "One step synthesis of NiO nanoparticles via solid-state thermal decomposition at low-temperature of novel aqua (2, 9-dimethyl-1, 10-phenanthroline) NiCl₂ complex," *International journal of molecular sciences*, vol. 14, pp. 23941-23954, 2013.
- [149] L. J. Matienzo, L. I. Yin, S. O. Grim, and W. E. Swartz, "X-Ray photoelectron spectroscopy of nickel compounds.," *Inorganic Chemistry* vol. 12, pp. 2763-2769, 1973.
- [150] J. A. Schreifels, P. C. Maybury, and W. E. S. Jr, "X-ray photoelectron spectroscopy of nickel boride catalysts: Correlation of surface states with reaction products in the hydrogenation of acrylonitrile.," *Journal of Catalysis* vol. 65, pp. 195-206., 1980.

- [151] A. M. Venezia, R. Bertocello, and G. Deganello, "X-ray photoelectron spectroscopy investigation of pumice-supported nickel catalysts," *Surface and Interface Analysis*, vol. 23, pp. 239-247, 1995.
- [152] A. Mansour, "Characterization of NiO by XPS," *Surface Science Spectra*, vol. 3, pp. 231-238, 1994.
- [153] M. Majumder, C. S. Rendall, J. A. Eukel, J. Y. Wang, N. Behabtu, C. L. Pint, *et al.*, "Overcoming the "coffee-stain" effect by compositional Marangoni-flow-assisted drop-drying," *J Phys Chem B*, vol. 116, pp. 6536-42, Jun 07 2012.
- [154] R. Duggal, F. Hussain, and M. Pasquali, "Self-Assembly of Single-Walled Carbon Nanotubes into a Sheet by Drop Drying," *Advanced Materials*, vol. 18, pp. 29-34, 2006.
- [155] M. A. Aziz, D. Theleritis, M. O. Al-Shehri, M. I. Ahmed, M. Qamaruddin, A. S. Hakeem, *et al.*, "A Simple and Direct Preparation of a Substrate-Free Interconnected Nanostructured Carbon Electrode from Date Palm Leaflets for Detecting Hydroquinone," *ChemistrySelect*, vol. 2, pp. 4787-4793, 2017.
- [156] J. D. Blakemore, R. H. Crabtree, and G. W. Brudvig, "Molecular Catalysts for Water Oxidation," *Chem Rev*, vol. 115, pp. 12974-3005, Dec 09 2015.
- [157] S. W. Sheehan, J. M. Thomsen, U. Hintermair, R. H. Crabtree, G. W. Brudvig, and C. A. Schmuttenmaer, "A molecular catalyst for water oxidation that binds to metal oxide surfaces," *Nat Commun*, vol. 6, p. 6469, Mar 11 2015.
- [158] Y. Fan, H. Shao, J. Wang, L. Liu, J. Zhang, and C. Cao, "Synthesis of foam-like freestanding Co₃O₄ nanosheets with enhanced electrochemical activities," *Chemical Communications*, vol. 47, pp. 3469-3471, 2011.
- [159] Y. Sun, S. Gao, F. Lei, J. Liu, L. Liang, and Y. Xie, "Atomically-thin non-layered cobalt oxide porous sheets for highly efficient oxygen-evolving electrocatalysts," *Chemical Science*, vol. 5, p. 3976, 2014.
- [160] J. Zhao, Y. Zou, X. Zou, T. Bai, Y. Liu, R. Gao, *et al.*, "Self-template construction of hollow Co₃O₄ microspheres from porous ultrathin nanosheets and efficient noble metal-free water oxidation catalysts," *Nanoscale*, vol. 6, pp. 7255-62, Jul 07 2014.
- [161] M. Aziz, D. Theleritis, M. O. Al-Shehri, M. I. Ahmed, M. Qamaruddin, A. S. Hakeem, *et al.*, "A Simple and Direct Preparation of a Substrate-Free Interconnected Nanostructured Carbon Electrode from Date Palm Leaflets for Detecting Hydroquinone," *ChemistrySelect*, vol. 2, pp. 4787-4793, 2017.
- [162] B. Abu-Zied and S. Soliman, "Nitrous oxide decomposition over MCO₃-Co₃O₄ (M= Ca, Sr, Ba) catalysts," *Catalysis letters*, vol. 132, p. 299, 2009.
- [163] G. A. El-Shobaky and A. E.-M. M. Turkey, "Catalytic decomposition of H₂O₂ on Co₃O₄ doped with MgO and V₂O₅," *Colloids and Surfaces A: Physicochemical and Engineering Aspects*, vol. 170, pp. 161-172, 2000.
- [164] M. A. Nejad and M. Jonsson, "Reactivity of hydrogen peroxide towards Fe₃O₄, Fe₂CoO₄ and Fe₂NiO₄," *Journal of Nuclear Materials*, vol. 334, pp. 28-34, 2004.
- [165] S. Jung, C. C. McCrory, I. M. Ferrer, J. C. Peters, and T. F. Jaramillo, "Benchmarking nanoparticulate metal oxide electrocatalysts for the alkaline water oxidation reaction," *Journal of Materials Chemistry A*, vol. 4, pp. 3068-3076, 2016.

Vitae

Name	Mohammed Ameen Ahmed Qasem
Nationality	Yemeni
Date of Birth	1/1/1987
Email	mohammedameen201032@gmail.com
Address	Ibb/ Yemen

Academic Background

- Master of science, chemical engineering(Sep,2015-Dec,2017)
- Bachelor of science, Chemical Engineering, (Sep,2009-Jan,2015). Honor student

Outcome of the Work

- " Preparation of nano- Co_3O_4 by direct thermal decomposition of $\text{Co}(\text{NO}_3)_2 \cdot 6\text{H}_2\text{O}$ for electrochemical water oxidation "(Accepted).
- " Influence of pamoic acid as a complexing agent in the thermal preparation of NiO nanoparticles: application to electrochemical water oxidation "(Accepted).